Computer-Aided Design Software for Torsional Analysis

Timothy R. Griffin

Thesis submitted to the Faculty of the
Virginia Polytechnic Institute and State University
in partial fulfillment of the requirements for the degree of

Master of Science
in
Mechanical Engineering

Larry D. Mitchell, Chairman
Reginald G. Mitchiner
Robert L. West, Jr.

March 5, 1998
Blacksburg, Virginia

Keywords: Torsion, Transfer Matrix, Multi-Rotor, Planetary Gear Train, Eigenvalues, Forced Response

Computer-Aided Design Software for Torsional Analysis

Timothy R. Griffin

(ABSTRACT)

The goal of this research has been the development of an effective design tool for torsional analysis. In the hopes of achieving this goal the computer program, *Torsion 1*, has been created. This torsional transfer matrix program provides the user with the ability to easily model multi-rotor systems using a simple user-interface. The program is capable of modeling such components or system characteristics as continuously distributed mass, viscous and structural damping, vibration absorbers, and gear meshes with gear tooth flexibility. The analysis capabilities of the program include forced-response and free-vibration analyses. The forced-response analysis module is capable of determining a system's response to a static or harmonic torsional load. The free-vibration analysis module allows is capable of determining the eigenvalues and eigenvectors for damped and undamped systems. This thesis includes an explanation of the multi-rotor transfer matrix technique employed in *Torsion 1*. The derivation of transfer matrices for visco-elastic vibration absorbers, pendulum absorbers, flexible gear meshes, and planetary gear trains are included in this work. Finally, the validity of the program results is verified with a set of benchmark examples.

Acknowledgements

I would like to express my sincere gratitude to my advisor, Dr. Larry D. Mitchell, for his guidance, advice, and support throughout the course of my graduate studies. His contributions to this research extend far beyond the references cited in this work. I would also like to thank my committee members, Dr. Reginald G. Mitchiner and Dr. Robert L. West, Jr., for their help in reviewing this work.

My deepest appreciation is extended to my parents whose love and support has among other things helped me to achieve my goals as a student thus far. I am also grateful for the knowledge and friendship shared with me by my brother, Geoff. I would like to thank the rest of my family for their fellowship and encouragement throughout my studies. In addition, I am grateful to my friends and fellow graduate students who have made the time spent at Virginia Tech interesting and rewarding.

The willingness of fellow graduate students Tim Poppe, Anaita Dolasa, and Pavan Thallapragada to share programming experiences and resources has been instrumental in the completion of my work. It should also be noted that the computer program, *Torsion 1*, is the latest in a series of transfer matrix programs developed by graduate students advised by Dr. Mitchell. *Torsion 1* makes use of several subroutines developed by others.

Table of Contents

List of Figures

List of Tables

Chapter 1. Introduction

1.1 Motivation: A Design Tool for Torsional Analysis

Mechanical power transmission systems are often subjected to static or periodic torsional loading that necessitates the analysis of the torsional characteristics of the system. For example, the drive train of a typical automobile is subjected to a periodically varying torque. This torque variation occurs due to the cyclical nature of the internal combustion engine that supplies the power[1].[*] If the frequency of the engine's torque variation matches one of the resonance frequencies of the engine/drive train system, large torsional deflections and internal shear stresses can occur. Continued operation of the machinery under such conditions can lead to early fatigue failure of system components. Thus, an engineer designing such a system needs to able to predict its torsional natural frequencies and be able to easily determine what effects design changes might have on those natural frequencies.

A design tool for predicting torsional natural frequencies of a piece of machinery should be capable of modeling the important characteristics of the system in a timely manner. Accurately modeling a system in the early stages of a design can reduce costs by decreasing the number of changes needed at later stages in the design process. In the case of modeling torsional system characteristics, it is common to find machinery with vibration dampers, tuned absorbers, and multiple shafts connected by gear trains that can significantly affect the system's dynamic performance. An accurate model of the system must be flexible enough to account for such components. However, a balance must be maintained between the accuracy of the model being created and the amount of time and effort needed to create the model. Therefore, a valuable design tool for torsional analysis would allow the engineer to quickly create a model of the system that provides insight about the system characteristics.

The transfer matrix method has certain advantages when compared to other techniques for modeling torsional systems. For example, the scope of problems which can be solved using commercially available finite element packages is often very broad (not limited specifically to torsional cases). Thus, a transfer matrix program designed specifically for modeling torsional systems can be much easier to learn and use effectively for torsional analysis. Of course the finite element method could be used in a computer program customized to torsional analysis as well. However, the transfer matrix method has the advantage of being able to easily model such system characteristics as continuously distributed mass and non-proportional damping. In addition transfer matrix techniques exist for modeling multi-rotor torsional systems with ease. Thus, a computer program using the transfer matrix method can provide valuable information about the torsional characteristics of a piece of equipment. When coupled with a simple user interface such a program can serve as an effective design tool.

---

[*] Superscripted numbers refer to references at the end of this thesis.

1.2 Literature Review

A review of the literature reveals the following topics:

- the origin of interest in the torsional analysis of machinery
- methods for modeling torsional system components
- the transfer matrix method for determining torsional natural frequencies and the forced response of a torsional system
- techniques for modeling multi-rotor systems
- transfer matrix computer programs with torsional capabilities
- methods for estimating the stiffness of a gear mesh

Wilson[2] gives a historical review of the early development of modern torsional analysis. It is reported that failures in marine and aeronautical drive trains were the original source of interest in the dynamic torsional behavior of machinery. The Holzer method, an iterative procedure for calculating the torsional natural frequencies of multi-mass systems, was developed in the early 1900's.

Wilson[3] and Nestorides[4] describe methods for modeling the various elements of torsional systems. These references include methods for determining equivalent inertias and/or stiffnesses for a variety of machinery components including crankshafts, flywheels, couplings, absorbers, etc. It is common for machinery systems to consist of multiple shafts geared together in non-branched or branched configurations as depicted in Figure 1.1. Both references describe a method for modeling non-branched, multi-shaft systems as an equivalent single-shaft system as well as a procedure for performing Holzer method calculations for branched systems.

The transfer matrix method for determining natural frequencies of torsional systems is an extension of the Holzer method in which the equations relating the displacements and internal forces of the system are written in matrix form. Pestel and Leckie[5] provide a thorough reference for the application of the transfer matrix method to a wide variety of problems including the determination of natural frequencies and mode shapes for undamped and damped torsional systems. In the process of determining the eigenvalues of a torsional system or the system's response to a torsional excitation the boundary conditions of the model must be applied. Pilkey and Chang[6] present a

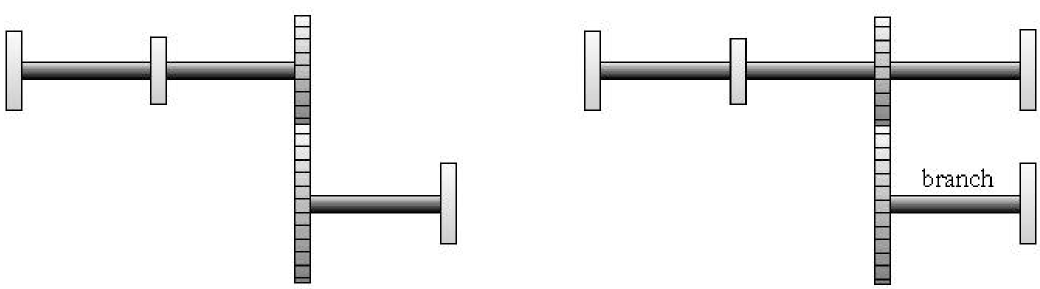

(a) Non-Branched System **(b) Branched System**

Figure 1.1: Two-Shaft Non-Branched and Branched System Examples

generalized method for applying the boundary conditions to a torsional transfer matrix model that is useful in developing an algorithm to accomplish the desired analysis. Pilkey and Chang also present a number of useful torsional transfer matrices and describe a computer program, *TWIST*, capable of performing torsional analysis for branched systems.

A transfer matrix technique for analyzing a branched-torsional system is described by Pestel and Leckie[7] that involves reducing the branched system to an equivalent single-shaft system. This method requires lumping the characteristics of the branch at the point on the main system where the branch is attached. That technique requires the elimination of the branch's state relations from the global transfer matrix and can result in numerical difficulties when using a root finding routine to determine natural frequencies. These numerical difficulties result from infinity wraps that can be observed by plotting the characteristic determinant curve for a branched system over a range of frequency values as demonstrated in Figure 1.2.

Sankar[8] presents one multi-shaft torsional transfer matrix approach that maintains the state information for the entire model in the global transfer matrix. This method involves building the transfer matrix for each branch separately, applying compatibility relations at the junction where the branches join, and then using the boundary conditions to find the characteristic determinant of the system. However, that method is cumbersome for complicated systems with multiple branches.

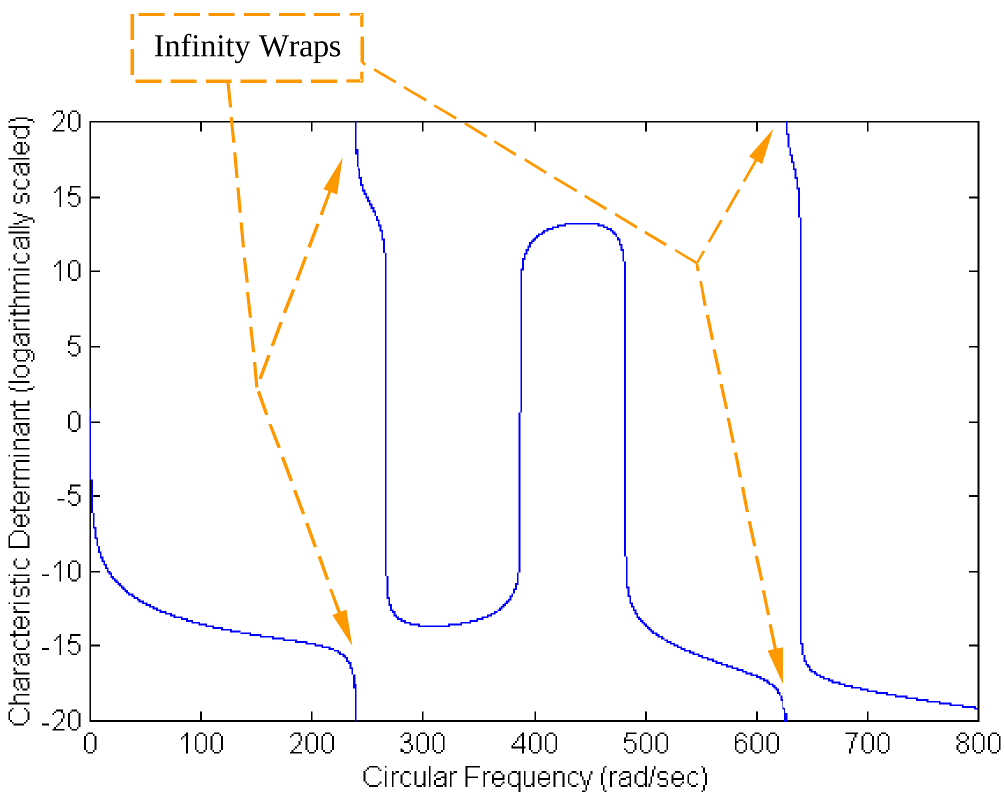

Figure 1.2: Infinity Wraps in the Plot of a Characteristic Determinant Curve, adapted from Pestel and Leckie[9]

Abhary[10] advocates the use of a semi-graphical approach for modeling lumped-parameter torsional systems. The graphical part of the technique is simply a bookkeeping tool to aid the analyst in performing equivalence calculations for systems with several branches. Once the equivalent model has been created, the author suggests writing the equations of motion for the system in matrix form and performing an eigenvalue analysis with the aid of a commercial software package. However, for complicated systems the necessary equivalence calculations can become time consuming and tedious. Therefore, this technique is not optimal for use in a design tool for torsional analysis.

Mitchell[11] has modified a multi-rotor transfer matrix approach for geared-torsional systems which was originally developed by Hibner[12] for shafts experiencing lateral vibrations. This multi-rotor transfer matrix approach is a simple and effective method for modeling multi-shaft systems. The advantages of this method include that it:

- eliminates much of the equivalence calculation needed with some other methods
- provides a simple transfer matrix to relate the states on either side of a gear mesh
- allows for the insertion of a gear tooth flexibility into the model
- permits the insertion of gear mesh transmission errors
- carries all the state information in the global transfer matrix
- models systems that many branches with ease

The model building procedure associated with this method can be readily generalized for application in a computer program.

Blanding[13] describes a transfer matrix computer program that implements the Hibner/Mitchell multi-rotor transfer matrix approach for analyzing the three-dimensional, harmonically forced response of multiple-shaft systems. This three-dimensional response includes not only torsional response but also axial and lateral responses. This model includes coupling terms between the different degrees of freedom. The program has the capability to represent the time-varying stiffness of a pair of meshing spur gears. In addition gear mesh errors can also be included in the model to determine their effects on the response. These added modeling capabilities increase the program’s ability to model a system accurately and as such are significant contributions to the development of the transfer matrix method for modeling rotors. However, including such advanced modeling capabilities comes at the expense of increasing the complexity of the program. Tsai and Kuang[14] also report of a computer program which implements the multi-rotor transfer technique for coupled lateral-torsional vibration analysis of geared rotors. Tsai and Kuang present an example uncoupled torsional analysis of a three-shaft system. However, some of the parameters used for modeling the system have inappropriate units. Therefore, the results they obtained cannot be used as a test case for a new computer program.

Doughty and Vafaee[15] report on a transfer matrix computer program capable of determining the damped natural frequencies and mode shapes of simple torsional systems. Two example problems with solutions are provided to demonstrate the technique. However, analysis using the program is limited to systems for which an equivalent single-shaft system can be developed. The root search method used in this case is a Newton-Raphson algorithm that has certain drawbacks. The Newton-Raphson technique requires an initial root estimate that can affect the success of the routine in finding roots. In addition this root-finding method requires the calculation of derivatives of the function being considered. For the transfer matrix problem these derivatives must be approximated in a somewhat arbitrary fashion which can also affect the success of the root-finding efforts. Huang and Horng[16] also describe a transfer matrix computer program that uses the Newton-Raphson technique for finding the roots of damped torsional systems. This program implements the Pestel and Leckie branching technique for a two-shaft system. Because this technique keeps track of only the main system state values and not those of the branch, calculating the complete eigenvectors for a two-shaft system using their program requires two separate system models.

Methods for modeling the stiffness of a pair of meshing gears are abundant in the literature. Among those techniques is a linear, algebraic model developed by Daws[17] for calculating the stiffness of a single spur gear tooth by modeling the tooth as a tapered beam. This model neglects the longitudinal compression and Hertzian contact deformation modes. The assumption is also made that the gear disk is rigid. However, because this tooth stiffness model is linear and algebraic it can be easily generalized and implemented in a computer program. A few of the references suggesting alternate methods for modeling gear tooth stiffness include Blanding[18], Neriya et al[19], Oswald et al[20], and Kuang and Yang[21].

1.3 Goals of this Research

The primary goal of this research is to develop a user-friendly transfer matrix program capable of modeling the torsional characteristics of common machinery systems. The computer program, *Torsion 1*, is written in the Visual Basic 4.0 language for systems running the Windows 95 operating system. *Torsion 1* allows the user to model the behavior of such components or system characteristics as uniformly distributed loads, pendulum absorbers, visco-elastic dampers, shafts with continuously distributed mass, foundations with uniformly distributed flexibility, gear meshes with a constant gear tooth stiffness, and planetary gear trains.

The program provides the user with the ability to perform forced-response and free-vibration analyses of multi-rotor systems with ease. The free-vibration analysis module is capable of automatically determining the undamped and damped natural frequencies and mode shapes using a Muller-Method[22] root-search routine. The forced-response analysis module provides the capability to determine the steady-state response of a damped or undamped system to a harmonic excitation. Static analysis of a torsional system can be performed with the forced-response module by specifying an excitation frequency of zero (a static load). Analysis results are displayed graphically and can be saved to a text file or a bitmap image for easy manipulation using other programs.

Chapter 2. The Transfer Matrix Method for Single-Shaft Torsional Systems

2.1 State Vector, Coordinate System, and Sign Convention

As mentioned previously, the transfer matrix method involves writing in matrix form the equations which relate the displacements and internal forces at one point in a system to the displacements and internal forces at another point in the system. In terms of transfer matrix terminology the displacements and internal forces at a point describe the "state" of the system at that point. A state vector is simply the combination of the displacements and internal forces of the system in a column-vector form. In the case of torsional analysis the displacement of concern is the angle of twist of a shaft and the internal force considered is an internal torque. Thus, the state vector for a torsional system can be represented as shown in Figure 2.1.

Transfer matrix models are typically divided into a series of fields and points. A field is a piece of the model having some non-zero length, such as a shaft segment in a torsional system. The points in a model represent characteristics which are not distributed over a length, but rather are lumped at a single position. For example, it is a common practice to lump the inertia of a large disk at a point on the system model. Figure 2.2 demonstrates the convention used in this reference for numbering fields, points, and state vectors in single-shaft transfer matrix models. The points in a model are numbered from zero. A field is given the same number as the point to its right. State vectors are numbered with respect to the points in the system (i.e. $\vec{z}_i^{\,L}$ is the state vector to the left of point "i").

The coordinate system used for the torsional transfer matrix model consists of the x-axis which coincides with the axis of the rotor. A positive angular displacement is defined as one whose right-hand-rule vector points in the positive x-direction. The definition of a positive torque is dependent on whether the face on which the torque acts

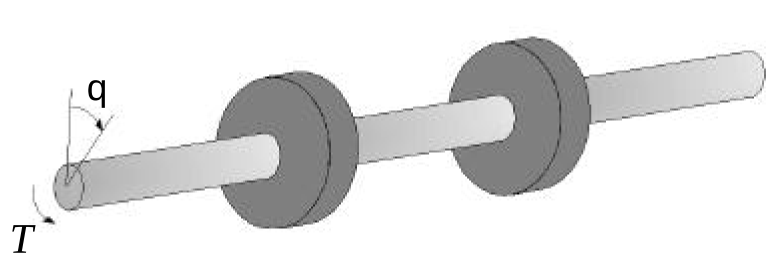

State Vector: $\vec{z} = \begin{Bmatrix} q \\ T \end{Bmatrix}$ Where: $q =$ angular displacement, $T =$ internal torque

Figure 2.1: State Vector for the Torsional System, adapted from Pestel and Leckie[23]

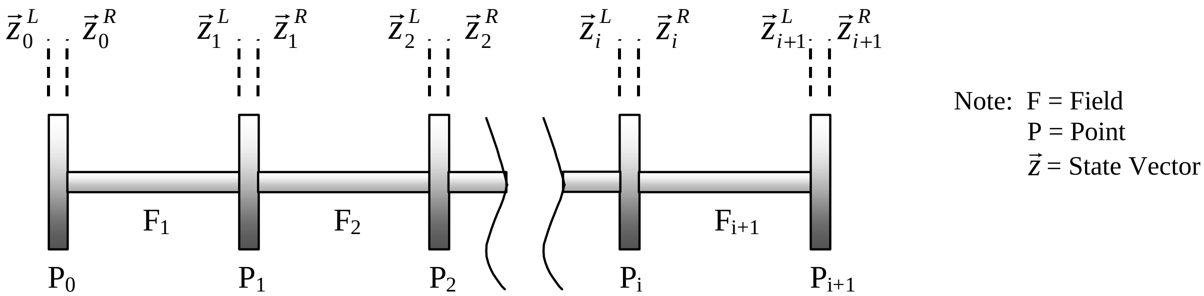

Figure 2.2: Numbering Convention for Single-Shaft Torsional Systems, adapted from Pestel and Leckie[24]

is a positive or negative one. A positive face has an outwardly directed normal that points in the direction of the positive x-axis. A negative face has an outward normal pointing in a direction opposite that of the positive x-axis. This concept of a positive and negative face is demonstrated in Figure 2.3. A positive torque can now be defined as one whose right-hand-rule vector points in the positive x-direction if it acts on a positive face. The vector for a positive torque acting on a negative face points in the negative x-direction. Shown in Figure 2.4 are vector representations of positive angular displacements and a positive internal torque pair for a length of shaft.

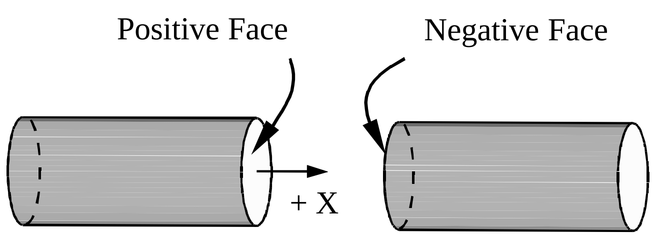

Figure 2.3: Positive and Negative Faces of a Shaft, adapted from Pestel and Leckie[25]

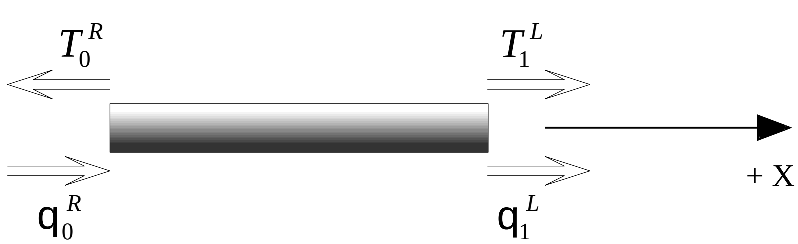

Figure 2.4: Positive Torsional States on Opposite Ends of a Shaft Section, adapted from Pestel and Leckie[26]

2.2 Building the Global Transfer Matrix

The global transfer matrix for a system relates the state at one end of the system to the state at the opposite end. The global transfer matrix is needed to obtain the desired solution (forced-response results or free-vibration characteristics of a torsional system in this case). Typically the global transfer matrix is assembled from individual transfer matrices that describe the characteristics of smaller elements of the system. In other words, the system model is first broken up into smaller elements (fields and points) for which the transfer matrices can be easily written. Then the global, or total system, transfer matrix is obtained by multiplying the individual transfer matrices together as will be demonstrated in the following paragraphs.

A field matrix is a transfer matrix that relates the states on either side of a field element. For example, a length of shaft with constant cross-section is often modeled with a field transfer matrix. The field transfer matrix for an elastic, massless shaft (as shown in Figure 2.4) is developed by first applying the mechanics of materials relation shown in Equation (2.1) that describes the angular displacement of a linear, elastic shaft with length l, shear modulus G, and torsional constant J.

$$\theta_1^L - \theta_0^R = \frac{T_0^R l}{JG} \tag{2.1}$$

Assuming no external torques are applied to the shaft, the torque equilibrium equation is then written as

$$T_1^L = T_0^R \tag{2.2}$$

Equation (2.1) and Equation (2.2) are combined in matrix form resulting in

$$\begin{Bmatrix} \theta \\ T \end{Bmatrix}_1^L = \begin{bmatrix} 1 & \frac{l}{JG} \\ 0 & 1 \end{bmatrix} \cdot \begin{Bmatrix} \theta \\ T \end{Bmatrix}_0^R \tag{2.3}$$

Note that the field transfer matrix for a massless, elastic shaft is found to be

$$\mathrm{TM}_{\text{massless, elastic shaft}} = \begin{bmatrix} 1 & \frac{l}{JG} \\ 0 & 1 \end{bmatrix} \tag{2.4}$$

A transfer matrix that relates the states on either side of a model element having zero length is referred to as a point transfer matrix. A rigid disk with its inertia lumped at a point, which can be represented as shown in Figure 2.5, is an example of a torsional element that can be modeled with a point transfer matrix. The point transfer matrix for the rigid disk is developed by first reasoning that the displacements θ_1^L and θ_1^R are equivalent because the disk has no flexibility. The equilibrium equation for the disk with polar mass moment of inertia, I, undergoing harmonic oscillation with frequency, ω, can be written as

$$T_1^R = T_1^L - I\omega^2\theta_1^L \tag{2.5}$$

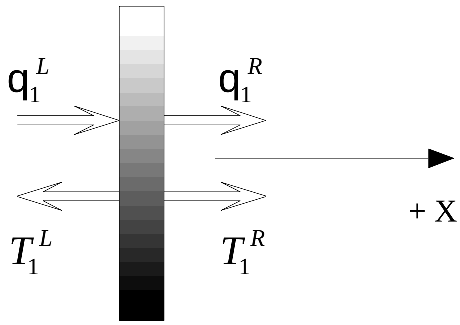

Figure 2.5: Rigid Disk Modeled with Inertia Lumped at a Point, adapted from Pestel and Leckie[27]

The matrix equation relating the states to the left and right of the rigid disk is shown in Equation (2.6).

$$\begin{Bmatrix} \theta \\ T \end{Bmatrix}_1^R = \begin{bmatrix} 1 & 0 \\ -I\omega^2 & 1 \end{bmatrix} \cdot \begin{Bmatrix} \theta \\ T \end{Bmatrix}_1^L \tag{2.6}$$

The point transfer matrix for the rigid disk with lumped inertia is then

$$\mathrm{TM}_{\text{rigid disk with lumped inertia}} = \begin{bmatrix} 1 & 0 \\ -I\omega^2 & 1 \end{bmatrix} \tag{2.7}$$

Assembling a transfer matrix that relates the states on opposite ends of a series of elements that are connected end to end involves a simple matrix multiplication of the elemental transfer matrices. For example, the transfer matrix for the combination of an elastic, massless shaft and a rigid disk with lumped inertia, as shown in Figure 2.6, is assembled by noting that the states to the right of the shaft and to the left of the disk are equivalent. Therefore, Equation (2.3) can be substituted into Equation (2.6) resulting in

$$\begin{Bmatrix} \theta \\ T \end{Bmatrix}_1^R = \begin{bmatrix} 1 & 0 \\ -I\omega^2 & 1 \end{bmatrix} \cdot \begin{bmatrix} 1 & \dfrac{l}{JG} \\ 0 & 1 \end{bmatrix} \cdot \begin{Bmatrix} \theta \\ T \end{Bmatrix}_0^R \tag{2.8}$$

Therefore, the transfer matrix for the shaft-disk combination can be written as

$$\mathrm{TM}_{\text{massless, elastic shaft + rigid disk with lumped inertia}} = \begin{bmatrix} 1 & 0 \\ -I\omega^2 & 1 \end{bmatrix} \cdot \begin{bmatrix} 1 & \dfrac{l}{JG} \\ 0 & 1 \end{bmatrix} \tag{2.9}$$

Note that the transfer matrix for the shaft-disk combination is equal to the transfer matrix for the first element (the shaft) pre-multiplied by the transfer matrix for the second element (the disk). The global transfer matrix for a larger model can be assembled in the same manner by simply multiplying the transfer matrices of the individual elements in the proper order.

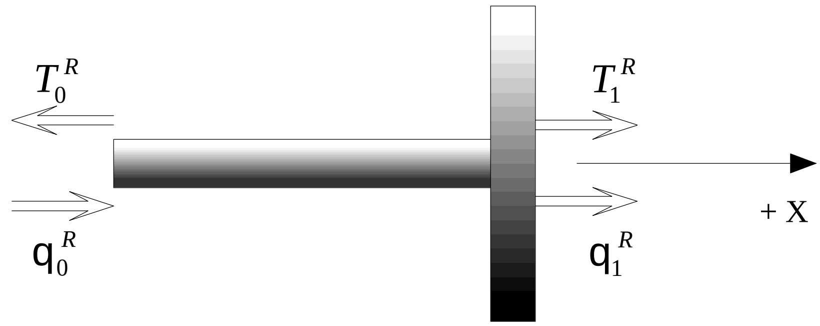

Figure 2.6: Massless Shaft and Lumped Inertia

2.3 Forced-Response Analysis of Simple Torsional Systems

Static analysis of a torsional system involves finding the shaft deflections that correspond to some applied load. As such, static analysis is an example of a forced-response analysis for which the applied load is steady and not cyclic. Pestel and Leckie[28] discuss a useful technique for including applied loads (both static and harmonically varying) in a transfer matrix model that involves expanding the size of the transfer matrix. For example, the partitioned transfer matrix for a positive torque, $T_{applied}$, applied at a point on a rotor is given as

$$\mathrm{TM}_{\text{applied torque}} = \left[\begin{array}{cc:c} 1 & 0 & 0 \\ 0 & 1 & -T_{applied} \\ \hdashline 0 & 0 & 1 \end{array}\right] \tag{2.10}$$

where the corresponding state vector must also be expanded as shown in Equation (2.11).

$$\text{Expanded State Vector} = \left\{\begin{array}{c} q \\ T \\ \hdashline 1 \end{array}\right\} \tag{2.11}$$

Note that all other transfer matrices in an externally loaded system model must also be expanded and partitioned as will be demonstrated in the example to follow. Once the expanded global transfer matrix is determined, the boundary conditions are applied and the remaining unknowns can be solved for.

As an example, consider the shaft shown in Figure 2.7 which is fixed on the left end and has an applied static torque on its right end which is free to rotate. The global transfer matrix is assembled by expanding the transfer matrix for the shaft given in Equation (2.4) and pre-multiplying by the transfer matrix given in Equation (2.10) as demonstrated in Equation (2.12).

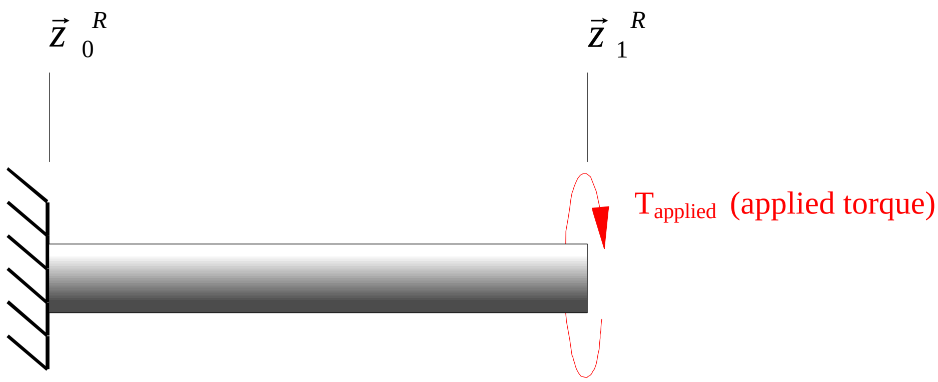

Figure 2.7: Fixed-Free Shaft with Static Load

$$TM_{global} = \begin{bmatrix} 1 & 0 & 0 \\ 0 & 1 & -T_{applied} \\ 0 & 0 & 1 \end{bmatrix} \cdot \begin{bmatrix} 1 & \frac{l}{JG} & 0 \\ 0 & 1 & 0 \\ 0 & 0 & 1 \end{bmatrix} \tag{2.12}$$

Carrying out the matrix multiplication in Equation (2.12) the following expression can be derived:

$$\begin{Bmatrix} \theta \\ T \\ 1 \end{Bmatrix}_1^R = \begin{bmatrix} 1 & \frac{l}{JG} & 0 \\ 0 & 1 & -T_{applied} \\ 0 & 0 & 1 \end{bmatrix} \cdot \begin{Bmatrix} \theta \\ T \\ 1 \end{Bmatrix}_0^R \tag{2.13}$$

Since the left end of the shaft is fixed, $\theta_0^R = 0$. It is also known that $T_1^R = 0$ since the right end is unrestrained (free). Applying those boundary conditions, Equation (2.13) can be reduced to the following two equations:

$$\theta_1^R = \frac{T_0^R l}{JG} \tag{2.14}$$

$$T_0^R = T_{applied} \tag{2.15}$$

Equation (2.14) provides the solution for the displacement of the right end of the shaft due to the applied load. More complicated problems can be solved in the same manner.

For the more general forced-response case where the excitation varies with some known frequency, the analysis is performed in much the same way. However, in this case it is known that a linear system will oscillate at the same frequency as the excitation. Therefore, the excitation frequency is substituted as the oscillating frequency of the system into the transfer matrices which represent mass elements such as the transfer matrix for a lumped inertia shown in Equation (2.6). The global transfer matrix is then assembled in the usual manner and the unknowns in the left-hand-state vector are solved for as was demonstrated in the static case.

2.4 Free-Vibration Analysis of Simple Torsional Systems

In free-vibration analysis the goal is to determine system natural frequencies and mode shapes. The transfer matrix method for determining a system's torsional natural frequencies involves:

- building the global transfer matrix
- applying the boundary conditions to eliminate unknowns in the global matrix equations
- finding the frequencies of vibration which make a solution to the matrix equation possible

The mode shapes corresponding to the natural frequencies can be found by making an arbitrary assumption about the unknown values of the state at the left end of the system and then calculating the other displacements and torques of the system relative to the assumed values at the left end. This yields an arbitrarily scaled eigenvalue or mode shape.

To demonstrate the procedures described above, consider the problem of determining the natural frequencies and mode shapes of the system shown in Figure 2.8 which consists of a massless, elastic shaft and a lumped-inertia fixed on the left end and unrestrained on the right end. Noting that the transfer matrix for this system will be the same as for that shown in Figure 2.6, the global system equations can be determined by carrying out the matrix multiplication specified in Equation (2.8).

$$\begin{Bmatrix} \theta \\ T \end{Bmatrix}_1^R = \begin{bmatrix} 1 & \dfrac{l}{JG} \\ -I\omega^2 & 1-(I\omega^2)\left(\dfrac{l}{JG}\right) \end{bmatrix} \cdot \begin{Bmatrix} \theta \\ T \end{Bmatrix}_0^R \tag{2.16}$$

Next, the boundary conditions can be applied to eliminate unknowns from Equation (2.16). Since the left end is fixed, $\theta_0^R = 0$, and since the right end is unrestrained, $T_1^R = 0$. Those values can be inserted into Equation (2.16) and the matrix equation can be broken into its two component equations, Equation (2.17) and Equation (2.18).

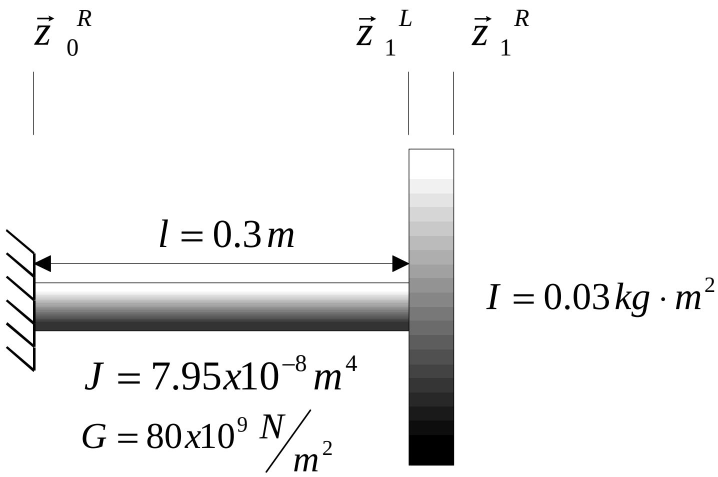

Figure 2.8: Shaft-Disk System Fixed on the Left End

$$\theta_1^R = \frac{T_0^R l}{JG} \tag{2.17}$$

$$0 = T_0^R \left\langle 1 - (I\omega^2)\left(\frac{l}{JG}\right)\right\rangle \tag{2.18}$$

In order for a non-zero solution to exist for these equations, the characteristic equation of the system, shown in Equation (2.19), must be true.

$$1 - (I\omega^2)\left(\frac{l}{JG}\right) = 0 \tag{2.19}$$

Typically, the frequencies, ω, which cause the expression on the left-hand-side of Equation (2.19) to equal zero are found by plotting the function

$$f(\omega) = 1 - (I\omega^2)\left(\frac{l}{JG}\right) \tag{2.20}$$

over a range of frequencies. The points where the function crosses the zero-axis can be shown to be the natural frequencies of the system. Using the definition of the variables shown in Figure 2.8, a plot of the characteristic determinant for the example problem is generated as shown in Figure 2.9. By examining the plot of the function over a smaller range than is shown in Figure 2.9 or by implementing a root search routine it can be determined that the natural frequency of the system is 840.63 rad/sec. The same procedure can be used to determine the natural frequencies of more complicated systems. For this simple system, Equation (2.19) can be rearranged as shown in Equation (2.21) to check that the natural frequency found from the determinant plot is accurate.

$$\omega = \sqrt{\frac{J \cdot G}{l \cdot I}} = \sqrt{\frac{(7.95\,x10^{-8}\,m^4)(80\,x10^9\,Pa)}{(0.3\,m)(0.03\,kg \cdot m^2)}} = 840.63\ {}^{rad}\!/_{\sec} \tag{2.21}$$

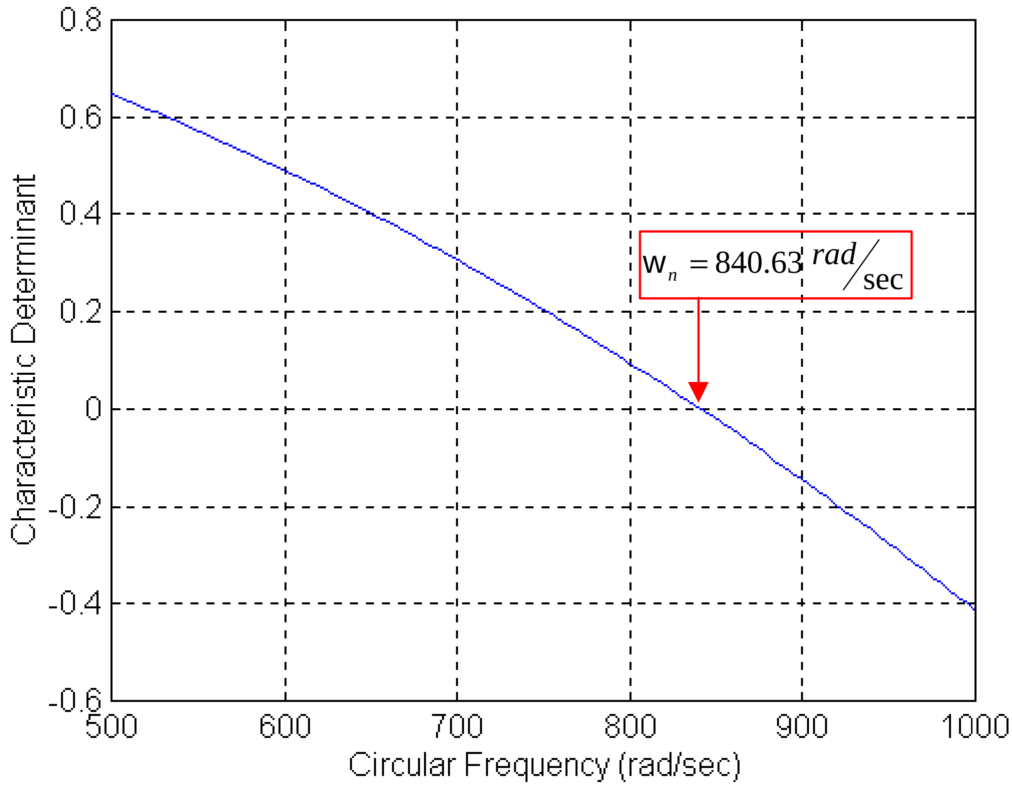

Figure 2.9: Characteristic Determinant of Shaft-Disk System

The mode shape for the system can be determined by assigning a value of one newton-meter to the unknown, T_0^R. The displacement, q_1^R, can then be calculated to be 4.716x10^{-5} radians using Equation (2.17). For more complicated systems determining the mode shapes is slightly more involved. Once values have been assigned to the unknowns of the left-hand state, the elemental transfer matrices can be used to transfer the state to the opposite side of each element. In the process, those states can be recorded and plotted to show the relative magnitudes of the displacements and torques along the length of the model.

2.5 Visco-elastic Absorber/Damper Transfer Matrix

An effective means of alleviating some torsional vibration problems involves the use of a vibration absorber or damper[29]. One category of such devices is composed of an auxiliary mass, referred to here as the seismic mass, that is coupled to the main system by some elastic and/or viscous medium as depicted in Figure 2.10(a). Such devices can include tuned and untuned absorbers as well as viscous damping devices sometimes referred to as Houdaille dampers. Tuned absorbers which have negligible damping are sometimes employed to shift the system's natural frequencies or to provide an anti-resonance at a particular frequency. Untuned absorbers which have a significant amount of damping are often used to reduce amplitude levels over a wider range of frequencies than tuned absorbers. Houdaille dampers serve as devices for dissipating vibratory energy.

Doughty[30] provides a derivation of the transfer matrix for this type of element. The derivation is begun by first applying Newton's second law to the main damper mass shown on the left in Figure 2.10(b).

$$\sum T = I_D \ddot{\theta}_D^L \tag{2.22}$$

$$T_D^R - T_D^L + k(\theta_S - \theta_D^R) + c(\dot{\theta}_S - \dot{\theta}_D^R) = I_D \ddot{\theta}_D^L \tag{2.23}$$

The damper mass is assumed to be a rigid disk. Therefore, the deflection on the left of the disk is equal to the deflection on the right as expressed below.

$$\theta_D^R = \theta_D^L \tag{2.24}$$

The velocities on opposite sides of the rigid disk will also be equivalent.

$$\dot{\theta}_D^R = \dot{\theta}_D^L \tag{2.25}$$

By substituting Equations (2.24) and (2.25) into Equation (2.23) and rearranging terms the following expression for the torque on the right side of the disk can be written.

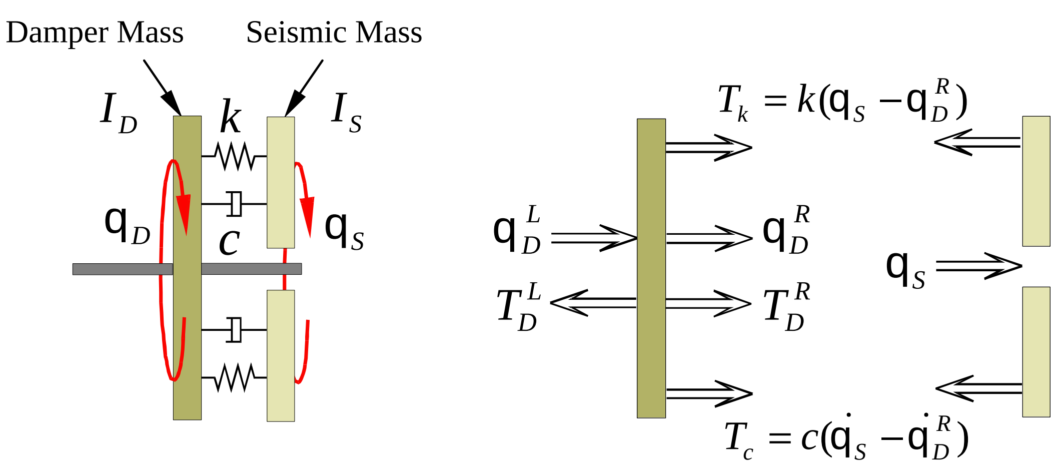

(a) Schematic **(b) Free-Body Diagram**

Figure 2.10: Torsional Visco-elastic Absorber/Damper

$$T_D^R = T_D^L + I_D \ddot{\theta}_D^L - k(\theta_S - \theta_D^L) - c(\dot{\theta}_S - \dot{\theta}_D^L) \tag{2.26}$$

By assuming that the motion of the damper is harmonic (oscillating sinusoidally with frequency ω) the velocity and acceleration of the damper can be expressed in terms of the damper displacement:

$$\theta_D^L = \bar{\theta}_D^L e^{j\omega t} \tag{2.27}$$

$$\dot{\theta}_D^L = j\omega\bar{\theta}_D^L e^{j\omega t} = j\omega\theta_D^L \tag{2.28}$$

$$\ddot{\theta}_D^L = -\omega^2\bar{\theta}_D^L e^{j\omega t} = -\omega^2\theta_D^L \tag{2.29}$$

Similarly, by assuming the motion of the seismic mass is harmonic, the velocity and the acceleration of the seismic mass can be written in terms of the displacement as:

$$\dot{\theta}_S = j\omega\theta_S \tag{2.30}$$

$$\ddot{\theta}_S = -\omega^2\theta_S \tag{2.31}$$

Substituting the expressions for velocity and acceleration in terms of displacement into Equation (2.26) results in the following expression:

$$T_D^R = T_D^L - I_D\omega^2\theta_D^L - k(\theta_S - \theta_D^L) - j\omega c(\theta_S - \theta_D^L) \tag{2.32}$$

To determine the relationship between θ_S and θ_D^L Newton's second law can be applied to the seismic mass:

$$\sum T = I_S\ddot{\theta}_S \tag{2.33}$$

$$-k(\theta_S - \theta_D^R) - c(\dot{\theta}_S - \dot{\theta}_D^R) = I_S\ddot{\theta}_S \tag{2.34}$$

Substituting Equation (2.24) and Equation (2.25) into Equation (2.34),

$$-k(\theta_S - \theta_D^L) - c(\dot{\theta}_S - \dot{\theta}_D^L) = I_S\ddot{\theta}_S \tag{2.35}$$

Next by substituting the expressions for velocity and acceleration written in terms of displacement and rearranging terms, the following expression is obtained:

$$\theta_S = \frac{k + j\omega c}{k + j\omega c - I_S\omega^2}\theta_D^L \tag{2.36}$$

By substituting Equation (2.36) into Equation (2.32) and rearranging terms the following expression can be written:

$$T_D^R = T_D^L + \left(k + j\omega c - I_D\omega^2 + \frac{(k + j\omega c)^2}{(k + j\omega c - I_S\omega^2)}\right)\theta_D^L \tag{2.37}$$

Finally, by writing Equation (2.24) and Equation (2.37) in matrix form the global transfer matrix can be expressed as:

$$\begin{Bmatrix} \theta_D^R \\ T_D^R \end{Bmatrix} = \begin{bmatrix} 1 & 0 \\ k + j\omega c - I_D\omega^2 + \dfrac{(k + j\omega c)^2}{(k + j\omega c - I_S\omega^2)} & 1 \end{bmatrix} \cdot \begin{Bmatrix} \theta_D^L \\ T_D^L \end{Bmatrix} \tag{2.38}$$

2.6 Pendulum Absorber Transfer Matrix

The pendulum absorber is another useful device for alleviating some torsional vibration problems. One of the unique features of the pendulum absorber is that its natural frequency is directly proportional to the rotational speed of the shaft on which it is employed. That feature is especially useful in such systems as internal combustion engines where some of the periodic torsional excitations within the system occur at specific multiples of the running speed.[31]

The transfer matrix for the pendulum absorber can be determined by making use of previously developed expressions for a pendulum absorber. Equation (2.39) is adapted from an expression given by Thomson and Dahleh[32] that describes the torque, T, applied to the disk by the pendulum. Note that the symbol, *n*, represents the bulk rotational speed of the shaft in radians/sec and ω represents the frequency of torsional oscillation also in radians/sec.

$$T = -\omega^2 \left[\frac{m(R+r)^2}{1 - r\omega^2 / Rn^2} \right] \cdot \theta_P^L \tag{2.39}$$

Applying Newton's second law to the disk to which the pendulum absorber is attached results in the following equation:

$$T_P^R - T_P^L - \omega^2 \left[\frac{m(R+r)^2}{1 - r\omega^2 / Rn^2} \right] \cdot \theta_P^L = -I\omega^2 \theta_P^L \tag{2.40}$$

Rearranging Equation (2.40),

$$T_P^R = T_P^L - \omega^2 \left(I + \left[\frac{m(R+r)^2}{1 - r\omega^2 / Rn^2} \right] \right) \theta_P^L \tag{2.41}$$

The pendulum disk is assumed to be rigid such that:

$$\theta_P^R = \theta_P^L \tag{2.42}$$

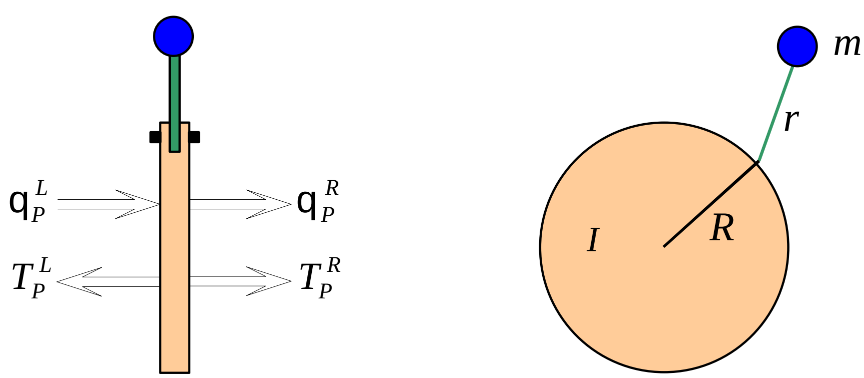

(a) Free-Body Diagram **(b) Parameters**

Figure 2.11: Pendulum Absorber

Writing Equation (2.41) and Equation (2.42) in matrix form leads to the transfer matrix for the pendulum absorber.

$$\begin{Bmatrix} \theta_P^R \\ T_P^R \end{Bmatrix} = \begin{bmatrix} 1 & 0 \\ -\omega^2\left(I + \left[\dfrac{m(R+r)^2}{1 - r\omega^2/Rn^2}\right]\right) & 1 \end{bmatrix} \cdot \begin{Bmatrix} \theta_P^L \\ T_P^L \end{Bmatrix} \tag{2.43}$$

2.7 Generalized Method for Applying Boundary Conditions to a Single-Shaft Model

As mentioned in the literature review, Pilkey and Chang[33] provide a generalized technique for applying the boundary conditions to single-shaft torsional systems. This technique is useful for computer-program applications of the transfer matrix method, and its extension to multi-shaft models will be demonstrated in Section 3.5. To help explain this technique a special notation is adopted here.

$$\vec{z} = \begin{Bmatrix} \theta \\ T \\ \hdashline 1 \end{Bmatrix} = \begin{Bmatrix} z(1) \\ z(2) \\ \hdashline 1 \end{Bmatrix} \tag{2.44}$$

Using this notation the global transfer matrix equation can be written as:

$$\begin{Bmatrix} z(1) \\ z(2) \\ \hdashline 1 \end{Bmatrix}_{right\,end} = \left[\begin{array}{cc:c} TM(1,1) & TM(1,2) & TM(1,3) \\ TM(2,1) & TM(2,2) & TM(2,3) \\ \hdashline 0 & 0 & 1 \end{array}\right] \cdot \begin{Bmatrix} z(1) \\ z(2) \\ \hdashline 1 \end{Bmatrix}_{left\,end} \tag{2.45}$$

The boundary condition on the left end of the model can be defined by $z(i)_{left\,end} = 0$, where i = 1 or 2. Similarly the boundary condition on the right end of the model can be defined by $z(j)_{right\,end} = 0$ where j = 1 or 2. The definitions of i and j are also shown in Table 2.1. For the forced-response case the value of the unknown left-end state variable, $z(3 - i)_{left\,end}$, must be determined. This can be done with the following equation written in terms of i and j:

$$z(3-i)_{left\,end} = \frac{-TM(j,3)}{TM(j,3-i)} \tag{2.46}$$

For the case of a free-vibration analysis it is necessary to apply the boundary conditions to determine the characteristic equation for the system. This characteristic equation can be defined by:

$$TM(j,3-i) = 0 \tag{2.47}$$

Table 2.1: Definition of Variables *i* and *j* For Use in the Generalized Method of Applying the Boundary Conditions, adapted from Pilkey and Chang[34]

Right End → / Left End ↓	**Fixed:** $z(1)_{\text{right end}} = 0$	**Free:** $z(2)_{\text{right end}} = 0$
Fixed: $z(1)_{\text{left end}} = 0$	$i = 1$ $j = 1$	$i = 1$ $j = 2$
Free: $z(2)_{\text{left end}} = 0$	$i = 2$ $j = 1$	$i = 2$ $j = 2$

Chapter 3. Multi-Rotor Transfer Matrix Technique

3.1 Expanded, Multi-Rotor Transfer Matrices

As mentioned in the Literature Review, an effective method for modeling torsional systems with multiple shafts involves using a multi-rotor transfer matrix technique developed by Mitchell[35]. That technique involves expanding the transfer matrix to keep track of the states of all shafts simultaneously. The numbering convention used here for the states of multi-shaft models involves adding the shaft number to the subscript as shown here: $\vec{z}^{\,L\,(Left)\,or\,R\,(Right)}_{Po\mathrm{int}\,Number\,,Shaft\,Number}$. To examine the concept of keeping track of the states for multiple shafts simultaneously, consider the system shown in Figure 3.1 which consists of two massless shafts that are not connected. The global transfer matrix for this system can be built by assembling the individual expanded transfer matrices. The transfer matrix equation relating the state on the right side of Shaft 1 to the state on its left end is given by:

$$\begin{Bmatrix} q^{L}_{1,1} \\ T^{L}_{1,1} \\ q^{R}_{0,2} \\ T^{R}_{0,2} \end{Bmatrix} = \begin{bmatrix} 1 & \left(\frac{l}{JG}\right)_{Shaft\,1} & 0 & 0 \\ 0 & 1 & 0 & 0 \\ 0 & 0 & 1 & 0 \\ 0 & 0 & 0 & 1 \end{bmatrix} \cdot \begin{Bmatrix} q^{R}_{0,1} \\ T^{R}_{0,1} \\ q^{R}_{0,2} \\ T^{R}_{0,2} \end{Bmatrix} = TM_{Shaft\,1} \cdot \begin{Bmatrix} q^{R}_{0,1} \\ T^{R}_{0,1} \\ q^{R}_{0,2} \\ T^{R}_{0,2} \end{Bmatrix} \tag{3.1}$$

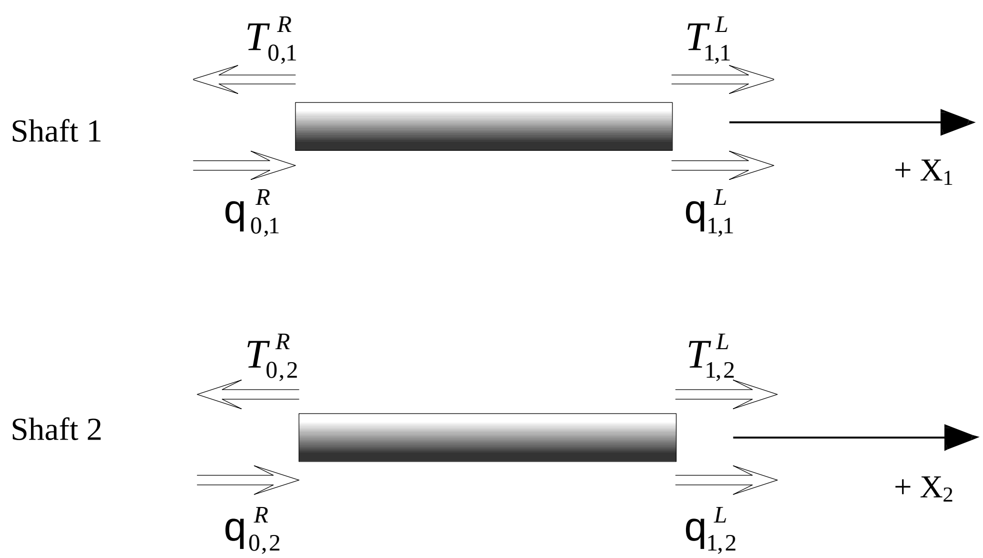

Figure 3.1: Two-Shaft Torsional System

The matrix equation relating the states to the left and right of Shaft 2 can be written as follows:

$$\begin{Bmatrix} q_{1,1}^{L} \\ T_{1,1}^{L} \\ q_{1,2}^{L} \\ T_{1,2}^{L} \end{Bmatrix} = \begin{bmatrix} 1 & 0 & 0 & 0 \\ 0 & 1 & 0 & 0 \\ 0 & 0 & 1 & \left(\dfrac{l}{JG}\right)_{Shaft\,2} \\ 0 & 0 & 0 & 1 \end{bmatrix} \cdot \begin{Bmatrix} q_{1,1}^{L} \\ T_{1,1}^{L} \\ q_{0,2}^{R} \\ T_{0,2}^{R} \end{Bmatrix} = TM_{Shaft\,2} \cdot \begin{Bmatrix} q_{1,1}^{L} \\ T_{1,1}^{L} \\ q_{0,2}^{R} \\ T_{0,2}^{R} \end{Bmatrix} \tag{3.2}$$

The global transfer matrix can then be assembled by substituting Equation (3.1) into Equation (3.2).

$$TM_{Global} = TM_{Shaft\,2} \cdot TM_{Shaft1} \tag{3.3}$$

The simple example presented above demonstrates the method of expanding the transfer matrix and state vector to simultaneously model multiple rotors. This multi-rotor transfer matrix technique is needed for modeling systems that have multiple shafts that are coupled in some manner. The following sections will discuss methods for modeling torsional systems that are gear coupled.

3.2 Transfer Matrix for a Compliant Gear Mesh Connecting Two Shafts

It is common to find multi-shaft torsional systems that are connected by a pair of meshing spur gears as shown in Figure 3.2(a). The transfer matrix that relates the states on either side of a pair of meshed spur gears can be derived by first writing the equations that relate the displacements and torques shown in Figure 3.2(b). The force, $F_{Gear\ Mesh}$, applied to the tooth of the driven gear acts along the pressure line which is perpendicular to the base radius, r_b, as shown in Figure 3.3. Therefore, the following equations can be developed:

$$q_{1,1}^{R} = q_{1,1}^{L} \tag{3.4}$$

$$T_{1,1}^{R} = T_{1,1}^{L} + r_{b1,1} \cdot F_{Gear\ Mesh} \tag{3.5}$$

$$q_{1,1}^{R} = q_{1,1}^{L} \tag{3.6}$$

$$T_{1,2}^{R} = T_{1,2}^{L} + r_{b1,2} \cdot F_{Gear\ Mesh} \tag{3.7}$$

Note that at this point the inertia of the gears is neglected because only the gear mesh itself is being modeled. The gear inertias can be modeled with separate point matrices.

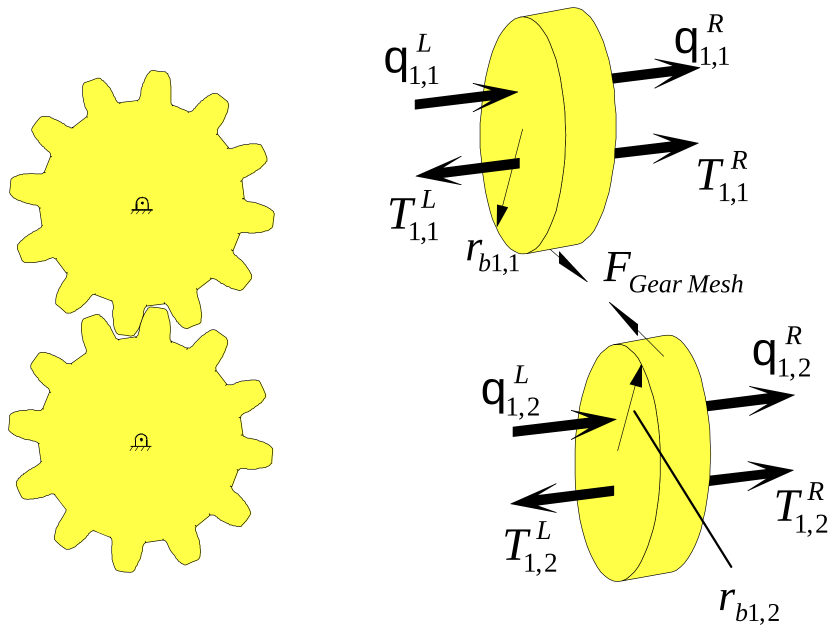

(a) Front View **(b) Free–Body Diagrams**

Figure 3.2: Two Meshing Spur Gears, adapted from Mitchell[36]

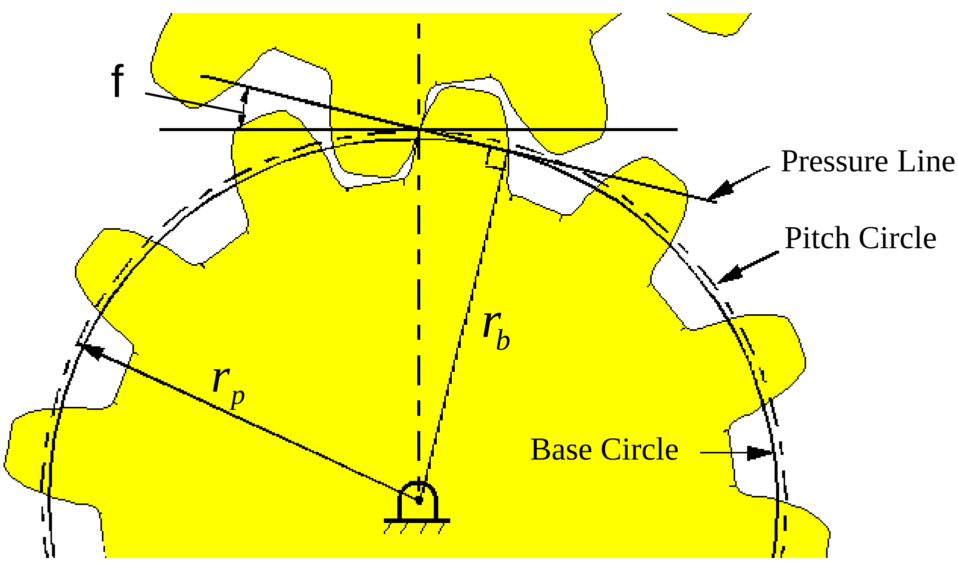

Figure 3.3: Spur Gear Terminology, adapted from Shigley and Mischke[37]

In this case the gear teeth on the spur gears connecting two shafts are modeled as having a constant linear stiffness as shown in Figure 3.4. An equivalent stiffness, K_e, for the gear mesh can be calculated as the series combination of $K_{T1,1}$ and $K_{T1,2}$ as shown in Equation (3.8).

$$K_e = \frac{K_{T1,1} \cdot K_{T1,2}}{K_{T1,1} + K_{T1,2}} \tag{3.8}$$

As mentioned in the Literature Review, several techniques are available for estimating this type of stiffness value for a gear tooth. The force on the gear teeth, $F_{Gear\ Mesh}$, can be defined in terms of the combined displacement of the two gear teeth, Δ.

$$F_{Gear\ Mesh} = K_e \cdot \Delta \tag{3.9}$$

$$\Delta = r_{b1,1} \cdot q_{1,1}^{L} + r_{b1,2} \cdot q_{1,2}^{L} \tag{3.10}$$

$$F_{Gear\ Mesh} = K_e \cdot (r_{b1,1} \cdot q_{1,1}^{L} + r_{b1,2} \cdot q_{1,2}^{L}) \tag{3.11}$$

By inserting Equation (3.11) into Equation (3.5) and Equation (3.7) and rearranging terms the following two equations result:

$$T_{1,1}^{R} = T_{1,1}^{L} + (r_{b1,1}{}^{2} \cdot K_e) \cdot q_{1,1}^{L} + (r_{b1,1} \cdot r_{b1,2} \cdot K_e) \cdot q_{1,2}^{L} \tag{3.12}$$

$$T_{1,2}^{R} = T_{1,2}^{L} + (r_{b1,1} \cdot r_{b1,2} \cdot K_e) \cdot q_{1,1}^{L} + (r_{b1,2}{}^{2} \cdot K_e) \cdot q_{1,2}^{L} \tag{3.13}$$

Equations (3.4), (3.6), (3.12), and (3.13) can be written in matrix form as:

$$\begin{Bmatrix} q_{1,1}^{R} \\ T_{1,1}^{R} \\ q_{1,2}^{R} \\ T_{1,2}^{R} \end{Bmatrix} = \begin{bmatrix} 1 & 0 & 0 & 0 \\ r_{b1,1}{}^{2} \cdot K_e & 1 & r_{b1,1} \cdot r_{b1,2} \cdot K_e & 0 \\ 0 & 0 & 1 & 0 \\ r_{b1,1} \cdot r_{b1,2} \cdot K_e & 0 & r_{b1,2}{}^{2} \cdot K_e & 1 \end{bmatrix} \begin{Bmatrix} q_{1,1}^{L} \\ T_{1,1}^{L} \\ q_{1,2}^{L} \\ T_{1,2}^{L} \end{Bmatrix} \tag{3.14}$$

Equation (3.14) defines the transfer matrix for a flexible gear mesh.

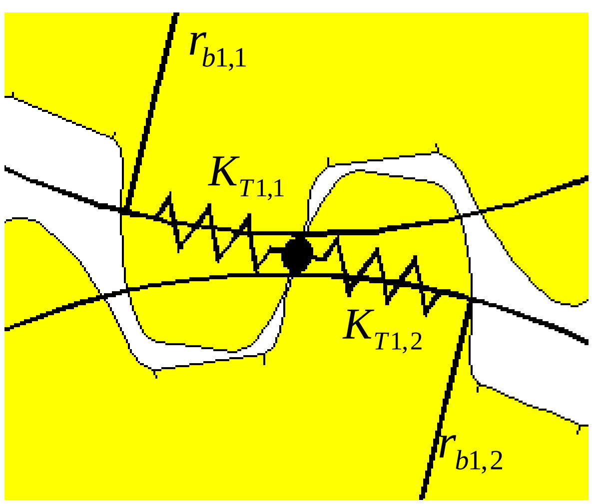

Figure 3.4: Linear Stiffness Representation of Meshing Spur Gear Teeth, adapted from Mitchell[38]

3.3 Planetary Gear Train Transfer Matrix

In order to obtain proper gear ratios in power transmission systems it is often advantageous to implement the use of planetary gear trains such as the one represented in Figure 3.5.[39] Modeling the torsional vibration characteristics of a system that includes one or more planetary gear trains can be a cumbersome task. If the modeling procedure involves the creation of a single-shaft equivalent model of the system, a significant amount of time must be spent performing equivalence calculations for the multiple components spinning at different speeds. Therefore, a multi-rotor transfer matrix technique that eliminates the need for equivalence calculations is ideally suited for such a task. As with the previously developed transfer matrix for a pair of meshing spur gears, the inertias of the gears can be modeled with separate point matrices. Thus, the matrix developed here transfers the state across the actual mesh of the gears (it doesn't include the gear inertias).

The development of a multi-rotor transfer matrix for a planetary gear train is begun here by examining the free-body diagram of the sun gear shown in Figure 3.6. Assuming the sun gear is a rigid disk with respect to its shaft attachment, the torsional displacements on either side of the sun gear will be equivalent.

$$\theta_S^R = \theta_S^L \tag{3.15}$$

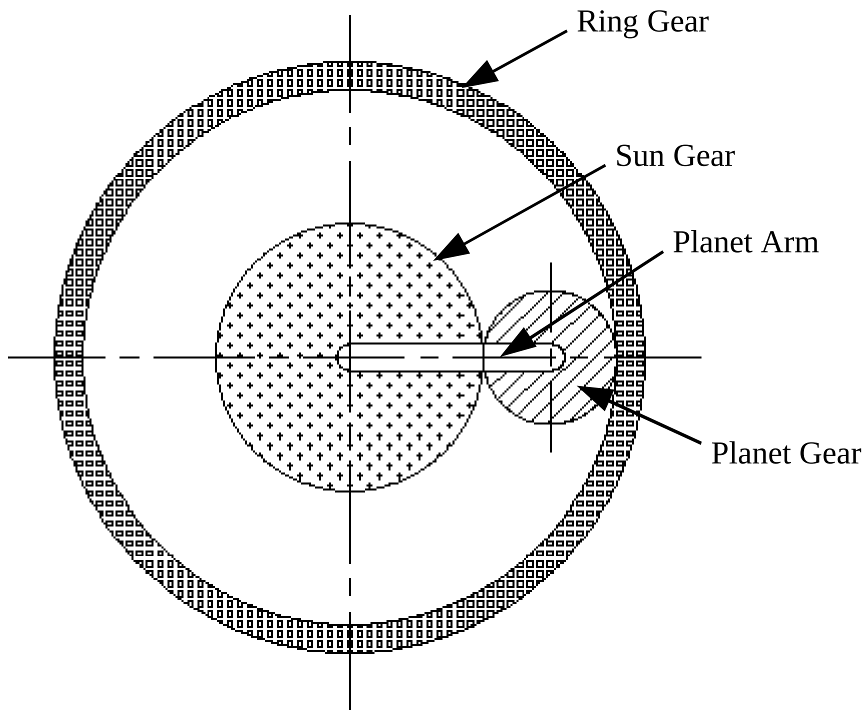

Figure 3.5: Planetary Gear Train

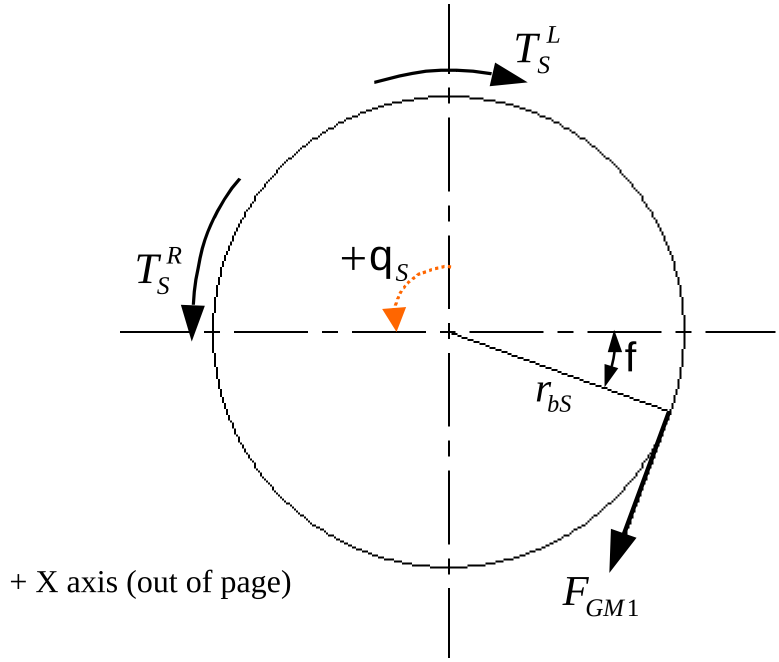

Figure 3.6: Free-Body Diagram of the Sun Gear

The torque equilibrium equation can be written as:

$$T_S^R = T_S^L + r_{bS} F_{GM1} \tag{3.16}$$

The free-body diagram of the planet gear is shown in Figure 3.7. The planet gear body is assumed to be rigid. Thus, the displacements on either side of the gear are equal as shown in Equation (3.17).

$$\theta_P^R = \theta_P^L \tag{3.17}$$

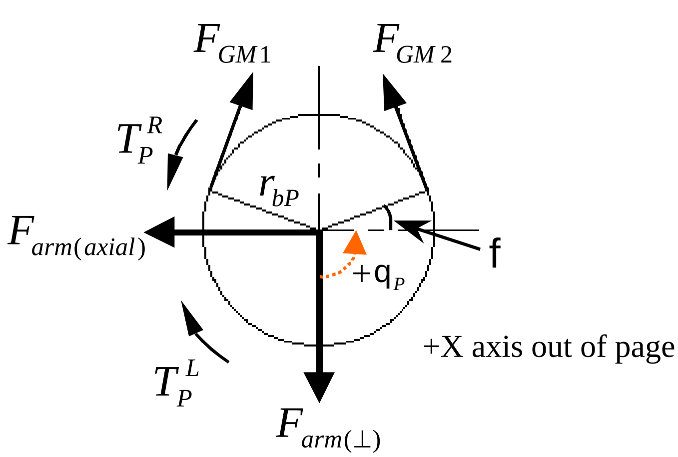

Figure 3.7: Free-Body Diagram of the Planet Gear

The torque equilibrium equation for the planet gear can be written as:

$$T_P^R = T_P^L + r_{bP} F_{GM1} - r_{bP} F_{GM2} \tag{3.18}$$

The equations that describe the relationship of the states on opposite sides of the planet arm can be developed by examining the free-body diagram shown in Figure 3.8. It is assumed that the planet arm is rigid such that,

$$q_A^R = q_A^L \tag{3.19}$$

The torque equilibrium equation for the planet arm is

$$T_A^R = T_A^L - r_{arm} F_{arm(\perp)} \tag{3.20}$$

Next, the equations governing the motion of the ring gear are developed by examining the free-body diagram shown in Figure 3.9. The assumption is made that the displacements on either side of the ring gear are equivalent.

$$q_R^R = q_R^L \tag{3.21}$$

The torque equilibrium equation for this gear can be written as:

$$T_R^R = T_R^L + r_{bR} F_{GM2} \tag{3.22}$$

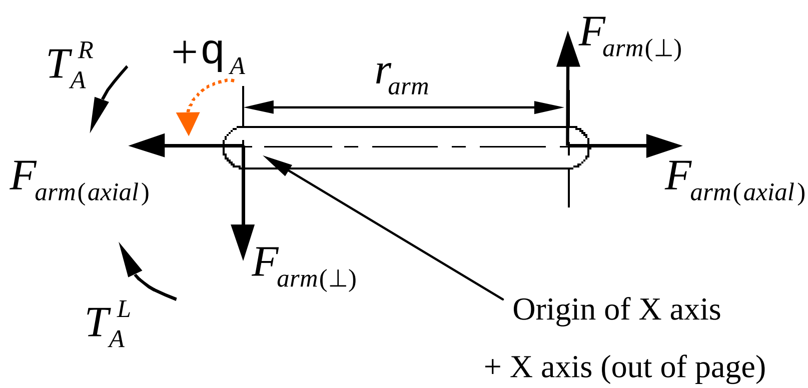

Figure 3.8: Free-Body Diagram of the Planet Arm

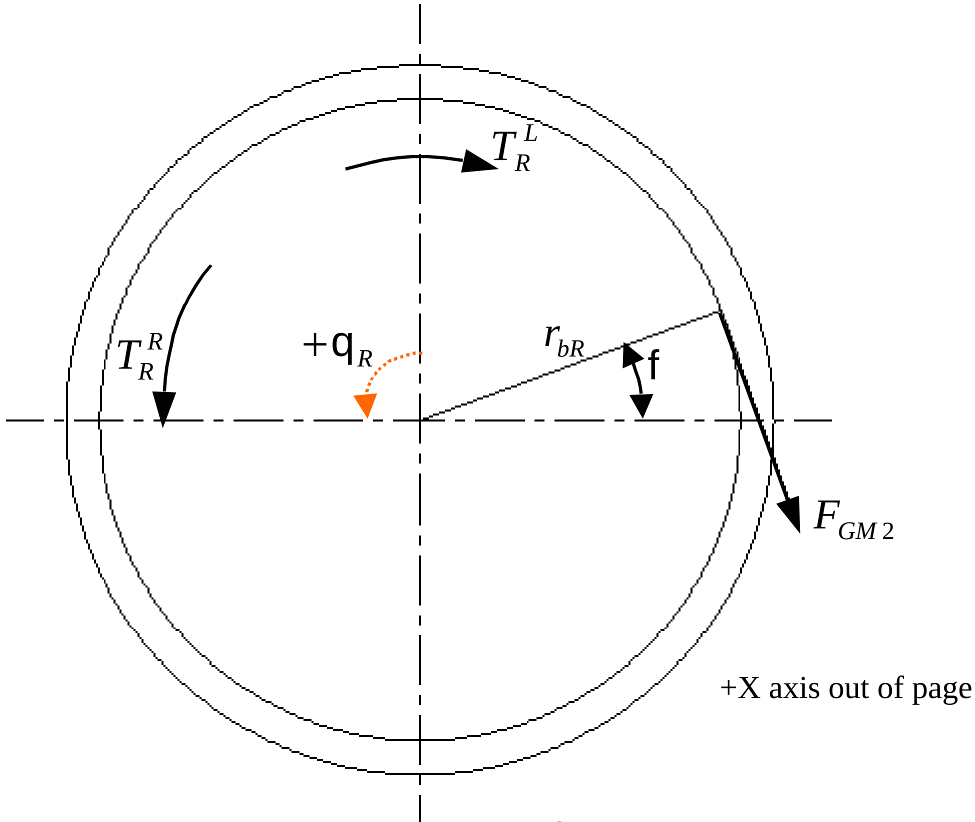

Figure 3.9: Free-Body Diagram of the Ring Gear

At this point, the equations for transferring the state across the planetary gear train mesh have been written, but the values of F_{GM1}, F_{GM2}, and $F_{arm(\perp)}$ have not yet been defined in terms of the state on the left side of the mesh. The meshing gear teeth in the planetary gear train will be treated as having a constant linear stiffness. This will allow the unknown forces F_{GM1}, F_{GM2}, and $F_{arm(\perp)}$ to be defined in terms of the torsional displacements of the gear train components. K_{e1}, the stiffness of the gear mesh between the sun and planet gears, will be equivalent to the series combination of the stiffness of a sun gear tooth, K_{TS}, and the stiffness of a planet gear tooth, K_{TP}.

$$K_{e1} = \frac{K_{TS} \cdot K_{TP}}{K_{TS} + K_{TP}} \tag{3.23}$$

Similarly, the stiffness of the gear mesh between the planet gear and the ring gear, K_{e2}, is defined as the series combination of the planet gear tooth stiffness and the stiffness of a ring gear tooth, K_{TR}.

$$K_{e2} = \frac{K_{TP} \cdot K_{TR}}{K_{TP} + K_{TR}} \tag{3.24}$$

The force, F_{GM1}, can be defined in terms of the combined linear displacement, Δ_1, of the sun gear tooth and the planet gear tooth.

$$F_{GM1} = K_{e1} \cdot \Delta_1 \tag{3.25}$$

Assuming that the torsional displacements of the sun gear, planet gear, and planet arm are small, Δ_1 can be defined as:

$$\Delta_1 = r_{bS} \cdot \theta_S^L \ + \ r_{bP} \cdot \theta_P^L \ - \ r_{bS} \cdot \theta_A^L \tag{3.26}$$

Substituting Equation (3.26) into Equation (3.25)

$$F_{GM1} = K_{e1} \cdot \left(r_{bS} \cdot \theta_S^L \ + \ r_{bP} \cdot \theta_P^L \ - \ r_{bS} \cdot \theta_A^L \right) \tag{3.27}$$

The force, F_{GM2}, can be defined in terms of the combined linear displacement, Δ_2, of the planet gear tooth and the ring gear tooth.

$$F_{GM2} = K_{e2} \cdot \Delta_2 \tag{3.28}$$

Assuming that the torsional displacements of the sun gear, planet gear, and planet arm are small, Δ_2 can be defined as:

$$\Delta_2 = r_{bR} \cdot \theta_R^L \ - \ r_{bP} \cdot \theta_P^L \ - \ r_{bR} \cdot \theta_A^L \tag{3.29}$$

Substituting Equation (3.29) into Equation (3.28)

$$F_{GM2} = K_{e2} \cdot \left(r_{bR} \cdot \theta_R^L \ - \ r_{bP} \cdot \theta_P^L \ - \ r_{bR} \cdot \theta_A^L \right) \tag{3.30}$$

The equilibrium equation for the forces on the planet gear in the direction perpendicular to the planet arm can be written to define the equation for $F_{arm(\perp)}$.

$$F_{arm(\perp)} = F_{GM1} \cos\phi \ + \ F_{GM2} \cos\phi \tag{3.31}$$

Substituting Equation (3.27) and Equation (3.30) into Equation (3.31),

$$F_{arm(\perp)} = \left[K_{e1} r_{bS} \theta_S^L + K_{e1} r_{bP} \theta_P^L - K_{e1} r_{bS} \theta_A^L + K_{e2} r_{bR} \theta_R^L - K_{e2} r_{bP} \theta_P^L - K_{e2} r_{bR} \theta_A^L \right] \cos\phi \tag{3.32}$$

Simplifying Equation (3.32),

$$F_{arm(\perp)} = \left[K_{e1} r_{bS} \theta_S^L + \left(K_{e1} - K_{e2} \right) r_{bP} \theta_P^L - \left(K_{e1} r_{bS} + K_{e2} r_{bR} \right) \theta_A^L + K_{e2} r_{bR} \theta_R^L \right] \cos\phi \tag{3.33}$$

The expressions for the forces, F_{GM1}, F_{GM2}, and $F_{arm(\perp)}$, that couple the planetary gear train components can now be substituted into the torque equations for each of the components. This is begun by substituting Equation (3.27) into Equation (3.16).

$$T_S^R = T_S^L + K_{e1} (r_{bS})^2 \theta_S^L + K_{e1} r_{bS} r_{bP} \theta_P^L - K_{e1} (r_{bS})^2 \theta_A^L \tag{3.34}$$

Substituting Equation (3.27) and Equation (3.30) into Equation (3.18) results in the following expression:

$$\begin{aligned} T_P^R = {} & T_P^L + K_{e1} r_{bS} r_{bP} \theta_S^L + \left(K_{e1} + K_{e2} \right) (r_{bP})^2 \theta_P^L \\ & + \left(K_{e2} r_{bR} - K_{e1} r_{bS} \right) r_{bP} \theta_A^L - K_{e2} r_{bP} r_{bR} \theta_R^L \end{aligned} \tag{3.35}$$

Equation (3.33) is substituted into Equation (3.20).

$$T_A^R = T_A^L + [-K_{e1} r_{bS} \theta_S^L + (K_{e2} - K_{e1}) r_{bP} \theta_P^L \\ + (K_{e1} r_{bS} + K_{e2} r_{bR}) \theta_A^L - K_{e2} r_{bR} \theta_R^L] r_{arm} \cos\phi \tag{3.36}$$

It is known that r_{arm} must equal the sum of the pitch radii of the sun gear and the planet gear. It is also known that the relationship between the base radius of a gear and pitch radius is given as:

$$r_b = r_{pitch} \cos\phi \tag{3.37}$$

Therefore, the following expression can be shown to be true:

$$r_{arm} \cos\phi = r_{bS} + r_{bP} \tag{3.38}$$

Equation (3.38) is now substituted into Equation (3.36).

$$T_A^R = T_A^L + [-K_{e1} r_{bS} \theta_S^L + (K_{e2} - K_{e1}) r_{bP} \theta_P^L \\ + (K_{e1} r_{bS} + K_{e2} r_{bR}) \theta_A^L - K_{e2} r_{bR} \theta_R^L]\{r_{bS} + r_{bP}\} \tag{3.39}$$

The expression for transferring the torque component of the state across the ring gear can be written by substituting Equation (3.30) into Equation (3.22).

$$T_R^R = T_R^L - K_{e2} r_{bP} r_{bR} \theta_P^L - K_{e2} (r_{bR})^2 \theta_A^L + K_{e2} (r_{bR})^2 \theta_R^L \tag{3.40}$$

The transfer matrix equation for the planetary gear mesh can now be written by writing Equations (3.15), (3.17), (3.19), (3.21), (3.34), (3.35), (3.36), and (3.40) in matrix form.

$$\begin{Bmatrix} \theta_S^R \\ T_S^R \\ \theta_P^R \\ T_P^R \\ \theta_A^R \\ T_A^R \\ \theta_R^R \\ T_R^R \end{Bmatrix} = \begin{bmatrix} 1 & 0 & 0 & 0 & 0 & 0 & 0 & 0 \\ u_1 & 1 & u_2 & 0 & u_3 & 0 & 0 & 0 \\ 0 & 0 & 1 & 0 & 0 & 0 & 0 & 0 \\ u_4 & 0 & u_5 & 1 & u_6 & 0 & u_7 & 0 \\ 0 & 0 & 0 & 0 & 1 & 0 & 0 & 0 \\ u_8 & 0 & u_9 & 0 & u_{10} & 1 & u_{11} & 0 \\ 0 & 0 & 0 & 0 & 0 & 0 & 1 & 0 \\ 0 & 0 & u_{12} & 0 & u_{13} & 0 & u_{14} & 1 \end{bmatrix} \cdot \begin{Bmatrix} \theta_S^L \\ T_S^L \\ \theta_P^L \\ T_P^L \\ \theta_A^L \\ T_A^L \\ \theta_R^L \\ T_R^L \end{Bmatrix} \tag{3.41}$$

Where

$$u_1 = K_{e1} \cdot (r_{bS})^2 \tag{3.42}$$

$$u_2 = K_{e1} \cdot r_{bS} \cdot r_{bP} \tag{3.43}$$

$$u_3 = -K_{e1} \cdot (r_{bS})^2 \tag{3.44}$$

$$u_4 = K_{e1} \cdot r_{bS} \cdot r_{bP} \tag{3.45}$$

$$u_5 = (K_{e1} + K_{e2})(r_{bP})^2 \tag{3.46}$$

$$u_6 = \left(K_{e2} \cdot r_{bR} - K_{e1} \cdot r_{bS}\right) \cdot r_{bP} \tag{3.47}$$

$$u_7 = -K_{e2} \cdot r_{bP} \cdot r_{bR} \tag{3.48}$$

$$u_8 = -K_{e1} \cdot r_{bS} \cdot \left(r_{bS} + r_{bP}\right) \tag{3.49}$$

$$u_9 = \left(K_{e2} - K_{e1}\right) \cdot r_{bP} \cdot \left(r_{bS} + r_{bP}\right) \tag{3.50}$$

$$u_{10} = \left(K_{e1} \cdot r_{bS} + K_{e2} \cdot r_{bR}\right) \cdot \left(r_{bS} + r_{bP}\right) \tag{3.51}$$

$$u_{11} = -K_{e2} \cdot r_{bR} \cdot \left(r_{bS} + r_{bP}\right) \tag{3.52}$$

$$u_{12} = -K_{e2} \cdot r_{bP} \cdot r_{bR} \tag{3.53}$$

$$u_{13} = -K_{e2} \cdot (r_{bR})^2 \tag{3.54}$$

$$u_{14} = K_{e2} \cdot (r_{bR})^2 \tag{3.55}$$

Equations (3.41) through (3.55) define the transfer matrix for the planetary gear mesh. That transfer matrix enables the creation of models with any number of planetary gear sets for static or dynamic analysis.

Care must be exercised in modeling the inertias of the planetary gear train components. Note from Figure 3.7 that the displacements of the planet gear shaft, θ_P, correspond to rotations about the central axis of the planet gear. The planet gear also revolves about the axis of the sun along with the planet arm. However, the displacements of the planet gear shaft, θ_P^L and θ_P^R, only represent the relative displacement of the planet gear with respect to its pivot on the planet arm. Therefore, special care must be taken in modeling the inertia of the planet gear. The inertia of the planet gear about the planet gear shaft's axis of rotation should be lumped on the planet gear shaft. The planet gear shaft's axis of rotation is labeled in Figure 3.10. However, the inertia of the planet gear about the rotational axis of the planet arm should be algebraically added to the inertia of the planet arm on the planet arm shaft. In other words, the inertial resistance to acceleration about the planet arm shaft's axis of rotation is equal to the total inertia of the planet arm and planet gear assembly about that axis. Wilson[40] and Nestorides[41] describe analytical and experimental methods for calculating these polar mass moments of inertia for a variety of different geometries. Those discussions include techniques for calculating the polar mass moment of inertia for a component whose axis of rotation does not pass through its center of gravity (i.e. the inertia of a planet gear about the axis of rotation of the planet arm.)

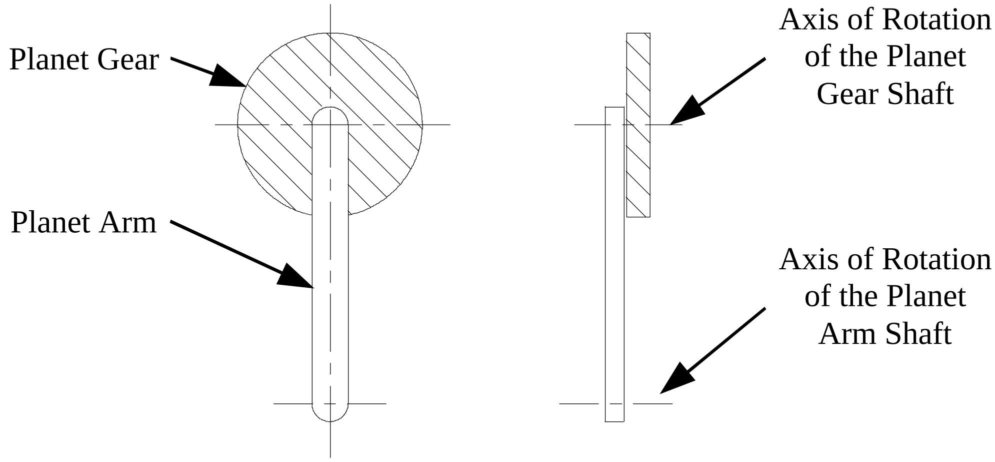

Figure 3.10: Axes of Rotation of the Planet Gear Shaft and the Planet Arm Shaft

3.4 Building the Global Transfer Matrix for a Multi-Shaft Model

A standard procedure for assembling the global transfer matrix for a multi-shaft system is demonstrated with an example system shown in Figure 3.11. $[F]_{i,j}$ is an expanded field matrix describing the properties of the i^{th} field section on shaft number *j*. Likewise $[P]_{i,j}$ represents an expanded point matrix for the i^{th} point on shaft *j*. $[GM]$ is a gear mesh transfer matrix that describes the connection of the two shafts. The gear mesh is defined as a point in the model on both shafts and the state vector at that point is labeled as $\vec{z}^{\,L(Left)\ or\ R(Right)}_{GM,\,Shaft\ Number}$.

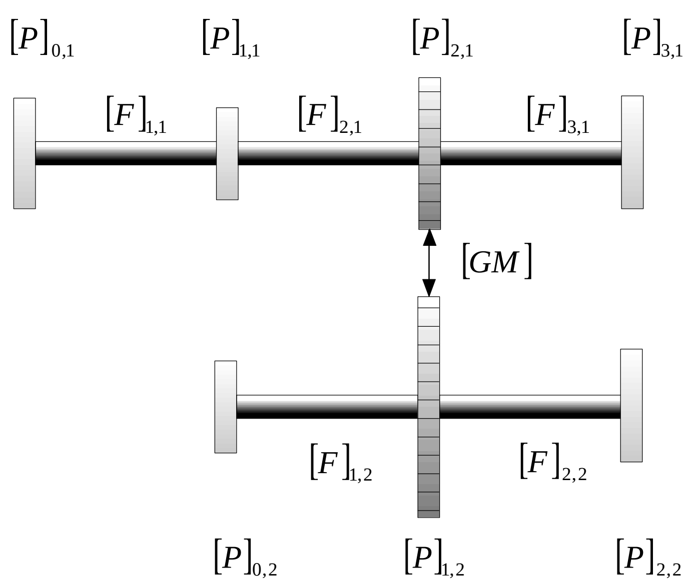

Figure 3.11: Elemental Transfer Matrices for a Geared, Two-Shaft Torsional System

The global transfer matrix assembly for this system can proceed by first transferring the state on the left end of the first shaft up to the gear mesh.

$$\begin{Bmatrix} \theta_{GM,1}^{L} \\ T_{GM,1}^{L} \\ \theta_{0,2}^{L} \\ T_{0,2}^{L} \end{Bmatrix} = [P]_{2,1}\cdot[F]_{2,1}\cdot[P]_{1,1}\cdot[F]_{1,1}\cdot[P]_{0,1}\cdot\begin{Bmatrix} \theta_{0,1}^{R} \\ T_{0,1}^{R} \\ \theta_{0,2}^{R} \\ T_{0,2}^{R} \end{Bmatrix} \tag{3.56}$$

The gear mesh transfer matrix should not be added to the global transfer matrix until the state on shaft 2 has been transferred up to the same point. This is accomplished by the following multiplication:

$$\begin{Bmatrix} \theta_{GM,1}^{L} \\ T_{GM,1}^{L} \\ \theta_{GM,2}^{L} \\ T_{GM,2}^{L} \end{Bmatrix} = [P]_{1,2}\cdot[F]_{1,2}\cdot[P]_{0,2}\cdot\begin{Bmatrix} \theta_{GM,1}^{L} \\ T_{GM,1}^{L} \\ \theta_{0,2}^{R} \\ T_{0,2}^{R} \end{Bmatrix} \tag{3.57}$$

Next, the state is transferred across the gear mesh.

$$\begin{Bmatrix} \theta_{GM,1}^{R} \\ T_{GM,1}^{R} \\ \theta_{GM,2}^{R} \\ T_{GM,2}^{R} \end{Bmatrix} = [GM]\begin{Bmatrix} \theta_{GM,1}^{L} \\ T_{GM,1}^{L} \\ \theta_{GM,2}^{L} \\ T_{GM,2}^{L} \end{Bmatrix} \tag{3.58}$$

The state can be transferred to the end of shaft 1 with the following equation.

$$\begin{Bmatrix} \theta_{3,1}^{R} \\ T_{3,1}^{R} \\ \theta_{GM,2}^{R} \\ T_{GM,2}^{R} \end{Bmatrix} = [P]_{3,1}\cdot[F]_{3,1}\cdot\begin{Bmatrix} \theta_{GM,1}^{R} \\ T_{GM,1}^{R} \\ \theta_{GM,2}^{R} \\ T_{GM,2}^{R} \end{Bmatrix} \tag{3.59}$$

The state can then be transferred to the end of shaft 2 as shown:

$$\begin{Bmatrix} \theta_{3,1}^{R} \\ T_{3,1}^{R} \\ \theta_{2,2}^{R} \\ T_{2,2}^{R} \end{Bmatrix} = [P]_{2,2}\cdot[F]_{2,2}\cdot\begin{Bmatrix} \theta_{3,1}^{R} \\ T_{3,1}^{R} \\ \theta_{GM,2}^{R} \\ T_{GM,2}^{R} \end{Bmatrix} \tag{3.60}$$

Finally the global transfer matrix can be assembled by combining Equations (3.56) through (3.60).

$$\mathrm{TM}_{\mathrm{global}} = [P]_{2,2}[F]_{2,2}[P]_{3,1}[F]_{3,1}[GM][P]_{1,2}[F]_{1,2}[P]_{0,2}[P]_{2,1}[F]_{2,1}[P]_{1,1}[F]_{1,1}[P]_{0,1} \tag{3.61}$$

3.5 Generalized Method for Applying Boundary Conditions to a Multi-Shaft Model

To determine the desired solution, the boundary conditions of the system must be applied to the global transfer matrix as was already demonstrated for single-shaft models. However, a multi-shaft system has more boundary conditions to be applied - the left and right end of each shaft is either fixed or free. Therefore, a method for applying these boundary conditions will first be demonstrated with a two-shaft example. Finally, the generalized procedure for applying the boundary conditions to a system with an arbitrary number of shafts will be presented.

To demonstrate the process of applying the boundary conditions to a multi-shaft system, consider performing a forced-response analysis for a two-shaft system having both shafts fixed on the left end and free on the right end with some intermediate loading. The global transfer matrix and the end state vectors for such a system can be written as

$$\begin{Bmatrix} q_{right,1} \\ 0 \\ q_{right,2} \\ 0 \\ \hdashline 1 \end{Bmatrix} = \left[\begin{array}{cccc:c} TM(1,1) & TM(1,2) & TM(1,3) & TM(1,4) & TM(1,5) \\ TM(2,1) & TM(2,2) & TM(2,3) & TM(2,4) & TM(2,5) \\ TM(3,1) & TM(3,2) & TM(3,3) & TM(3,4) & TM(3,5) \\ TM(4,1) & TM(4,2) & TM(4,3) & TM(4,4) & TM(4,5) \\ \hdashline 0 & 0 & 0 & 0 & 1 \end{array}\right] \cdot \begin{Bmatrix} 0 \\ T_{left,1} \\ 0 \\ T_{left,2} \\ \hdashline 1 \end{Bmatrix} \tag{3.62}$$

The second and fourth equations (the equations with a "0" in the vector on the left-hand side of the expression) in the matrix expression above can simplified to the following two equations:

$$TM(2,2)\cdot T_{left,1} + TM(2,4)\cdot T_{left,2} = -TM(2,5) \tag{3.63}$$

$$TM(4,2)\cdot T_{left,1} + TM(4,4)\cdot T_{left,2} = -TM(4,5) \tag{3.64}$$

This set of two equations and two unknowns can be solved for the remaining unknowns in the left-hand state vector, $T_{left,1}$ and $T_{left,2}$, using Cramer's Rule.

$$T_{left,1} = \frac{\begin{vmatrix} -TM(2,5) & TM(2,4) \\ -TM(4,5) & TM(4,4) \end{vmatrix}}{\begin{vmatrix} TM(2,2) & TM(2,4) \\ TM(4,2) & TM(4,4) \end{vmatrix}} \tag{3.65}$$

$$T_{left,2} = \frac{\begin{vmatrix} TM(2,2) & -TM(2,5) \\ TM(4,2) & -TM(4,5) \end{vmatrix}}{\begin{vmatrix} TM(2,2) & TM(2,4) \\ TM(4,2) & TM(4,4) \end{vmatrix}} \tag{3.66}$$

Similarly, torsional systems with *x* shafts will have *x* unknowns in the left-end state after applying the boundary conditions. For such a system, a set of *x* equations and *x* unknowns can be solved for the remaining unknowns using Cramer's Rule.

To determine the natural frequencies of the system with the global transfer matrix shown in Equation (3.62), it is necessary to determine the characteristic determinant of the system. The characteristic determinant can be found by first reasoning that loading terms (the terms in the fifth column of the global transfer matrix) will all be zero since this is a "free" vibration problem. The second and fourth equations from the matrix expression in Equation (3.62) can then be written as

$$TM(2,2) \cdot T_{left,1} + TM(2,4) \cdot T_{left,2} = 0 \tag{3.67}$$

$$TM(4,2) \cdot T_{left,1} + TM(4,4) \cdot T_{left,2} = 0 \tag{3.68}$$

In order that this system of equations has a non-zero solution, the determinant of the coefficients must equal zero as expressed in Equation (3.69).

$$\begin{vmatrix} TM(2,2) & TM(2,4) \\ TM(4,2) & TM(4,4) \end{vmatrix} = 0 \tag{3.69}$$

The determinant in Equation (3.69) is the characteristic determinant for this system, and finding the system's natural frequencies entails finding the roots of the characteristic equation formed by evaluating that determinant. For systems with more shafts, the size of the characteristic determinant grows, but the procedure for finding the natural frequencies is the same.

Next, the equations used for applying the boundary conditions to a system with an arbitrary number of shafts will be defined. To help explain this generalized technique the following notation will be adopted for the state vectors:

$$\vec{z} = \begin{Bmatrix} q_{left\ or\ right\ end,1} \\ T_{left\ or\ right\ end,1} \\ q_{left\ or\ right\ end,2} \\ T_{left\ or\ right\ end,2} \\ \vdots \\ q_{left\ or\ right\ end,x} \\ T_{left\ or\ right\ end,x} \\ 1 \end{Bmatrix} = \begin{Bmatrix} z(1)_{left\ or\ right\ end,1} \\ z(2)_{left\ or\ right\ end,1} \\ z(1)_{left\ or\ right\ end,2} \\ z(2)_{left\ or\ right\ end,2} \\ \vdots \\ z(1)_{left\ or\ right\ end,x} \\ z(2)_{left\ or\ right\ end,x} \\ 1 \end{Bmatrix} \tag{3.70}$$

This notation is similar to that used in Section 2.7 with the exception that the shaft number has been added to the subscript. Also note that here x is equal to the total number of shafts in the model and the "$2 \cdot x + 1$" column of the transfer matrix would contain any applied torques.

The left end boundary condition for each shaft in the model can be defined by $z(i_m)_{left\ end,\mathrm{m}} = 0$ where $i_m = 1$ or 2 and m is the number of the shaft. Similarly the boundary condition on the right end of each shaft can be defined by $z(j_m)_{right\ end,\ m} = 0$ where $j_m = 1$ or 2. For the forced-response case the values of the m unknown left-end state variables, $z(3 - i_m)_{left\ end,\ m}$, must be determined. This can be done for each shaft, *m*, by applying the following equation:

$$z(3-i_m)_{left\,end,m} = \frac{\det[A]}{\det[B]} \tag{3.71}$$

The matrix, $[B]$, is formed from the non-zero coefficients of the global matrix equations which have a zero in the state vector for the right side of the model. In the example presented at the beginning of this section Equations (3.63) and (3.64) are the equations from Equation (3.62) that have a zero state term in the state vector for the right side of the model. The transfer matrix columns for the non-zero coefficients in Equations (3.63) and (3.64) correspond to the non-zero rows in the state vector for the left side of the model. The zero state term in the right side state vector corresponding to shaft number *p* is located in row number $j_p + 2*p - 2$. This defines the corresponding global transfer matrix row numbers of terms in row *p* of matrix $[B]$. The non-zero state term in the left side state vector corresponding to shaft number *p* is located in row number $1 + 2*p - i_p$. This defines the corresponding global transfer matrix column numbers of terms in column *p* of matrix $[B]$. Therefore matrix $[B]$ can be defined as:

$$[B]=\begin{bmatrix} TM(j_1+2\cdot 1-2,1+2\cdot 1-i_1) & TM(j_1+2\cdot 1-2,1+2\cdot 2-i_2) & \cdots & TM(j_1+2\cdot 1-2,1+2\cdot x-i_x) \\ TM(j_2+2\cdot 2-2,1+2\cdot 1-i_1) & TM(j_2+2\cdot 2-2,1+2\cdot 2-i_2) & \cdots & TM(j_2+2\cdot 2-2,1+2\cdot x-i_x) \\ \vdots & \vdots & & \vdots \\ TM(j_x+2\cdot x-2,1+2\cdot 1-i_1) & TM(j_x+2\cdot x-2,1+2\cdot 2-i_2) & \cdots & TM(j_x+2\cdot x-2,1+2\cdot x-i_x) \end{bmatrix} \tag{3.72}$$

The matrix, $[A]$, is identical to matrix $[B]$ except that the m^{th} column is replaced by:

$$\begin{matrix} -TM(j_1+2\cdot 1-2,2\cdot x+1) \\ -TM(j_2+2\cdot 2-2,2\cdot x+1) \\ \vdots \\ -TM(j_x+2\cdot x-2,2\cdot x+1) \end{matrix} \tag{3.73}$$

For the case of a free-vibration analysis the characteristic equation can be defined by:

$$\det[B] = 0 \tag{3.74}$$

where $[B]$ is defined in Equation (3.72).

Chapter 4. *Torsion 1*: A Transfer Matrix Computer Program for Torsional Analysis

4.1 Introduction

An effective design tool for torsional analysis, *Torsion 1*, has been created using the Visual Basic 4.0 programming language. This program is capable of performing linear, forced-response and free-vibration analyses for a torsional system. Additional transfer matrices that have not been derived in this text but are used by *Torsion 1* are catalogued in Appendix A. The modeling and analysis capabilities of the program allow multi-shaft systems connected by meshing gears to be analyzed with ease. The Visual Basic 4.0 programming environment has been chosen because it allows the programmer to easily create an effective graphical user interface. Figure 4.1 shows the main program window as it appears when the program is first run.

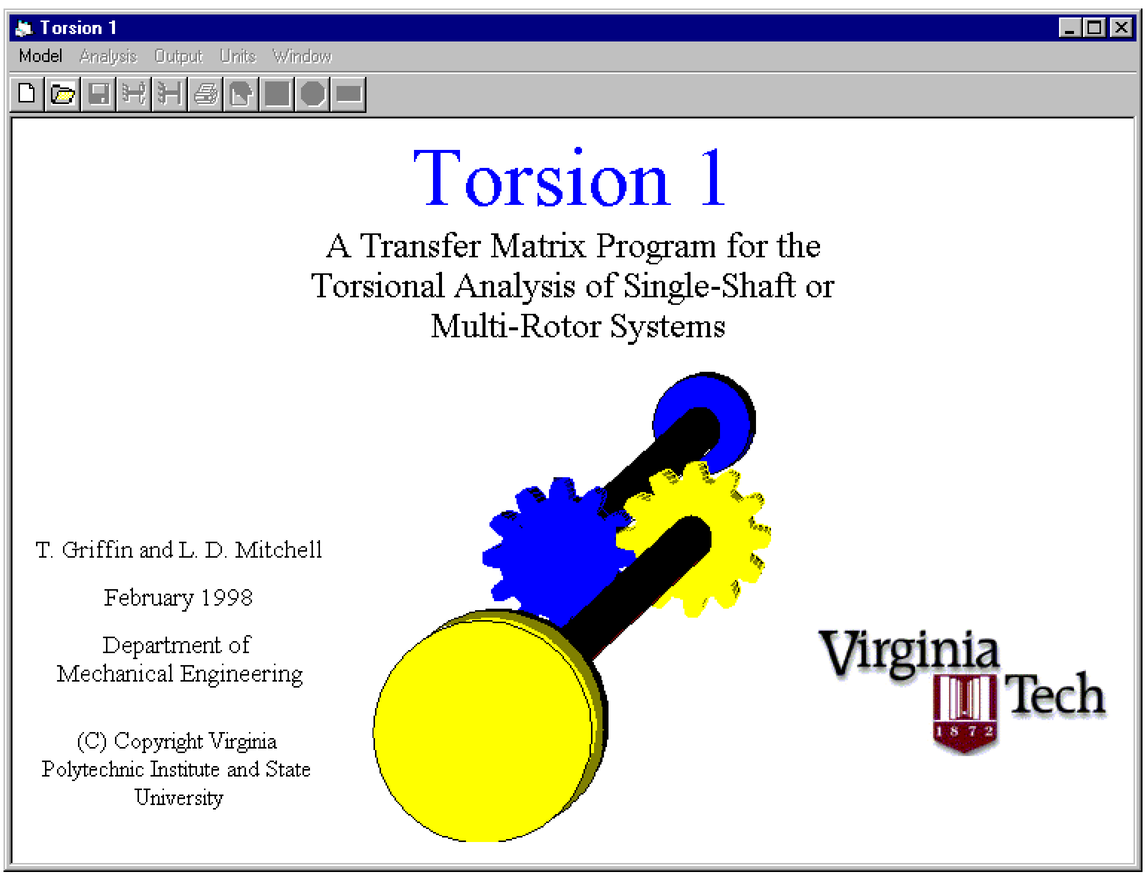

Figure 4.1: *Torsion 1* Title Screen

4.2 Organization of the Program

The bulk of the functionality for the program *Torsion 1* is accessed by the user from four basic forms. The organization and hierarchy of the forms within *Torsion 1* is depicted schematically in Figure 4.2. Note that the global interface for the program is a parent form. The parent form is the main window for a program within which the other program modules operate. Figure 4.3 is a picture of the global interface of *Torsion 1* with the three child forms open within the parent form. The global interface provides the program capabilities which are common to all the child forms such as sending output to the printer. The child forms which include the model editor, forced-response analysis module, and free-vibration analysis module perform the specific tasks for which they are named. The block in Figure 4.2 labeled "Public Code" represents the subroutines in the program which can be accessed by any of the program modules. The details of the parent form and the child forms within this program will be provided in the following sections.

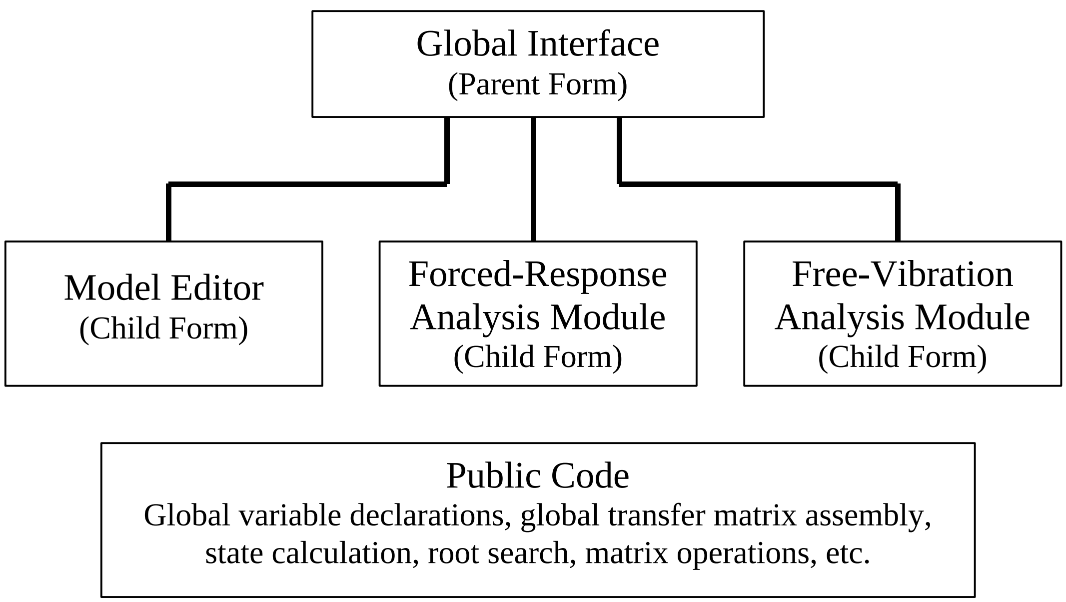

Figure 4.2: Schematic Diagram of *Torsion 1* Organization

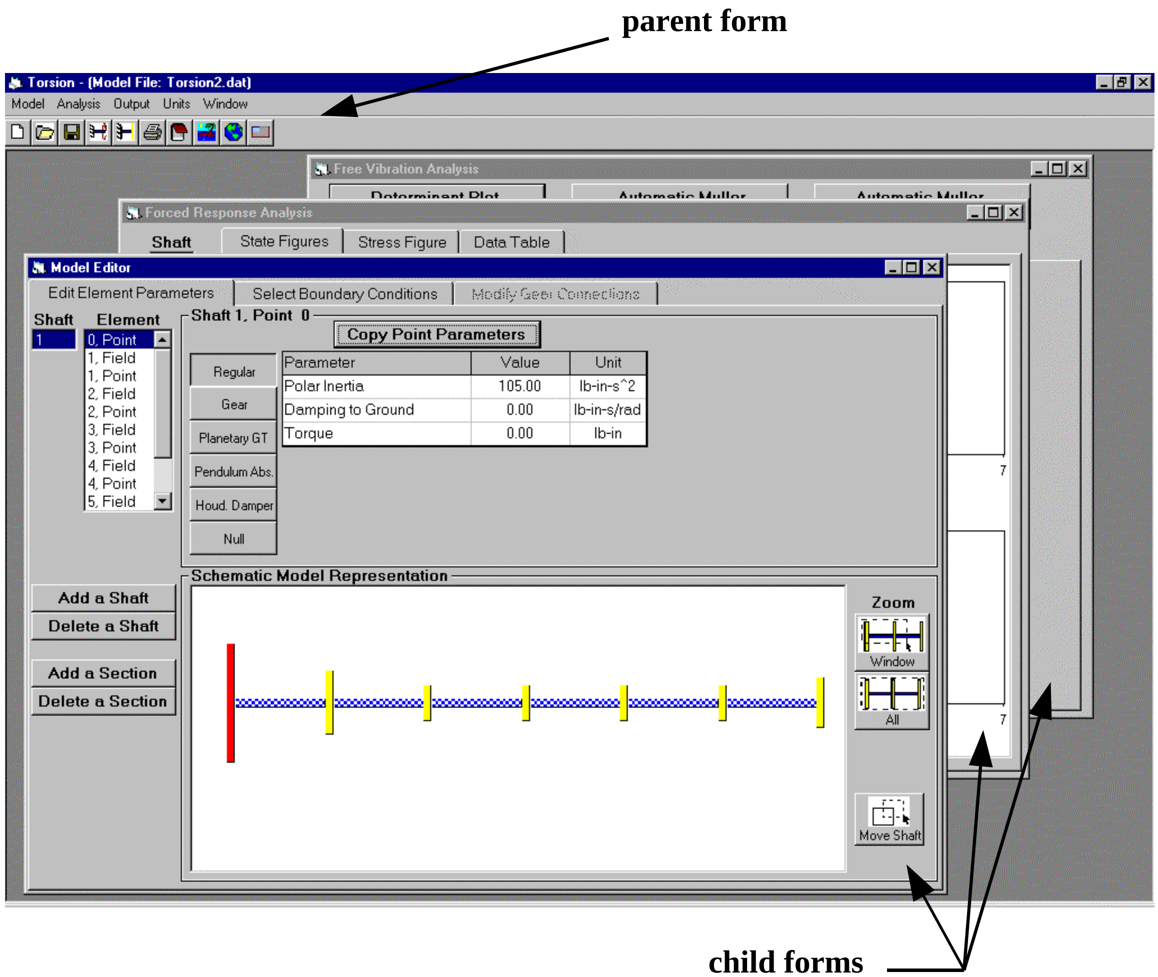

Figure 4.3: Parent Form/Child Form Hierarchy

4.3 Global Interface

The global interface for *Torsion 1* is the parent form depicted in Figure 4.3. Through the controls on the global interface the program user can save or load model parameters to or from a data file. The user can also choose to display one or more of the child forms or send analysis results to the printer or to a file. Another function of the controls on the global interface allows the user to change the system of units being used to model a system. The controls for the global interface include a menu and a toolbar, and they are located at the top, left corner of the form. Figure 4.4 shows a closer view of the menu and toolbar on the global interface.

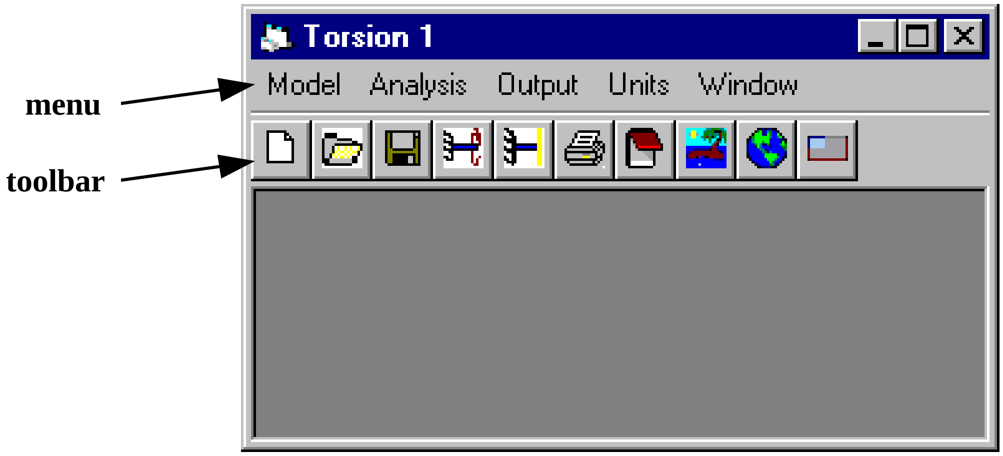

Figure 4.4: Global Interface Menu and Toolbar

When one of the menu options is selected by way of a mouse click, a second-level menu appears that provides the available options within the initially selected category. Selecting one of the second-level menu options initiates one of the functions of the global interface described in Table 4.1. The buttons in the toolbar provide the user with the ability to access the functions of the global interface more easily. Table 4.1 also shows the correspondence of the toolbar icons to the second-level menu options and the functions that can be accessed through them.

Table 4.1: Menu and Toolbar Functions

First-Level Menu	Second-Level Menu	Toolbar Icon	Function
Model			
	New	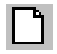	Open the Model Editor for a new model
	Load		Load an existing model from a data file
	Save		Save the current model parameters to a data file
Analysis			
	Forced-Response		Open the Forced-Response Analysis module
	Free-Vibration	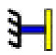	Open the Free-Vibration Analysis module
Output			
	Print		Print the image or text currently displayed
	Text File		Save results or model listing to a text file
	Bitmap Image		Save graphical display to a bitmap image
Units			
	SI	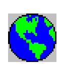	Convert to SI system of units
	English	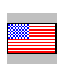	Convert to English Gravimetric system of units
Window			
	List of child forms that are currently open	(none)	Bring the selected child form to the front within the global interface and make it active (ready for input via the mouse or keyboard)

4.4 Model Editor

The Model Editor allows the user to create or edit the system model such that torsional analysis can be performed. Figure 4.5 shows the Model Editor open within the global interface. The controls on this form are grouped into three major categories: controls used to edit the element parameters, controls used to select the appropriate boundary conditions, and controls used to specify the nature of the gear connections in the model (if any exist). These controls are displayed on separate tabs (or pages) on the Model Editor form. Note that only one set of controls is displayed at a time. The user selects which set of controls is displayed by clicking on the appropriate tab label at the top of the Model Editor form.

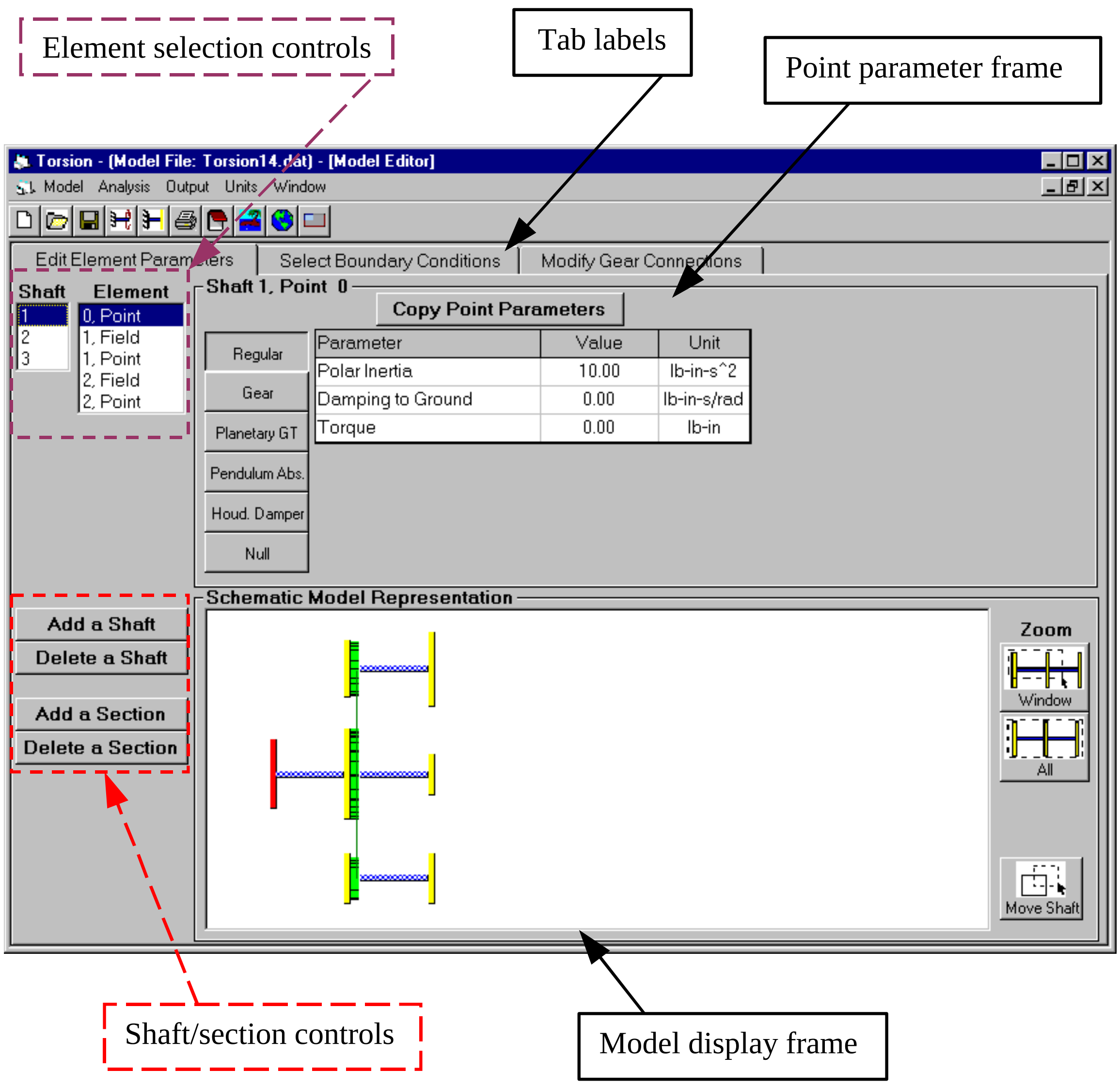

Figure 4.5: Model Editor Form, Edit Element Parameters Tab

The tab which has controls for editing the values of the element parameters is labeled “Edit Element Parameters” and is the selected tab in Figure 4.5. When modeling a system the user must edit one element at a time. The element selection controls shown in Figure 4.5 allow the user to specify which element in the model is to be edited. When the element selected is a point on the model the point parameter frame (a frame is a set of controls on a form bound by a black rectangle) appears. The controls on the point parameter frame display the pertinent values of the point parameters and allow those values to be changed. A similar field parameter frame appears in place of the point parameter frame whenever a field element is selected within the element selection controls. The shaft/section controls allow the user to change the number of shafts or field/point sections in the model. Finally, the model display frame shows a schematic representation of the model. This frame appears on all three tabs within the Model Editor, and the element, shaft, or gear connection that is selected appears highlighted in red. The controls on the model display frame allow the user to change the view in the display window and the relative positions of the shafts in the display.

One of the program options available on the point parameter frame is a tool window that can estimate the stiffness of a spur gear tooth based on standard gear dimensions provided by the user. The Gear Tooth Stiffness Estimator tool window is shown in Figure 4.6. This model uses an adapted version of the Daws’[42] model for calculating a tooth stiffness. Some additional assumptions have been made in using the equations presented by Daws such that a single, constant-stiffness estimate can be obtained for the gear tooth from a few basic parameters used to describe the spur gear (which can be seen in Figure 4.6). The assumptions used in conjunction with the equations listed in the Daws reference are presented here:

- The stiffness estimate is based on a model of the gear teeth in contact at their pitch point.
- The *addendum* and *dedendum* distances are assumed to match those for standard, coarse-pitch-involute spur gears as presented by Mabie and Reinholtz[43] :

$$addendum = \frac{1.000}{diametral\ pitch} \tag{4.1}$$

$$dedendum = \frac{1.250}{diametral\ pitch} \tag{4.2}$$

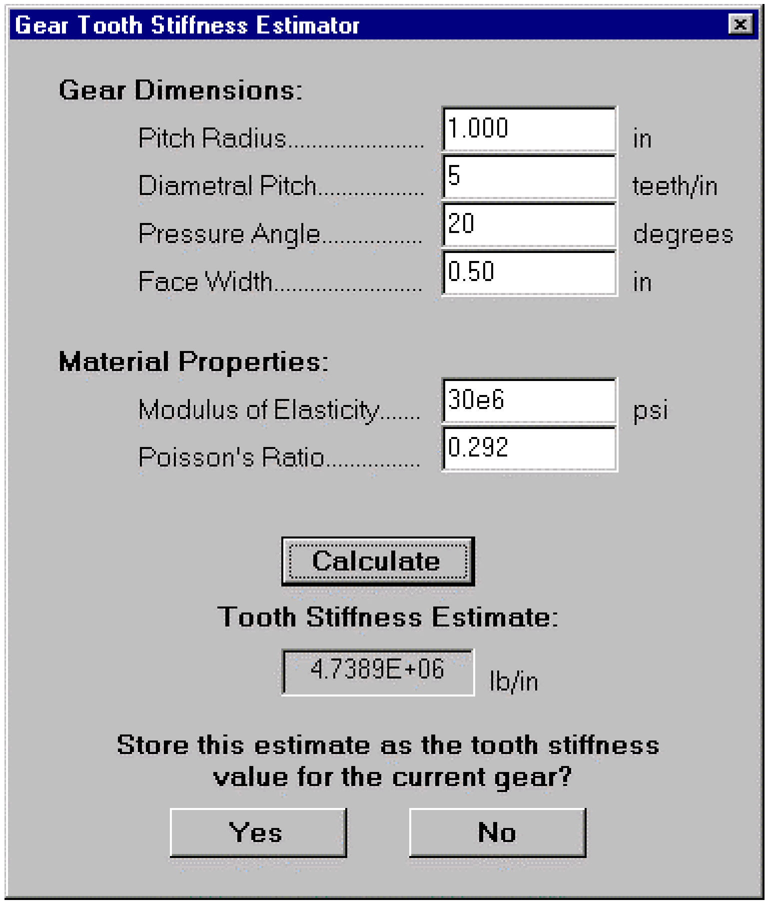

Figure 4.6: Gear Tooth Stiffness Estimator Tool Window

The tab on the Model Editor form which allows the user to select the boundary conditions for the model is labeled “Select Boundary Conditions”. The Select Boundary Conditions tab is the active tab in Figure 4.7. The shaft selection control on this tab allows the user to specify the shaft whose boundary conditions will be edited. The boundary condition frame contains controls which allow the user to specify whether the ends of the selected shaft are free or fixed.

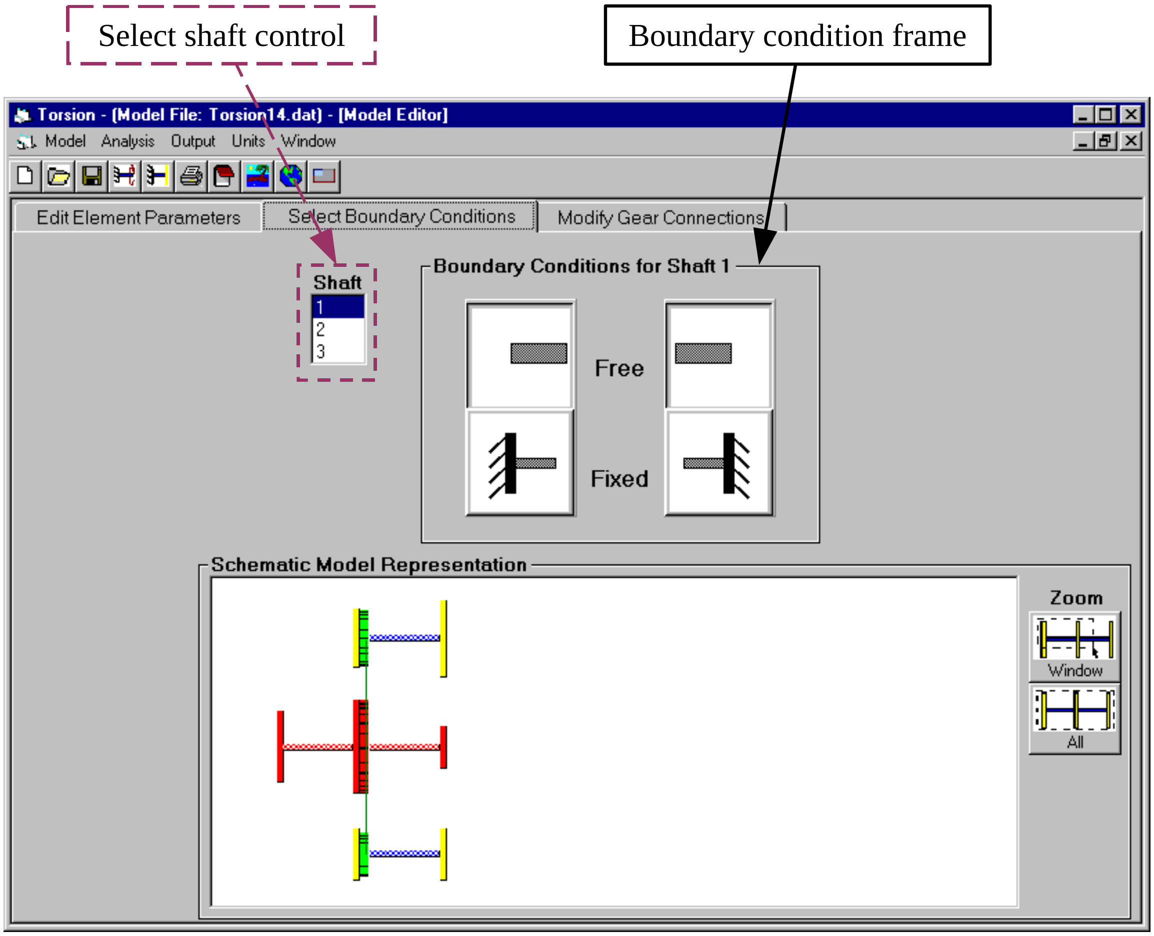

Figure 4.7: Model Editor Form, Select Boundary Conditions Tab

Finally, the Modify Gear Connections tab is shown in Figure 4.8. The controls on this tab allow the user to edit the gear connections within the system. The select gear mesh control allows the user to select one of the existing gear meshes as the active mesh. A description of the active mesh is provided in the gear mesh description frame. The add/delete gear mesh controls can be used to change the number and type of gear mesh connections. Whenever one of the add gear mesh controls is selected, the gear mesh connection frame appears. The controls on this frame can be used to specify the new gear connection to be added.

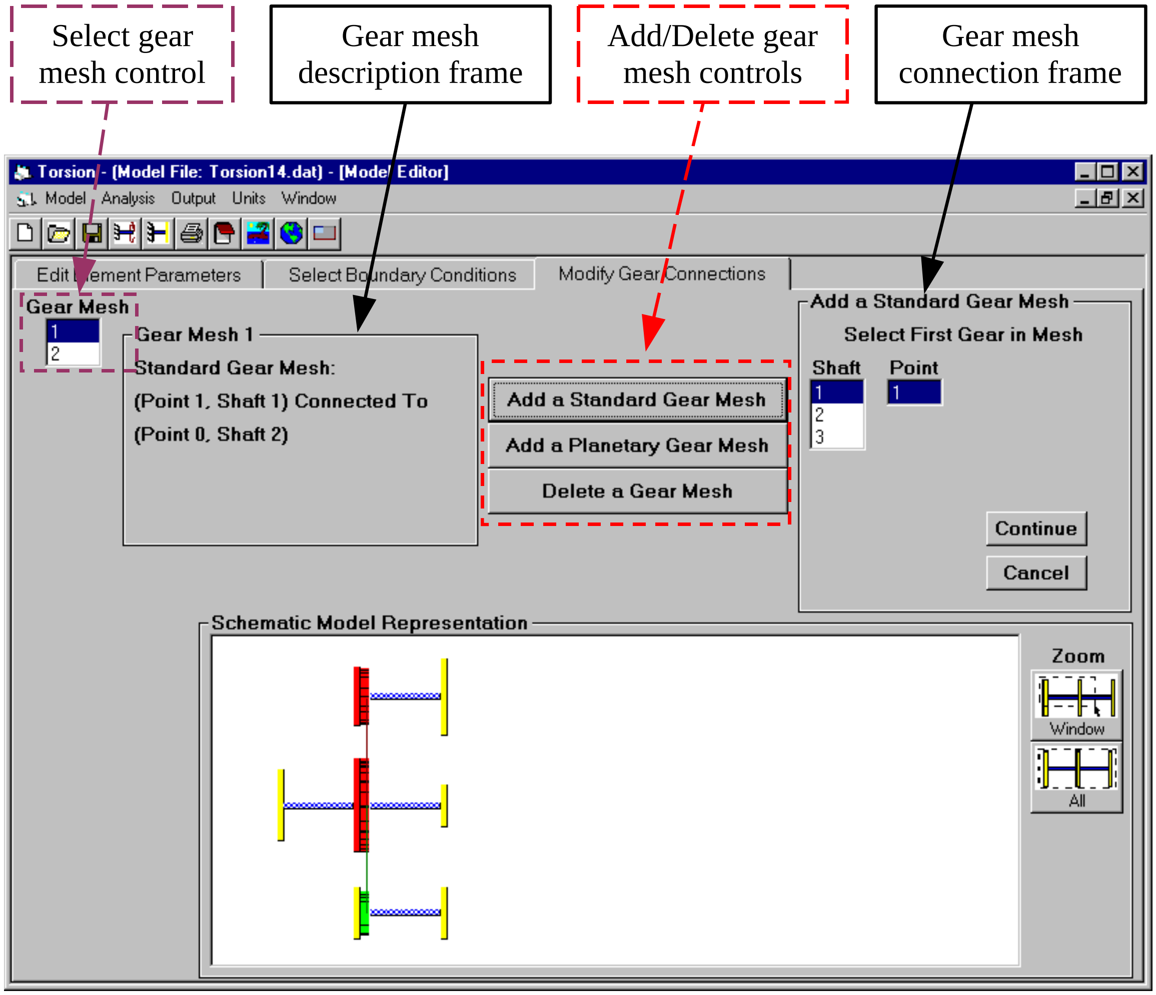

Figure 4.8: Model Editor Form, Modify Gear Connections Tab

4.5 Forced-Response Analysis Module

A static or dynamic forced-response analysis can be performed with the aid of the Forced-Response Analysis module of *Torsion 1*. The Forced-Response Analysis form is shown in Figure 4.9 with the State Figures tab active. Note that the controls on the left side of the form appear on the main form and not on any of the tabs. Thus, the controls on the left of the form can be accessed from any of the tabs. The shaft selection control allows the user to choose the shaft for which the response results will be displayed (the results are displayed for a single shaft at a time). The increment number controls are used to change the number of increments within each field section for which the state is calculated. The forcing frequency control is used to select the harmonic frequency for the loads whose magnitudes are specified on the Model Editor form. The user has the option of performing a damped or undamped analysis. This option is selected using the control at the bottom, left corner of the form. Note that the State Figures tab displays the displacement and internal torque results in graphical form. The Stress Figure tab, shown in Figure 4.10, provides a graphical representation of the stress analysis results. The displacement, torque, and stress results are all provided in tabular form on the Data Table tab shown in Figure 4.11.

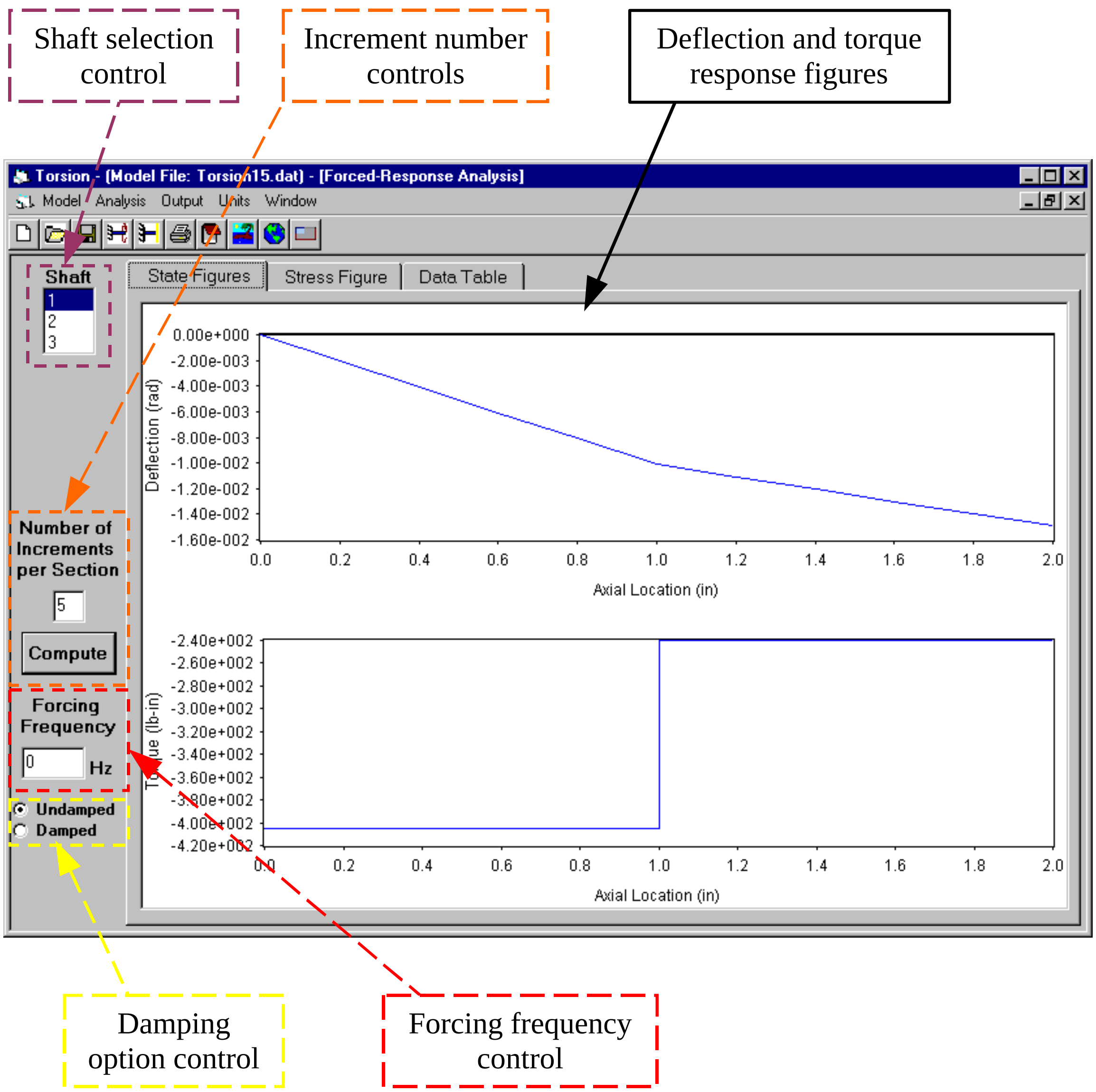

Figure 4.9: Forced-Response Analysis Form, State Figures Tab

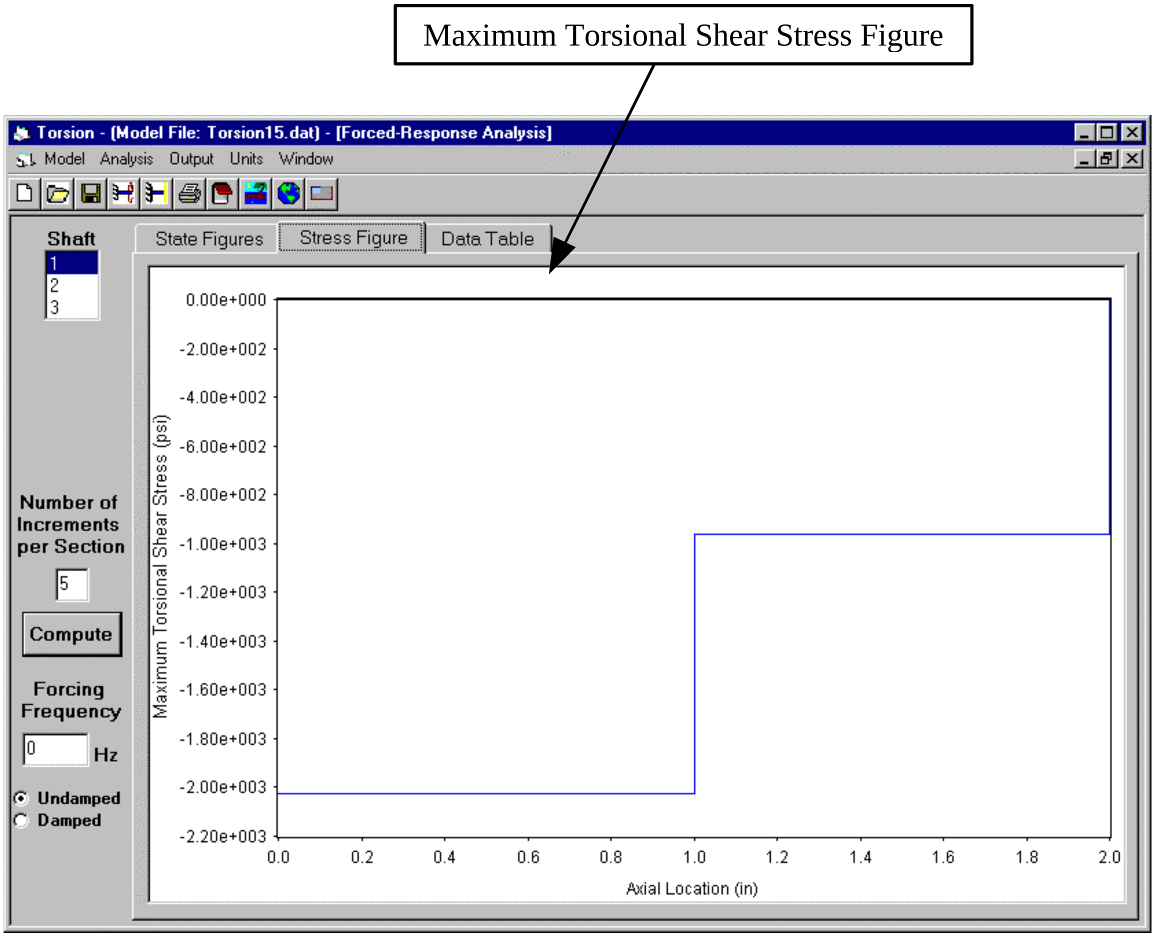

Figure 4.10: Forced-Response Analysis Form, Stress Figures Tab

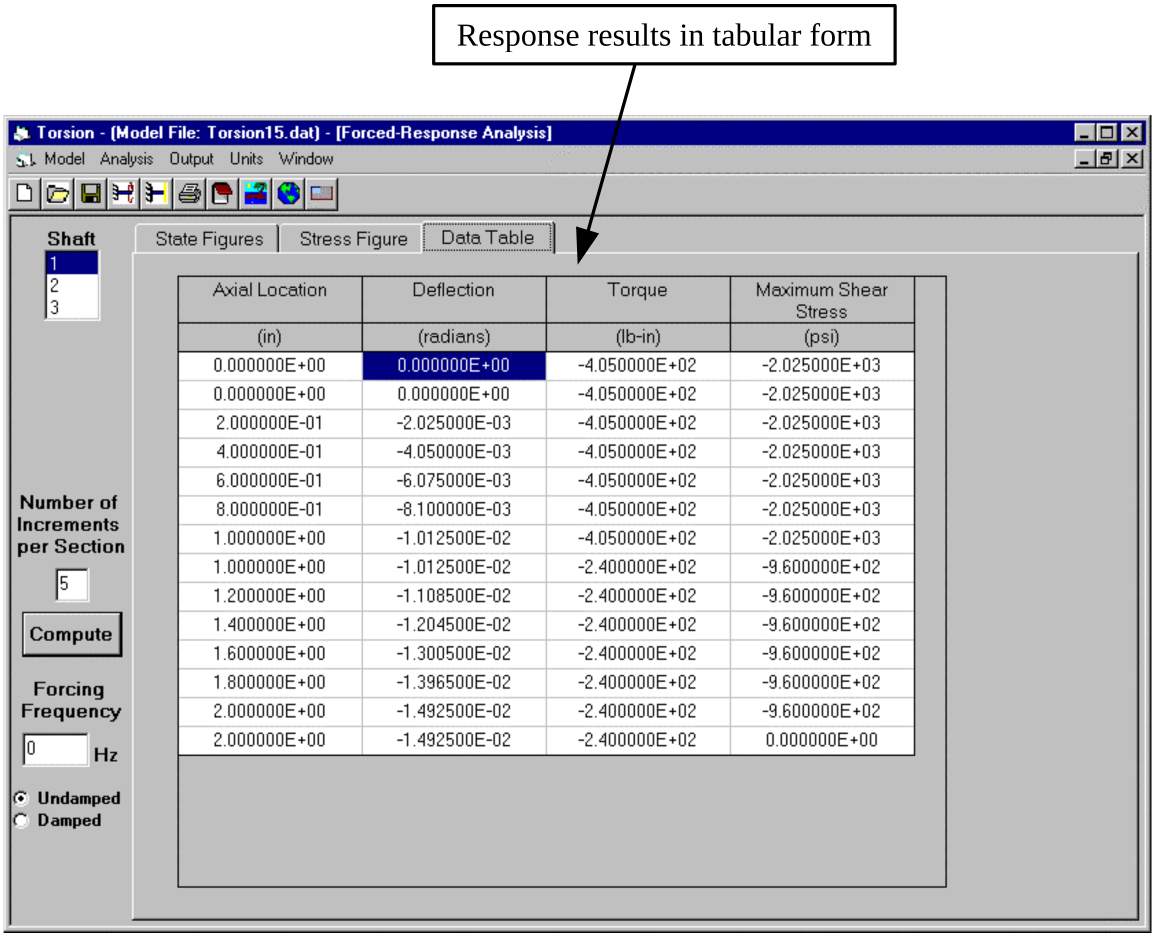

Axial Location (in)	Deflection (radians)	Torque (lb-in)	Maximum Shear Stress (psi)
0.000000E+00	0.000000E+00	-4.050000E+02	-2.025000E+03
0.000000E+00	0.000000E+00	-4.050000E+02	-2.025000E+03
2.000000E-01	-2.025000E-03	-4.050000E+02	-2.025000E+03
4.000000E-01	-4.050000E-03	-4.050000E+02	-2.025000E+03
6.000000E-01	-6.075000E-03	-4.050000E+02	-2.025000E+03
8.000000E-01	-8.100000E-03	-4.050000E+02	-2.025000E+03
1.000000E+00	-1.012500E-02	-4.050000E+02	-2.025000E+03
1.000000E+00	-1.012500E-02	-2.400000E+02	-9.600000E+02
1.200000E+00	-1.108500E-02	-2.400000E+02	-9.600000E+02
1.400000E+00	-1.204500E-02	-2.400000E+02	-9.600000E+02
1.600000E+00	-1.300500E-02	-2.400000E+02	-9.600000E+02
1.800000E+00	-1.396500E-02	-2.400000E+02	-9.600000E+02
2.000000E+00	-1.492500E-02	-2.400000E+02	-9.600000E+02
2.000000E+00	-1.492500E-02	-2.400000E+02	0.000000E+00

Figure 4.11: Forced-Response Analysis Form, Data Table Tab

4.6 Free-Vibration Analysis Module

The Free-Vibration Analysis form shown in Figures 4.12 through 4.15 can be used to determine the natural frequencies and modes shapes of a torsional system. The root-search controls at the top of the form allow the user to select the type of root search to be used in finding the natural frequencies. One of the options for finding the system natural frequencies is an automated Muller-Method root search for finding either damped or undamped roots. A second option for finding roots involves plotting the characteristic determinant curve for the system to visually approximate where the value of the determinant equals zero. This root approximation can be refined using a false position search routine. It should be noted that this second root-search option can only be used in finding the undamped natural frequencies.

The Eigenvalues tab of the Free-Vibration Analysis form, shown in Figure 4.12, displays the roots that have been found using the Muller-Method or false-position root searches. The Mode Shapes tab, which is shown in Figure 4.13, displays the arbitrarily scaled eigenvectors which correspond to the eigenvalues that have been found. The mode and shaft selection controls at the top, left corner of this tab allow the user to select the particular mode and shaft for which the eigenvector results are displayed. As was described for the Forced-Response Analysis form, the increment number controls allow the user to select the number of increments in each field section of the model for which the state vector is calculated. The mode selection, shaft selection, and increment number controls also appear on the Data Table tab shown in Figure 4.14 where they perform similar functions. The Data Table tab shows the eigenvector results in tabular form. Figure 4.15 is an image showing the Characteristic Determinant tab which can be used to view a logarithmically scaled plot of the determinant curve. The controls on that tab are used to set the range of frequencies displayed in the figure and allow the user to refine a root approximation using a false-position root-search routine.

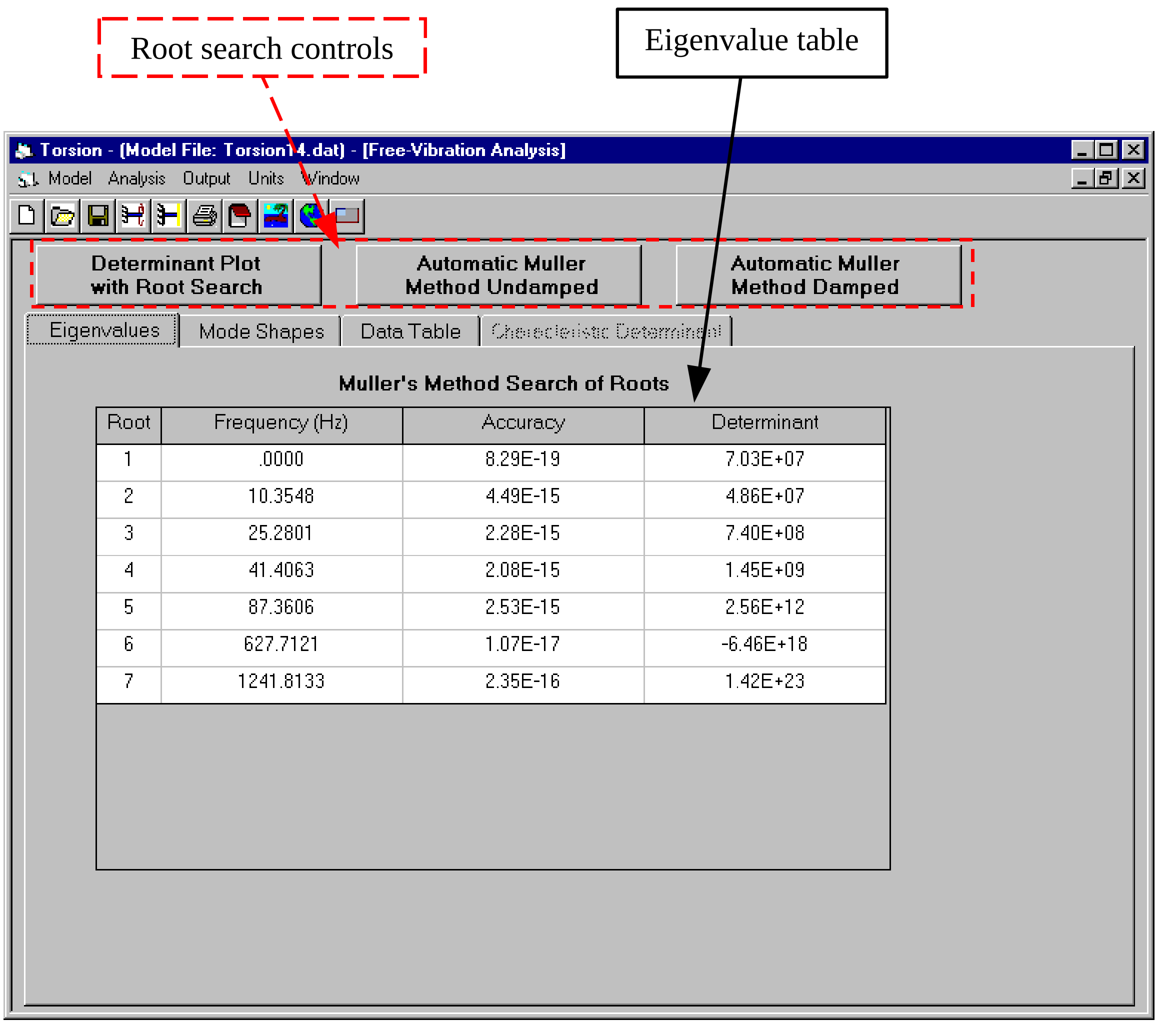

Figure 4.12: Free-Vibration Analysis Form, Eigenvalues Tab

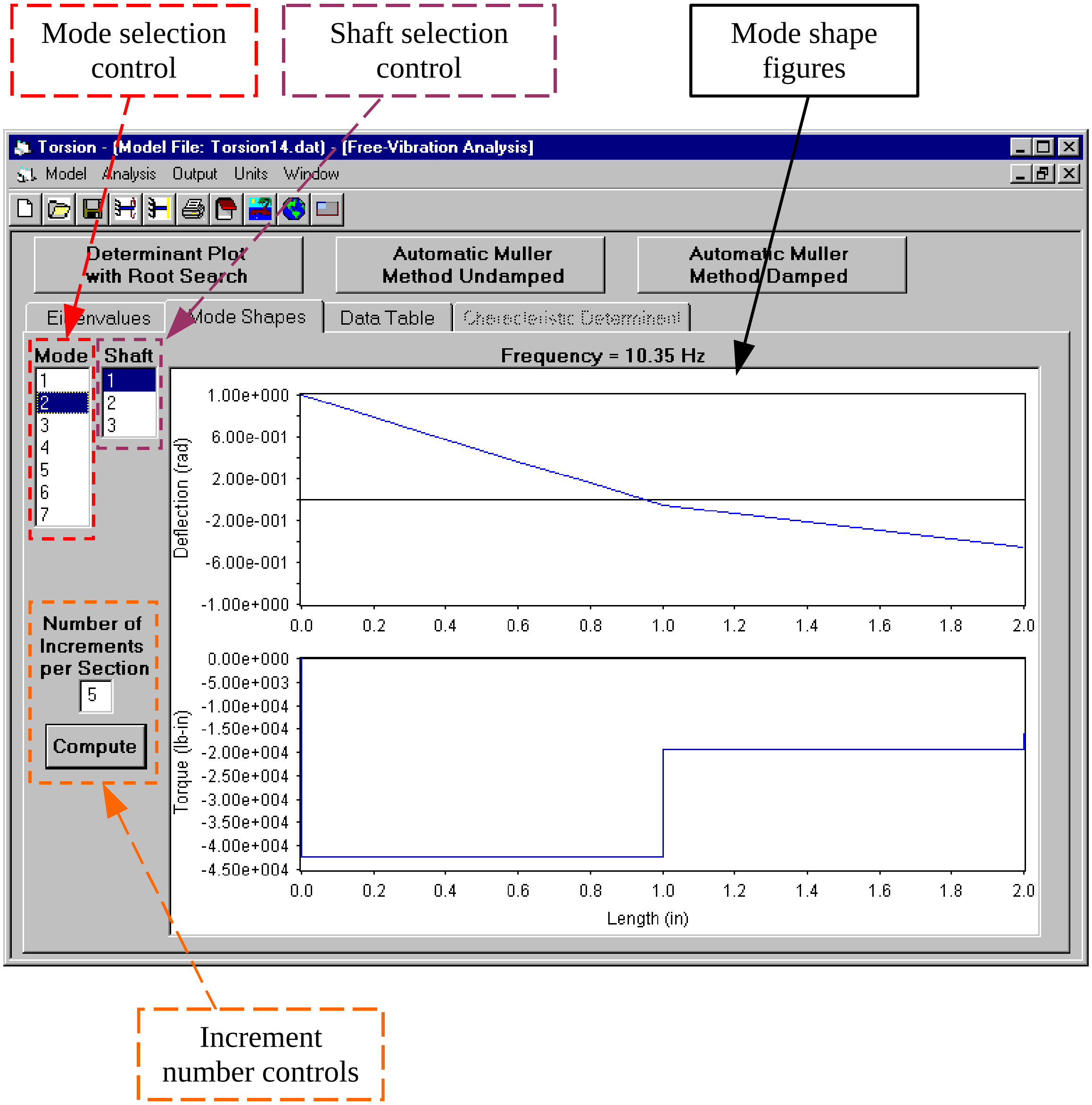

Figure 4.13: Free-Vibration Analysis Form, Mode Shapes Tab

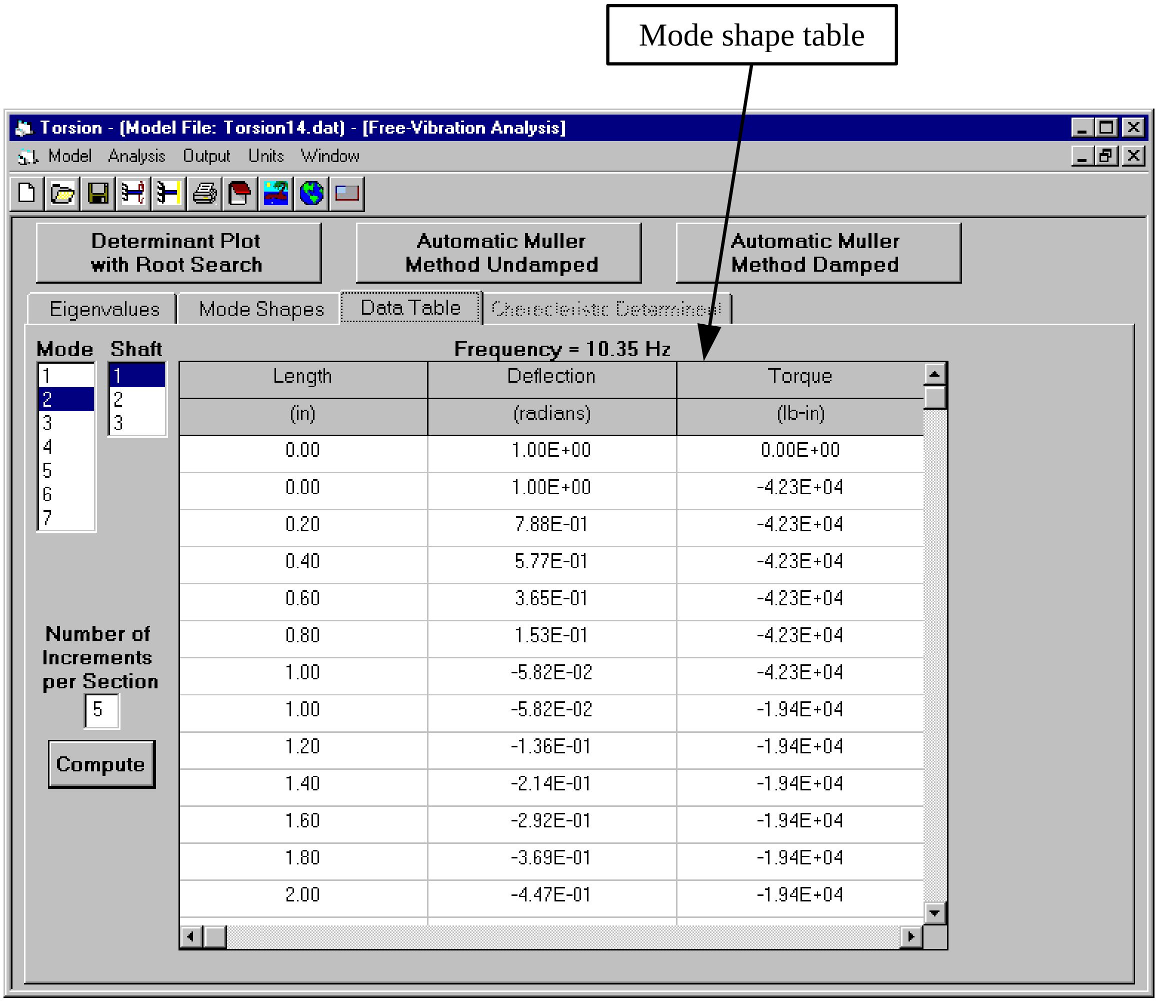

Figure 4.14: Free-Vibration Analysis Form, Data Table Tab

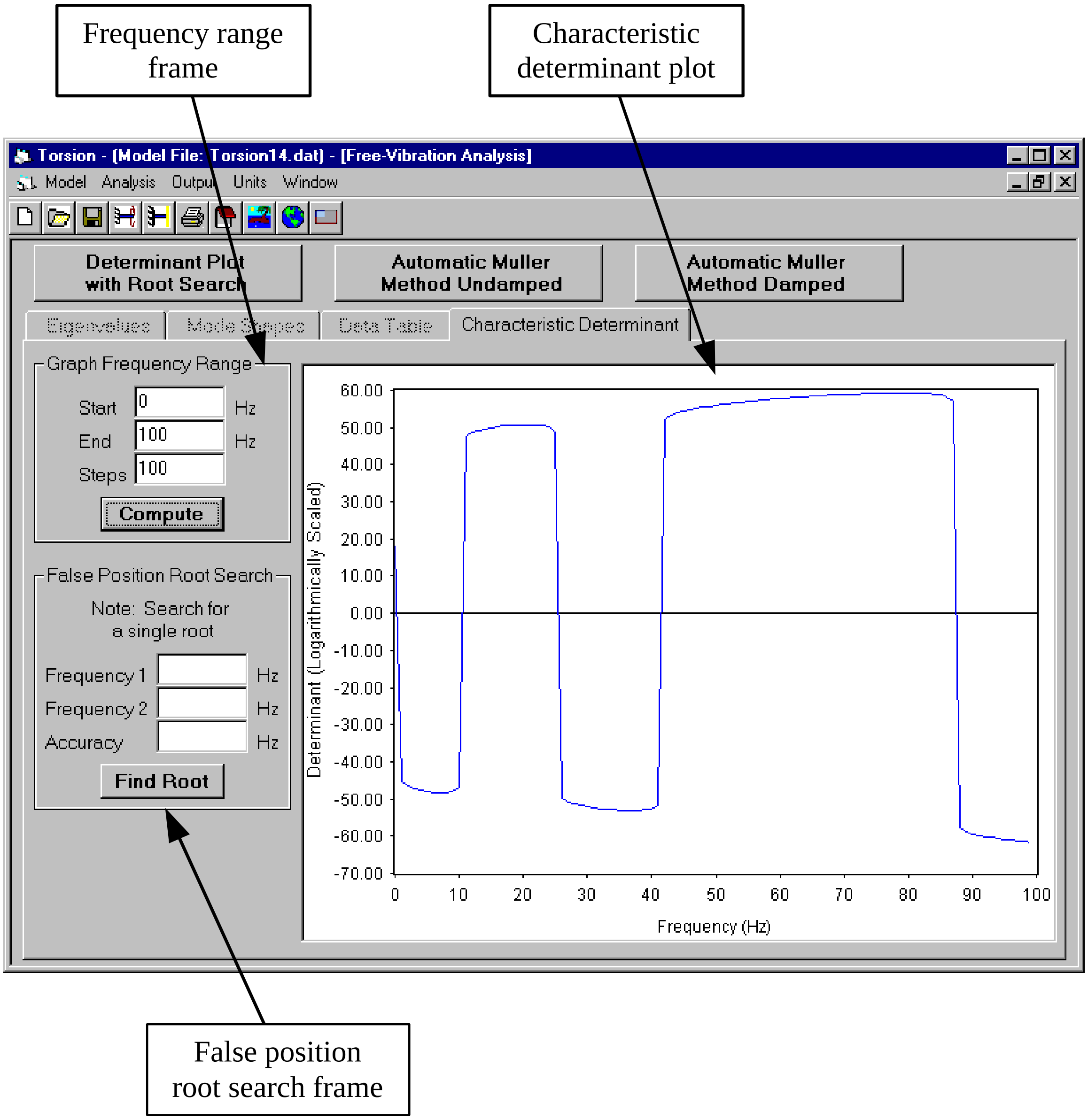

Figure 4.15: Free-Vibration Analysis Form, Characteristic Determinant Tab

Chapter 5. Verification of the Computer Program: A Set of Benchmark Solutions

5.1 Static Response of an Imbedded Bar

The first example problem presented here is taken from Pilkey and Chang[44] and involves determining the static response of a shaft that is imbedded in an elastic foundation as shown in Figure 5.1. The shaft is subjected to a uniformly distributed static torque, t. The magnitudes of the shaft's torsional constant (J), shear modulus (G), foundation stiffness modulus (k_t), section lengths (l_1, l_2, l_3), and loading (t) are specified in Figure 5.1. Pilkey and Chang present results from their computer program, *TWIST*. The deflection results from *TWIST* along with the results obtained from *Torsion 1* are shown in Table 5.1. Note that the difference between the results from the two programs is insignificant and can be explained by the different number of decimal places reported. The torque results from the two programs are shown in Table 5.2. The torque results compare favorably as well. The deflection and torque results from the *Torsion 1* program are shown in Table 5.3 in SI units. The same results are displayed graphically in Figure 5.2.

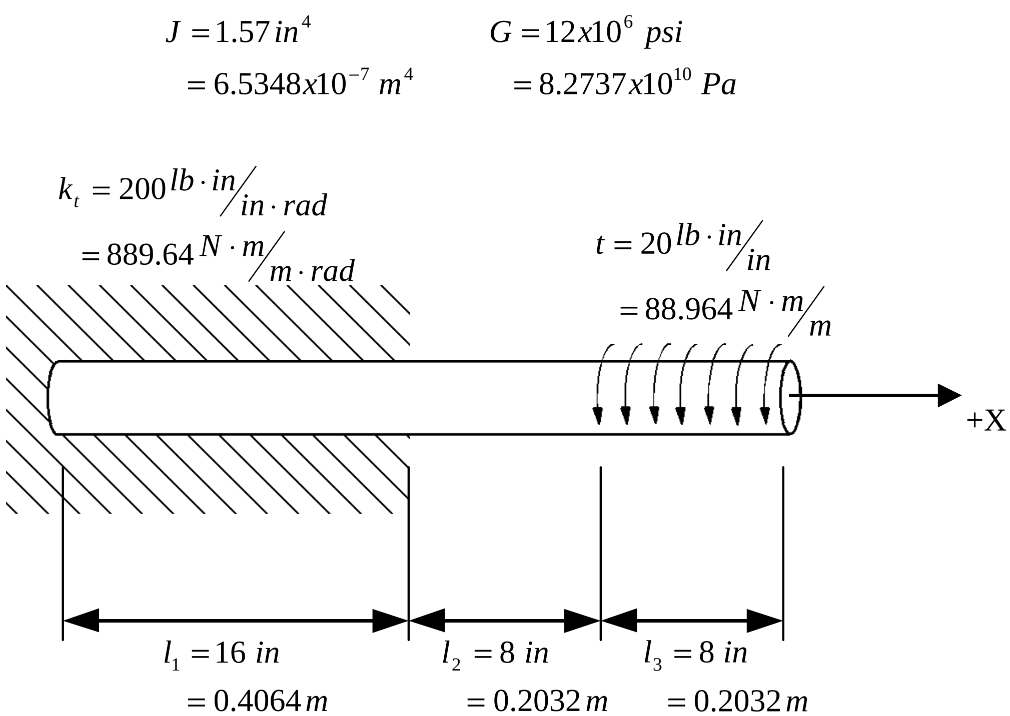

Figure 5.1: Shaft Imbedded in a Torsionally Flexible Foundation, adapted from Pilkey and Chang[45]

Table 5.1: Deflection Results From *TWIST* and *Torsion 1*

Axial Location (in)	***TWIST* Deflection (rad)**	***Torsion 1* Deflection (rad)**	**Percent Difference**
0.000000E+00	4.99774E-02	4.997736E-02	8.00E-05
5.333333E+00	4.99849E-02	4.998491E-02	2.00E-05
1.066667E+01	5.00075E-02	5.000755E-02	1.00E-04
1.600000E+01	5.00453E-02	5.004529E-02	2.00E-05
1.866667E+01	5.00679E-02	5.006793E-02	5.99E-05
2.133333E+01	5.00906E-02	5.009058E-02	3.99E-05
2.400000E+01	5.01132E-02	5.011323E-02	5.99E-05
2.666667E+01	5.01321E-02	5.013210E-02	0.00E+00
2.933333E+01	5.01434E-02	5.014342E-02	3.99E-05
3.200000E+01	5.01472E-02	5.014720E-02	0.00E+00

Table 5.2: Torque Results From *TWIST* and *Torsion 1*

Axial Location (in)	***TWIST* Torque (lb-in)**	***Torsion 1* Torque (lb-in)**	**Percent Difference**
0.000000E+00	0.00000E+00	0.000000E+00	0.00E+00
5.333333E+00	5.33119E+01	5.331187E+01	5.63E-05
1.066667E+01	1.06640E+02	1.066398E+02	1.88E-04
1.600000E+01	1.60000E+02	1.600000E+02	0.00E+00
1.866667E+01	1.60000E+02	1.600000E+02	0.00E+00
2.133333E+01	1.60000E+02	1.600000E+02	0.00E+00
2.400000E+01	1.60000E+02	1.600000E+02	0.00E+00
2.666667E+01	1.06667E+02	1.066667E+02	2.81E-04
2.933333E+01	5.33333E+01	5.333333E+01	5.63E-05
3.200000E+01	-9.09494E-13	0.000000E+00	N/A

Table 5.3: Deflection and Torque Results From *Torsion 1* in SI Units

Axial Location (m)	*Torsion 1* Deflection (rad)	*Torsion 1* Torque (N-m)
0.000000E+00	4.997736E-02	0.000000E+00
1.354667E-01	4.998491E-02	6.023432E+00
2.709333E-01	5.000755E-02	1.204868E+01
4.064000E-01	5.004529E-02	1.807757E+01
4.741333E-01	5.006793E-02	1.807757E+01
5.418667E-01	5.009058E-02	1.807757E+01
6.096000E-01	5.011323E-02	1.807757E+01
6.773333E-01	5.013210E-02	1.205172E+01
7.450667E-01	5.014342E-02	6.025858E+00
8.128000E-01	5.014720E-02	0.000000E+00

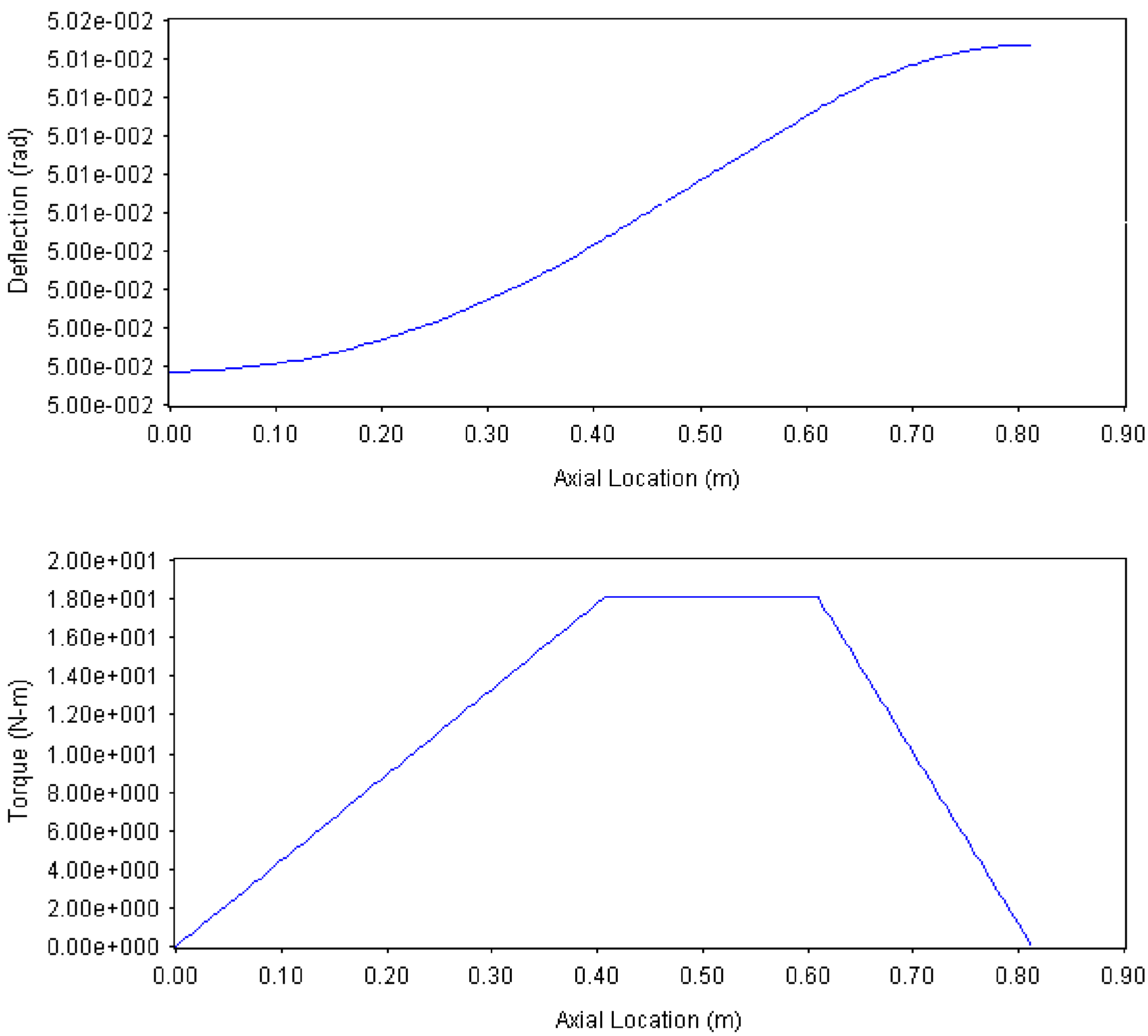

Figure 5.2: Deflection and Torque Response Results for the Imbedded Bar

5.2 Forced-Response Analysis of a Lumped-Parameter System

The second example problem consists of a three-mass system shown in Figure 5.3 which is subjected to a harmonically varying torque of magnitude, $\bar{T}$. This problem is taken from Wilson[46] who provides forced-response solutions corresponding to two different forcing frequencies. Wilson's solutions were obtained from hand calculations. A comparison of Wilson's results with the results obtained using *Torsion 1* corresponding to forcing frequency of 6.1640 Hz is shown in Table 5.4. Note that the difference between the results is less than 1%. Table 5.5 shows similar results when the torsional load varies harmonically with a frequency of 10.6764 Hz. These results have a slightly higher disparity which is probably due to round-off and lack of precision in the hand calculations.

$$\bar{T} = 50{,}000\, lb \cdot in$$
$$= 564{,}924\, N \cdot m$$

$$T = \bar{T}\sin(\mathrm{w}\, t)$$

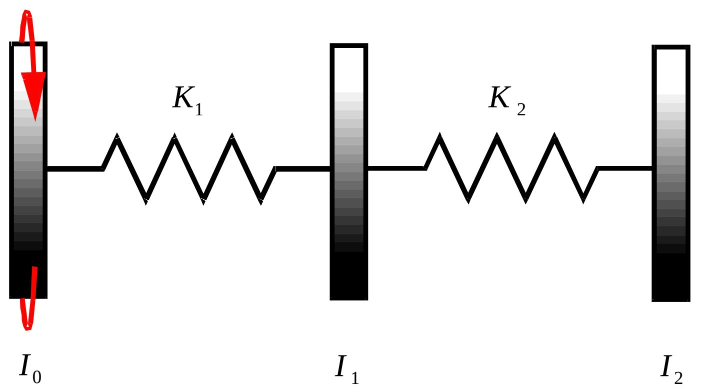

$$K_1 = K_2 = 4{,}000{,}000\, {}^{lb \cdot in}\!/_{rad} \qquad I_1 = I_2 = I_3 = 2000\, lb \cdot in \cdot s^2$$
$$= 451{,}939\, {}^{N \cdot m}\!/_{rad} \qquad = 225.970\, kg \cdot m^2$$

Figure 5.3: Three-Mass System with Harmonically Varying Torsional Load

Table 5.4: Steady-State Deflection of the Three-Mass System Due to a Load Varying Harmonically With Frequency = 6.1640 Hz

Point	**Wilson's Deflection (rad)**	***Torsion 1* Deflection (rad)**	**Percent Difference**
0	0.0204	0.02036920	0.15
1	-0.0074	-0.007407479	0.10
2	-0.0297	-0.02962863	0.24

Table 5.5: Steady-State Deflection of the Three-Mass System Due to a Load Varying Harmonically With Frequency = 10.6764 Hz

Point	Wilson's Deflection (rad)	*Torsion 1* Deflection (rad)	Percent Difference
0	-0.004	-0.004074211	1.86
1	-0.0074	-0.007407302	0.10
2	0.006	0.005925917	1.23

5.3 Damped and Undamped Free-Vibration Analysis of an Engine/Generator

Shown in Figure 5.4 is the schematic representation for a model of a 16 cylinder diesel engine coupled with an electric generator. Doughty and Vafaee[47] use a transfer matrix program to determine the eigenvalues and eigenvectors for this model corresponding to the parameter values shown in Table 5.6. The first five undamped eigenvalues obtained by Doughty and Vafaee are compared with results from *Torsion 1* in Table 5.7. The results obtained from *Torsion 1* show good correspondence with those provided by Doughty and Vafaee. A comparison of the eigenvector (mode shape) corresponding to the 118.298 Hz natural frequency obtained from the two computer programs is shown in Table 5.8.

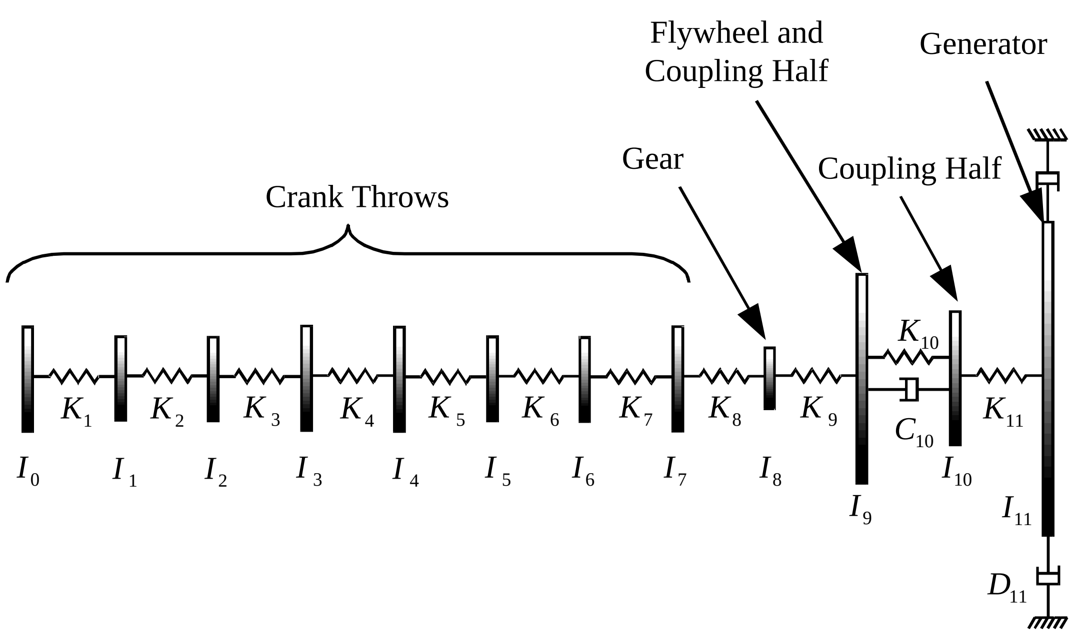

Figure 5.4: Lumped-Parameter Torsional Model of an Engine/Generator Set, adapted from Doughty and Vafaee[48]

Table 5.6: Parameter Values for the Engine/Generator Set, adapted from Doughty and Vafaee[49]

Section (Field+Point)	K_{field} Field Stiffness (N-m/rad)	C_{field} Field Damping (N-m-s/rad)	I_{point} Polar Inertia (kg-m^2)	D_{point} Damping to Ground (N-m-s/rad)
0	-	-	6	0
1	16	0	4.5	0
2	16	0	4.5	0
3	16	0	6	0
4	13	0	6	0
5	16	0	4.5	0
6	16	0	4.5	0
7	16	0	6	0
8	25	0	3.5	0
9	150	0	100	0
10	0.5	330	20	0
11	10	0	350	550

Table 5.7: Lower Natural Frequencies of the Undamped Engine/Generator Model

Root	Doughty and Vafaee Natural Frequency (Hz)	*Torsion 1* Natural Frequency (Hz)	Percent Difference
1	0.0	0.0000	0.0000
2	10.731	10.7309	0.0009
3	59.9513	59.9513	0.0000
4	118.298	118.2980	0.0000
5	157.216	157.2164	0.0002

Table 5.8: Undamped Mode Shape for the Engine/Generator Corresponding to 118.298 Hz Natural Frequency

Point	Doughty and Vafaee Deflection (rad)	*Torsion 1* Deflection (rad)	Percent Difference
0	1.0000	1.000000	0.000
1	0.7928	0.7928210	0.003
2	0.4625	0.4624502	0.011
3	0.0602	0.06022183	0.036
4	-0.4502	-0.4501844	0.003
5	-0.7716	-0.7716206	0.003
6	-0.9732	-0.9731593	0.004
7	-1.0235	-1.023484	0.002
8	-0.9200	-0.9199838	0.002
9	-0.8909	-0.8908741	0.003
10	106.2796	106.2796	0.000
11	-5.7960	-5.796002	0.000

Doughty and Vafaee also provide some of the results obtained from analyzing the damped torsional system. For example, the damped eigenvalues for the model are shown along with the corresponding results from *Torsion 1* in Table 5.9. Once again the agreement of most of the results provides confidence that the new program is functioning correctly. However, there is a very significant disagreement for the results of the two programs in the real component of roots 9 and 10. The following paragraph provides the intuitive reasoning used to conclude that the result provided by Doughty and Vafaee is possibly too large.

The real component of an eigenvalue represents the rate of decay of the oscillation experienced by a system. This decay term is representative of the effectiveness of the damping within the system for a particular mode. As an example, consider roots 7 and 8 in Table 5.9. The mode corresponding to these eigenvalues has a larger decay term than any of the other modes. The undamped mode shape corresponding to this mode (undamped natural frequency of 118.2890 Hz) has a large relative deflection between points 9 and 10 as can be seen in Figure 5.5. Therefore, the damper between points 9 and 10 would likely dissipate a significant amount of energy from this mode, and the large decay term makes sense.

Table 5.9: Lower Eigenvalues of the Damped Engine/Generator Model

Root	Doughty and Vafaee Eigenvalue		*Torsion 1* Eigenvalue		Percent Difference	
	Real (Hz)	Imaginary (Hz)	Real (Hz)	Imaginary (Hz)	Real	Imaginary
1	0.0	0.0	0.0000	0.0000	0.000	0.000
2	-0.1698	0.0	-0.1698	0.0000	0.000	0.000
3	-0.2605	10.728	-0.2605	10.7277	0.000	0.003
4	-0.2605	-10.728	-0.2605	-10.7277	0.000	0.003
5	-0.0528	59.9516	-0.0529	59.9517	0.189	0.000
6	-0.0528	-59.9516	-0.0529	-59.9517	0.189	0.000
7	-1.275	118.285	-1.2747	118.2853	0.024	0.000
8	-1.275	-118.285	-1.2747	-118.2853	0.024	0.000
9	-1.051	157.216	-0.0105	157.2160	99.001	0.000
10	-1.051	-157.216	-0.0105	-157.2160	99.001	0.000

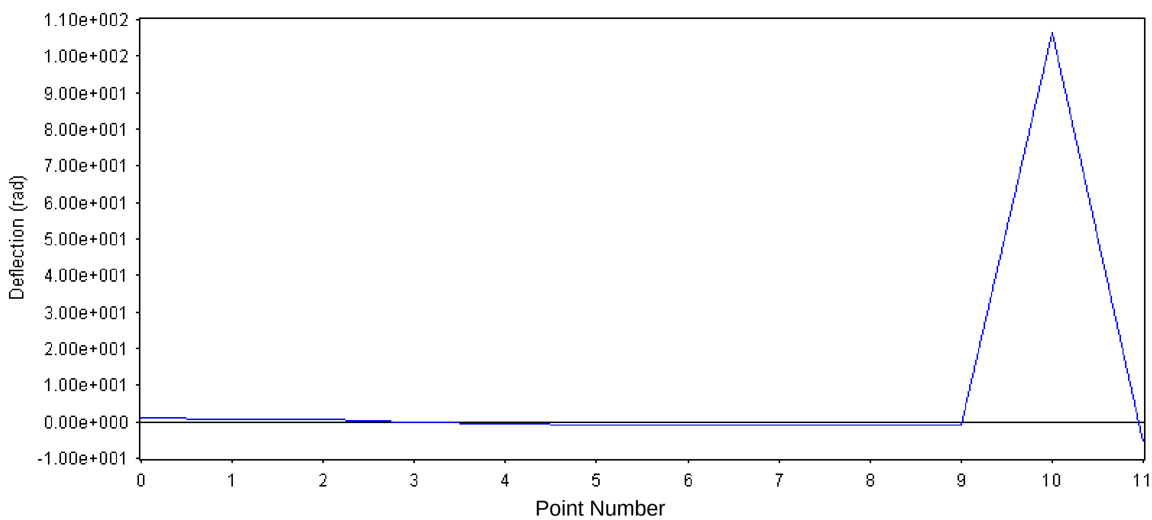

Figure 5.5: Undamped Mode Shape of Engine/Generator Corresponding to Natural Frequency of 118.2890 Hz

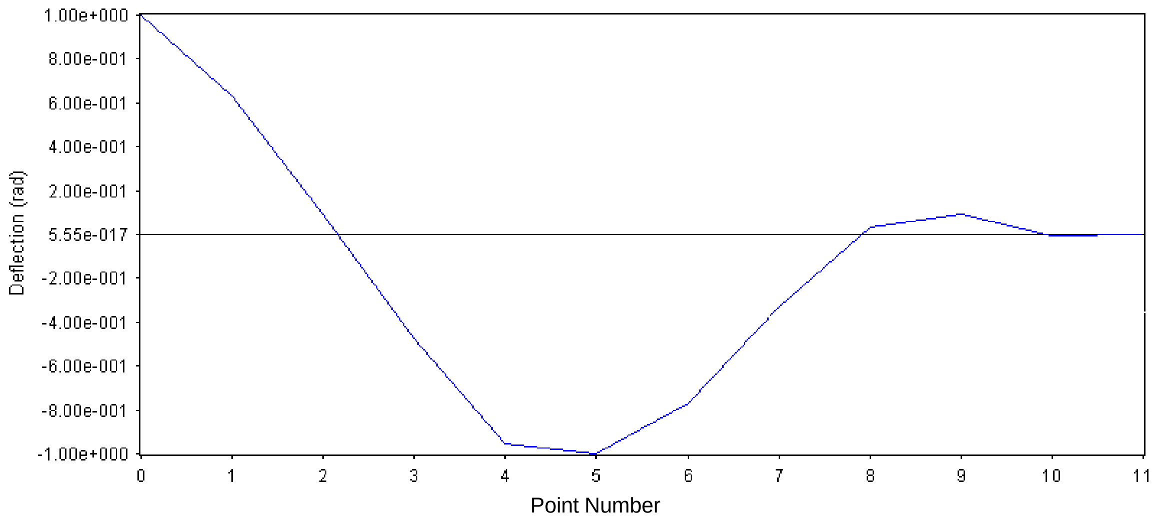

Figure 5.6: Undamped Mode Shape of Engine/Generator Corresponding to Natural Frequency of 157.2164 Hz

The decay term reported by Doughty and Vafaee for roots 9 and 10 is only about 18 percent less than the decay term for roots 7 and 8. By looking at the undamped mode shape corresponding to roots 9 and 10 (undamped natural frequency of 157.2164 Hz) shown in Figure 5.6, one notices that the relative deflection between points 9 and 10 is significantly less prominent in this mode than was observed in the previous mode shape. Also, the deflection at point 11 (location of the damper to ground) is essentially zero. If one assumes that these are valid mode shapes, it seems logical that the decay term for roots 9 and 10 presented by Doughty and Vafaee is too large. Although this is certainly not absolute proof that the results form *Torsion 1* are valid, the fact that the two results appear to be a factor of 100 off leads to the belief that the location of the decimal place in the decay term may have been misreported by Doughty and Vafaee. Since the eigenvalues for all of the other modes are in good agreement, this seems to be the most logical explanation for the discrepancy.

5.4 Undamped Free-Vibration Analysis of a Redundant Drive System

The system shown in Figure 5.7 is a redundant drive train for which Wilson[50] provides estimates of the systems natural frequencies. The analysis of the undamped natural frequencies of this system using *Torsion 1* is provided as a demonstration of the program's ability to provide valid natural frequency results for multi-rotor systems. The values of the inertias and stiffnesses used to model the system are shown in Table 5.8. Wilson states that Shaft 2 runs at twice the speed of Shaft 1 and assumes that the gear teeth are rigid. For the purpose of creating a multi-rotor model of the system, the values in Table 5.9 have been assumed for the gears in the system. The assumed radii provide the speed ratio specified by Wilson. The gear tooth stiffness values were successively increased until increasing the stiffness value no longer had a significant effect on the resulting estimates of the system's first two oscillatory natural frequencies.

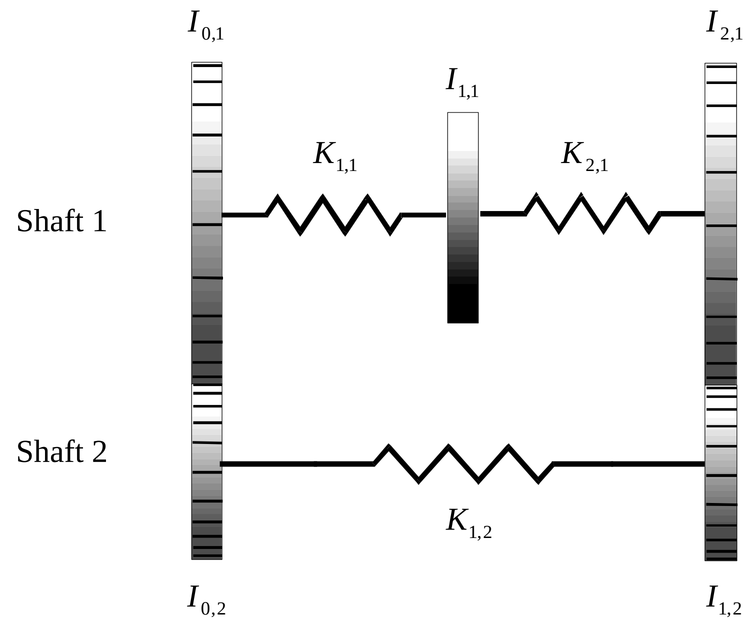

Figure 5.7: Redundant Drive System, adapted from Wilson[51]

Table 5.10: Inertia and Stiffness Parameter Values for the Redundant Drive System

Section Number	Polar Inertia, *I* (lb-in-s^2)	Polar Inertia, *I* (kg-m^2)	Field Stiffness, *K* (lb-in/rad)	Field Stiffness, *K* (N-m/rad)
0,1	1970	222.58	-	-
1,1	1000	112.99	4.0000E+6	4.5194E+5
2,1	2970	335.57	3.0000E+6	3.3895E+5
0,2	20	2.2597	-	-
1,2	2.5	0.28246	5.0000E+5	5.6492E+4

Table 5.11: Assumed Values of the Gear Parameters for Creating a Multi-Rotor Model of the Redundant Drive System Using *Torsion 1*

Section Number	Gear Base Radius (in)	Gear Base Radius (m)	Gear Tooth Stiffness (lb/in)	Gear Tooth Stiffness (N/m)
0,1	2	0.0508	1.0E+11	1.751E+13
2,1	2	0.0508	1.0E+11	1.751E+13
0,2	1	0.0254	1.0E+11	1.751E+13
1,2	1	0.0254	1.0E+11	1.751E+13

Table 5.12: Natural Frequency Estimates for the First Two Oscillatory Modes of the Redundant Drive System

Root	**Wilson's Natural Frequency Estimates (Hz)**	***Torsion 1* Natural Frequency Estimates (Hz)**	***Matlab* Model Natural Frequency Estimates (Hz)**
1	8.72	8.6784	8.6784
2	14.8	14.7863	14.7863

The estimates for the natural frequencies of the first two oscillatory modes of this system are provided in Table 5.12. Since the results from *Torsion 1* and the hand calculations performed by Wilson did not coincide exactly, a third model of the system was created by forming the mass and stiffness matrices for an equivalent single-speed system. Having formed the mass and stiffness matrices of the equivalent system (for which the gear teeth were assumed to be rigid), *Matlab* was used to determine the system eigenvalues. The results from this analysis are also shown in Table 5.12 and show very good agreement with the results from the multi-rotor, *Torsion 1* model.

5.5 Undamped Free-Vibration Analysis of a Petroleum Drill String Modeled with a Continuum Element

In the following example, an undamped free-vibration analysis is performed for the petroleum drill string model shown in Figure 5.8. Thomson and Dahleh[52] demonstrate the calculation of the first two natural frequencies for this system using an analytical technique. The estimates for the first two natural frequencies obtained from both the analytical technique and the *Torsion 1* computer program are provided in Table 5.13. The mode shapes which correspond to the first two natural frequencies are provided in Figure 5.9 and Figure 5.10.

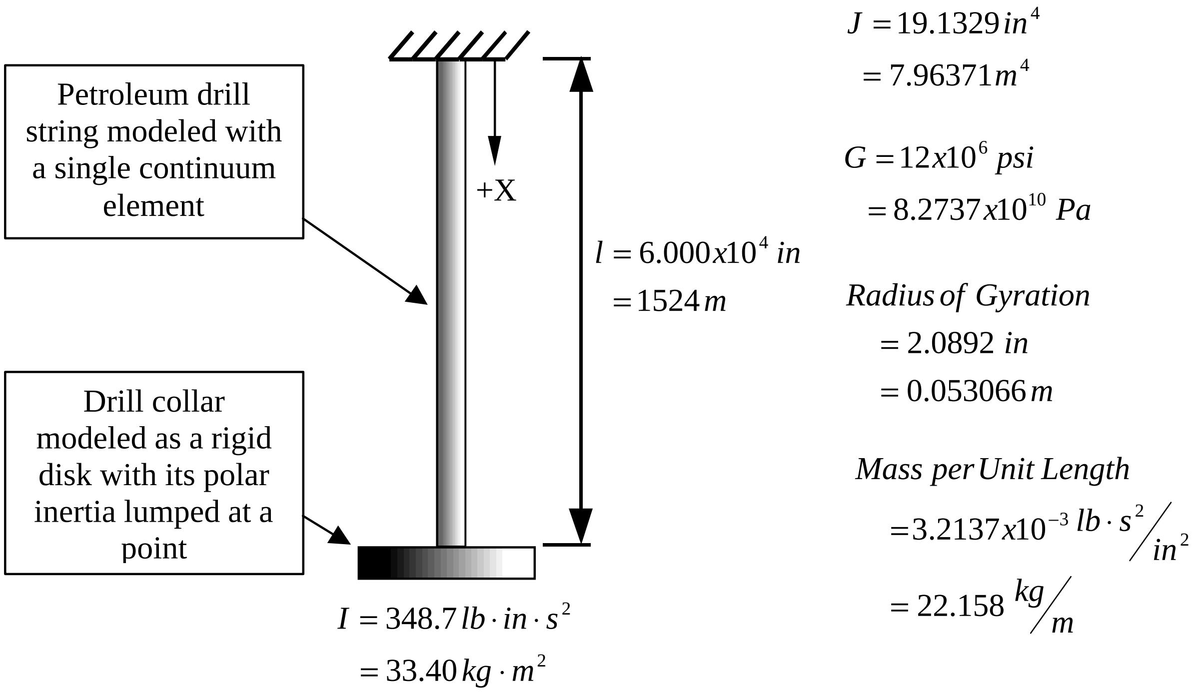

Figure 5.8: Petroleum Drill Sting Model, adapted from Thomson and Dahleh[53]

Table 5.13: First Two Natural Frequencies for the Petroleum Drill String Model

Root	**Analytically Determined Natural Frequency (Hz)**	***Torsion 1* Natural Frequency (Hz)**
1	0.384	0.3842
2	1.26	1.2616

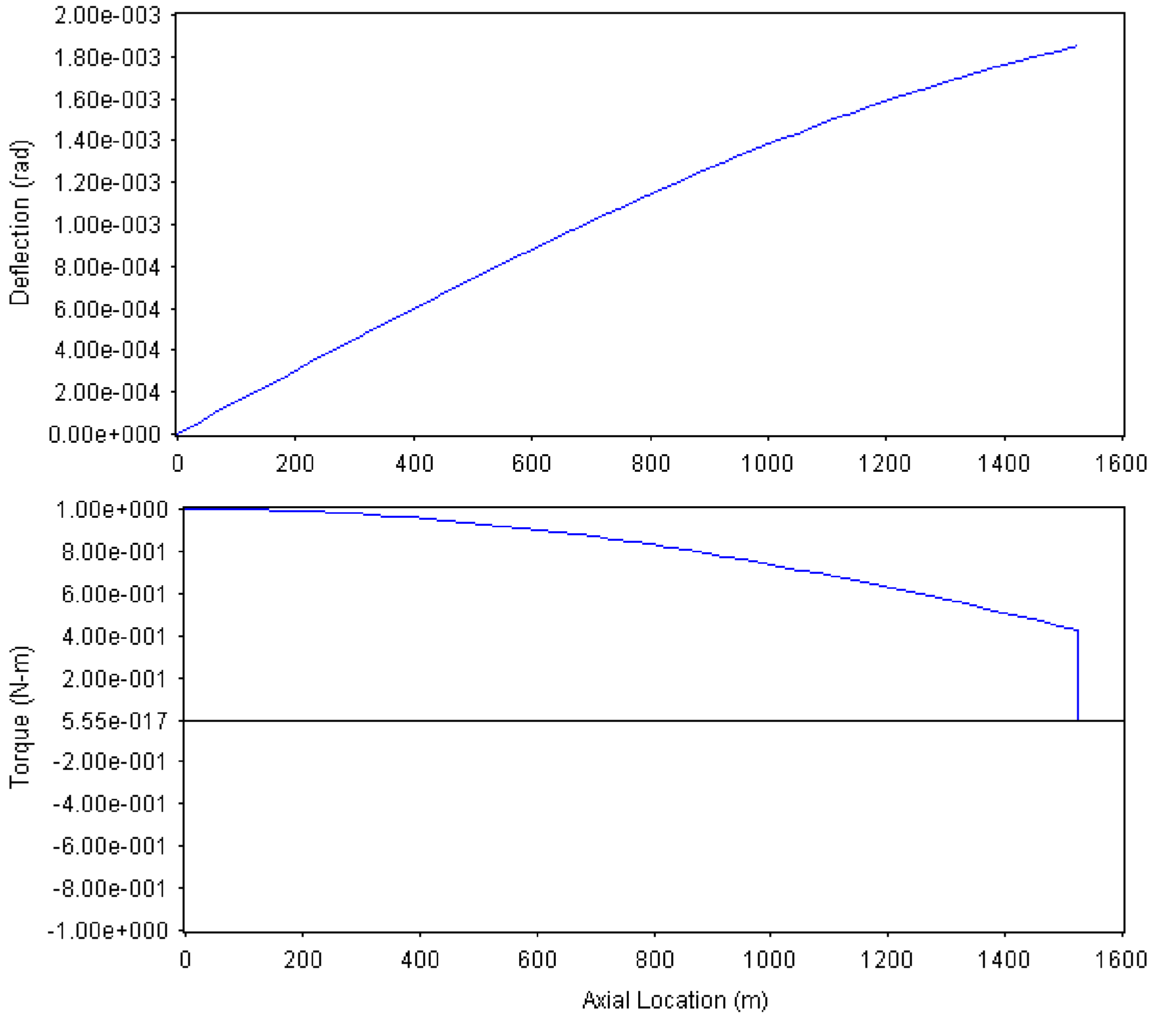

Figure 5.9: Petroleum Drill String Mode Shape Corresponding to a Natural Frequency of 0.3842 Hz

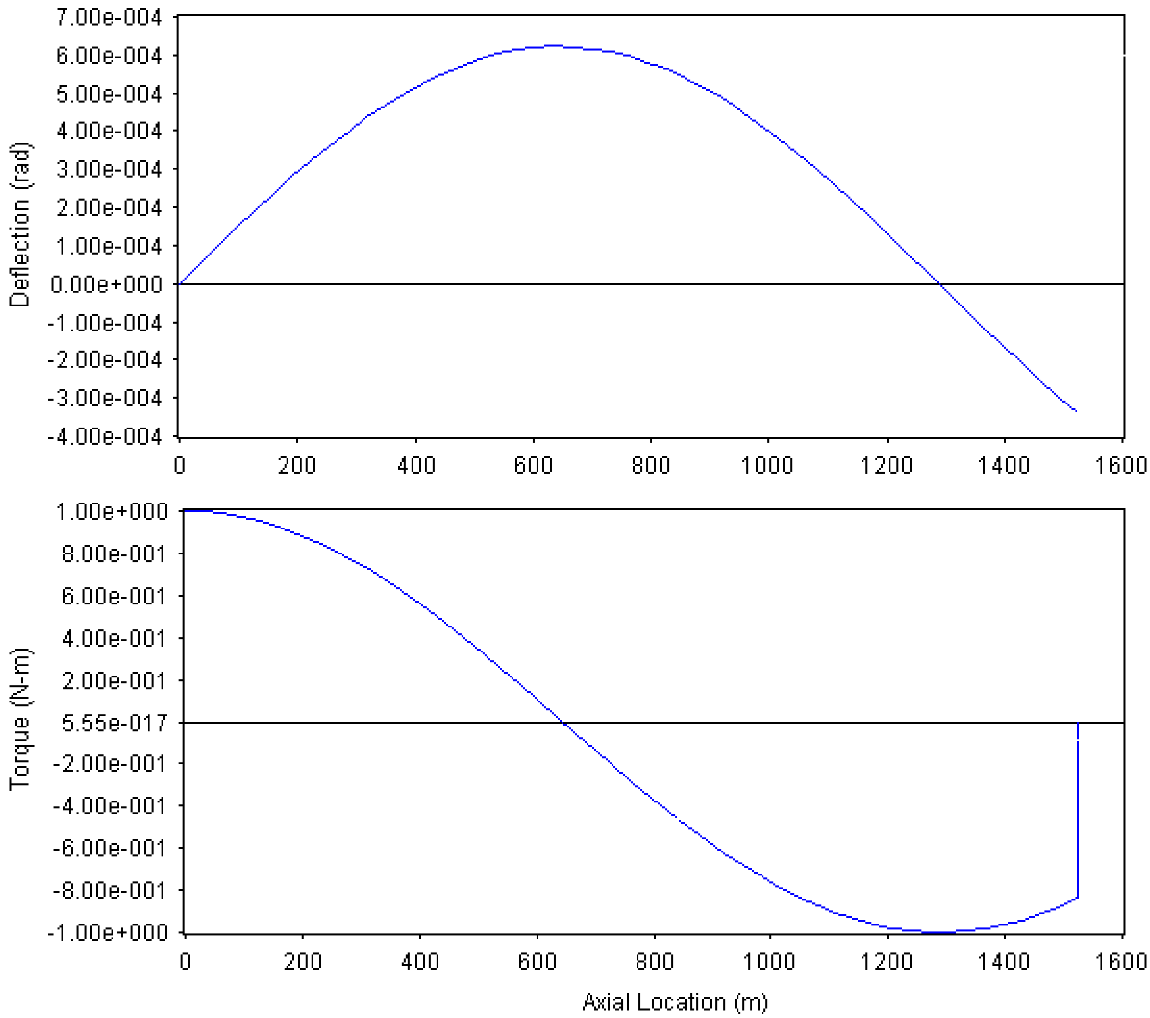

Figure 5.10: Petroleum Drill String Mode Shape Corresponding to a Natural Frequency of 1.2616 Hz

The correspondence of the natural frequency results from *Torsion 1* shown in Table 5.13 with the results obtained from Thomson and Dahleh's analytical expression helps to verify the proper operation of the routines in the *Torsion 1* computer program. However, examining the mode shape for the third root reported by the Muller method algorithm of *Torsion 1* reveals a problem. The mode shape for this third root (natural frequency of 3.2814 Hz) is shown in Figure 5.11. Note that the first vibration mode, shown in the deflection diagram of Figure 5.9, has only a single node at the left end. As would be expected, the second mode in Figure 5.10 has two nodes. Similarly, it would be expected that the third mode would have three nodes. However, the mode shape for the "third" root shown in Figure 5.11 has four nodes. The "third" root reported by the Muller method algorithm actually corresponds to the fourth vibratory mode of the system. The root-search algorithm failed to report the third natural frequency of the system. Thus, the program user must be certain that the results obtained make sense. When the characteristic determinant curve is plotted, as shown in Figure 5.12, it can be seen that natural frequency of 3.2814 Hz is actually the fourth root of this system. The false position root search routine can be used to determine the system's third natural frequency as 2.2507 Hz. The deflection and torque diagrams for the third mode of the system are shown in Figure 5.13.

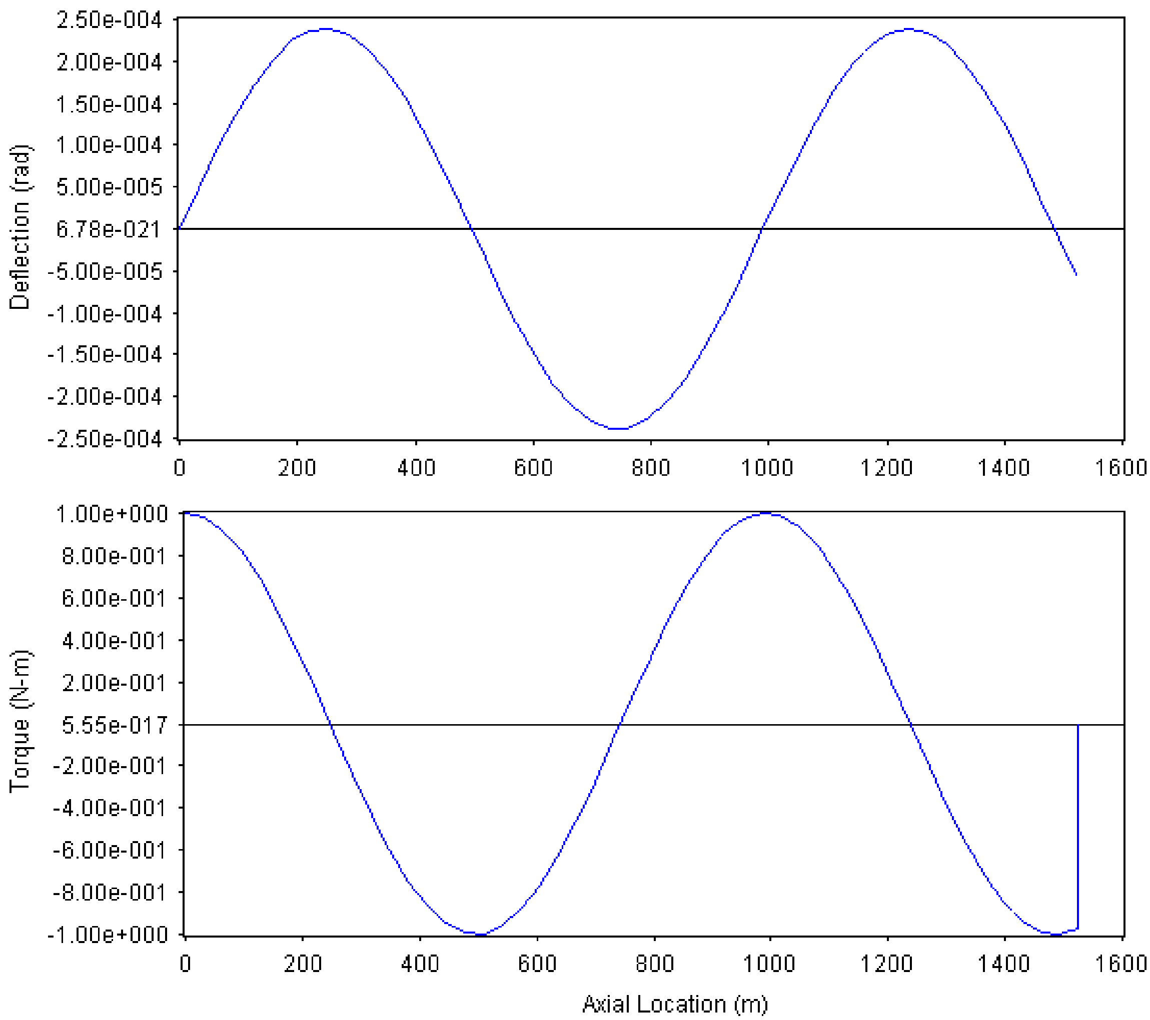

Figure 5.11: Petroleum Drill String Mode Shape Corresponding to a Natural Frequency of 3.2814 Hz

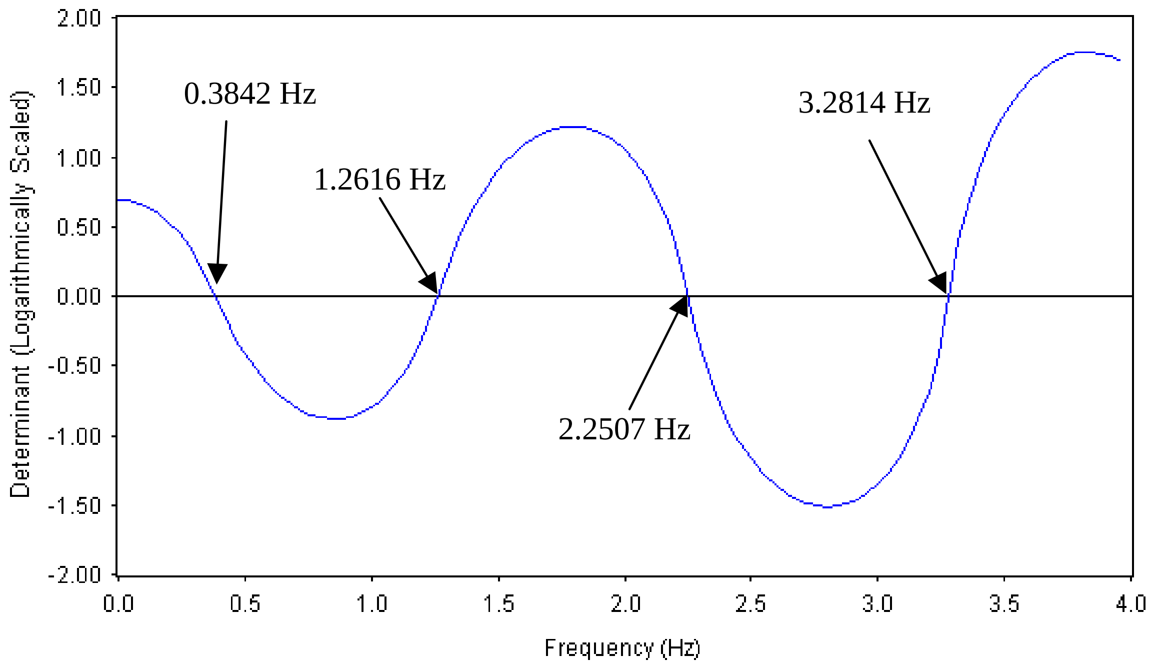

Figure 5.12: Plot of the Characteristic Determinant for the Petroleum Drill String

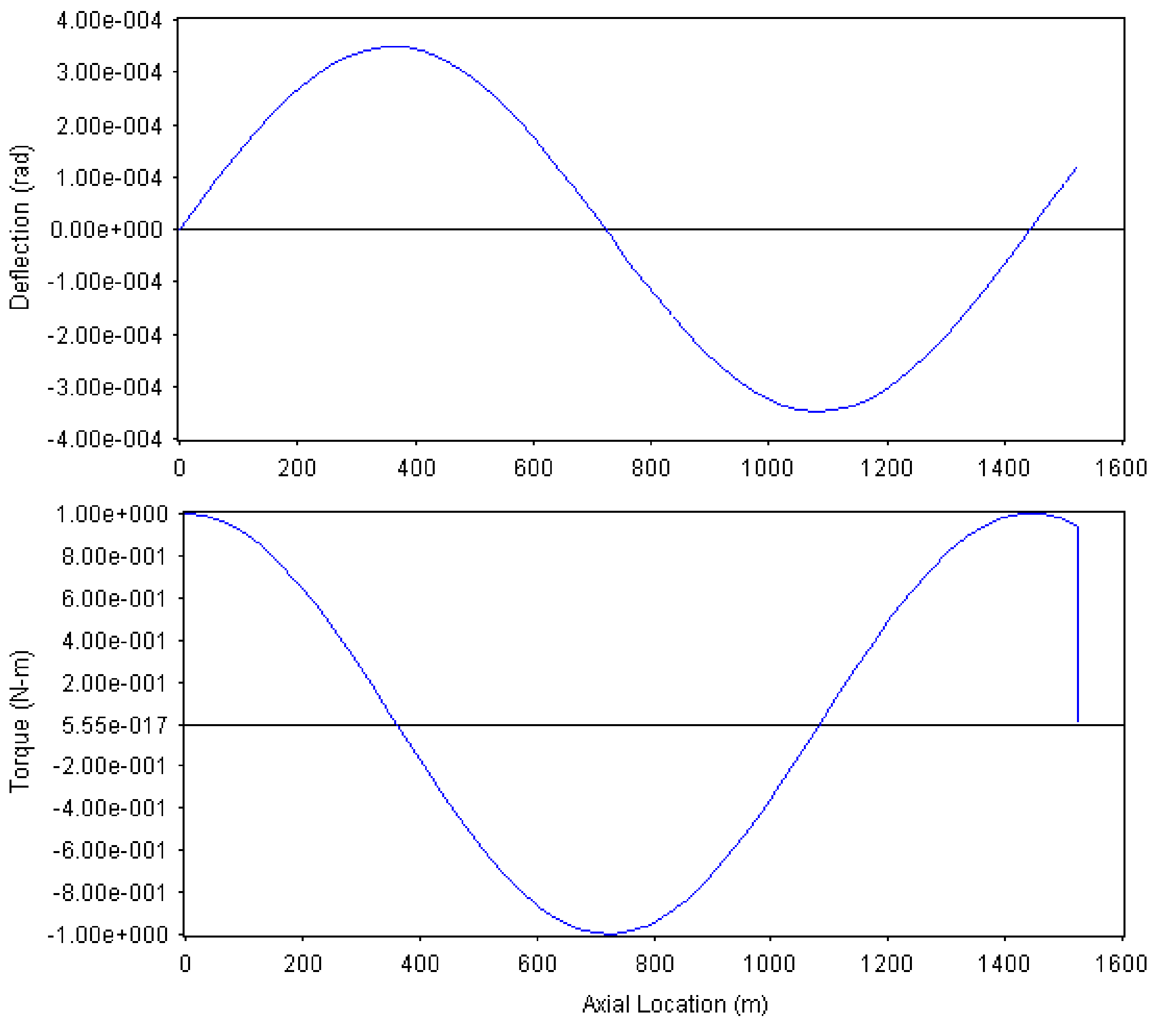

Figure 5.13: Petroleum Drill String Mode Shape Corresponding to a Natural Frequency of 2.2507 Hz

5.6 Undamped Free-Vibration Analysis of an Automatic Vehicle Transmission

The *Torsion 1* computer program can be used to effectively model the torsional free-vibration characteristics of a compound planetary gear train. This capability is demonstrated in the following example problem taken from Mandal, et al.[54] Shown in Figure 5.14 is a schematic representation of the lumped-parameter model used with *Torsion 1* to determine the torsional natural frequencies of an automatic transmission. Included in Appendix B is a listing of the model parameter values for this automatic transmission. This transmission was designed by CVRDE (Combat Vehicles Research and Development Establishment) for Indian Buses and Trucks.

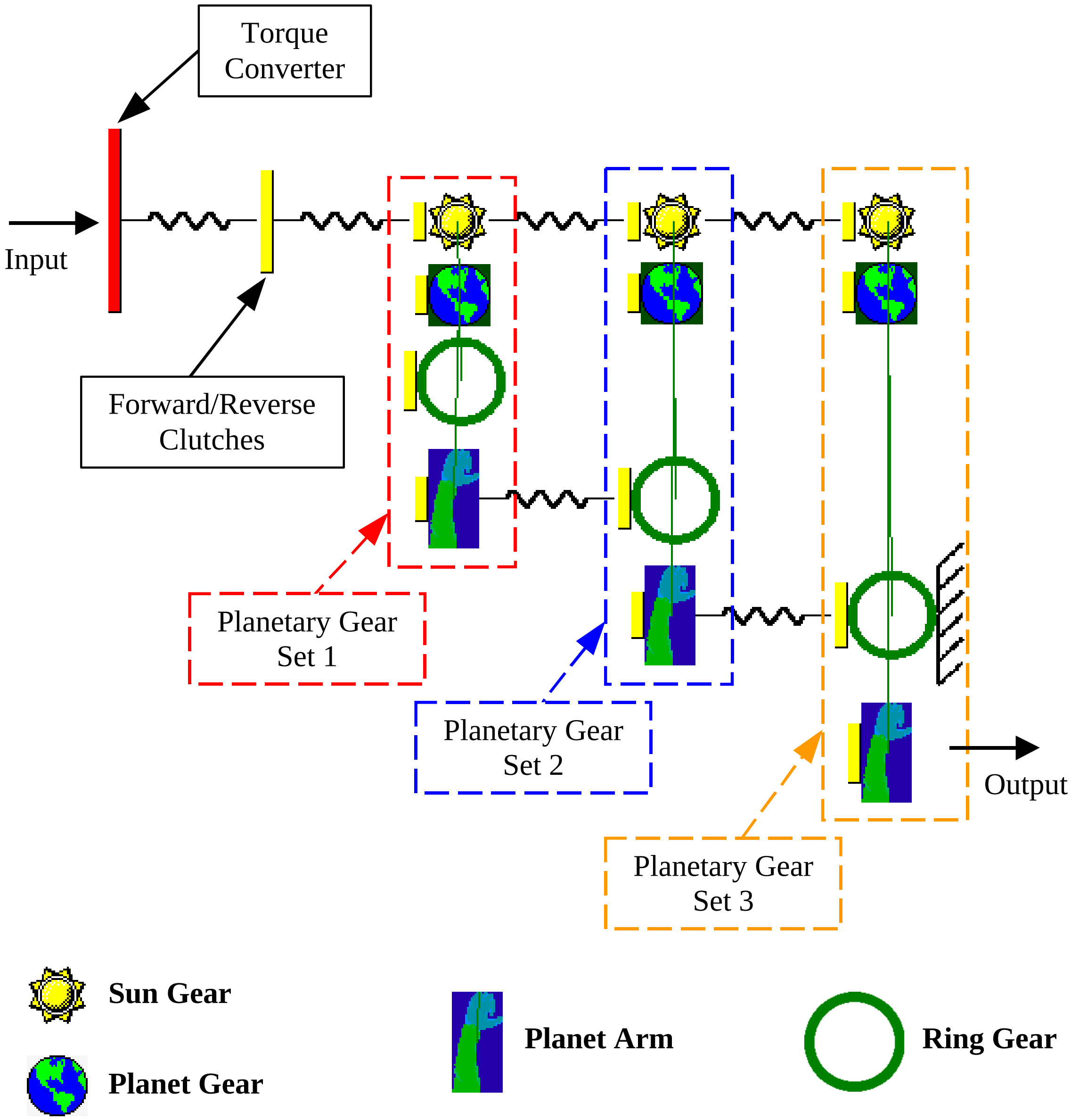

Figure 5.14: Schematic Model Representation for the Automatic Vehicle Transmission in Forward, First-Gear Configuration

Mandal, et al. describe the free-vibration analysis of a single-shaft equivalent torsional model of the transmission using a finite element program to perform the analysis. This method entails the creation of a separate model for each speed setting of the transmission, requires a significant number of equivalence calculations, and assumes the gear teeth in the system are rigid. In order to demonstrate that a *Torsion 1* multi-rotor model could be used to find results similar to those found using the equivalence technique, a series of analyses were performed on models of the system with different tooth stiffness values. The resulting values of the first oscillatory natural frequency from this analysis are shown in Figure 5.15. Similarly, the values obtained for the second oscillatory natural frequency of the system are plotted in Figure 5.16. Note that in each case the natural frequency estimate from the *Torsion 1* model approaches that of the equivalence model as the gear tooth stiffness is increased.

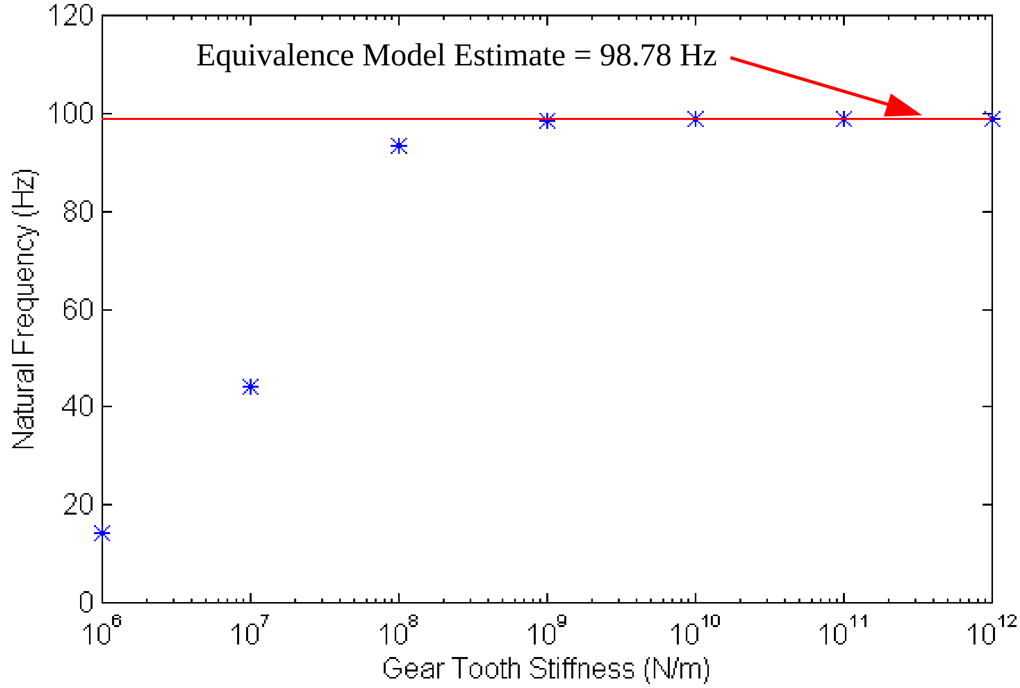

Figure 5.15: Variation of the Transmission's First Oscillatory Natural Frequency for a Range of Linear Gear Tooth Stiffness Values

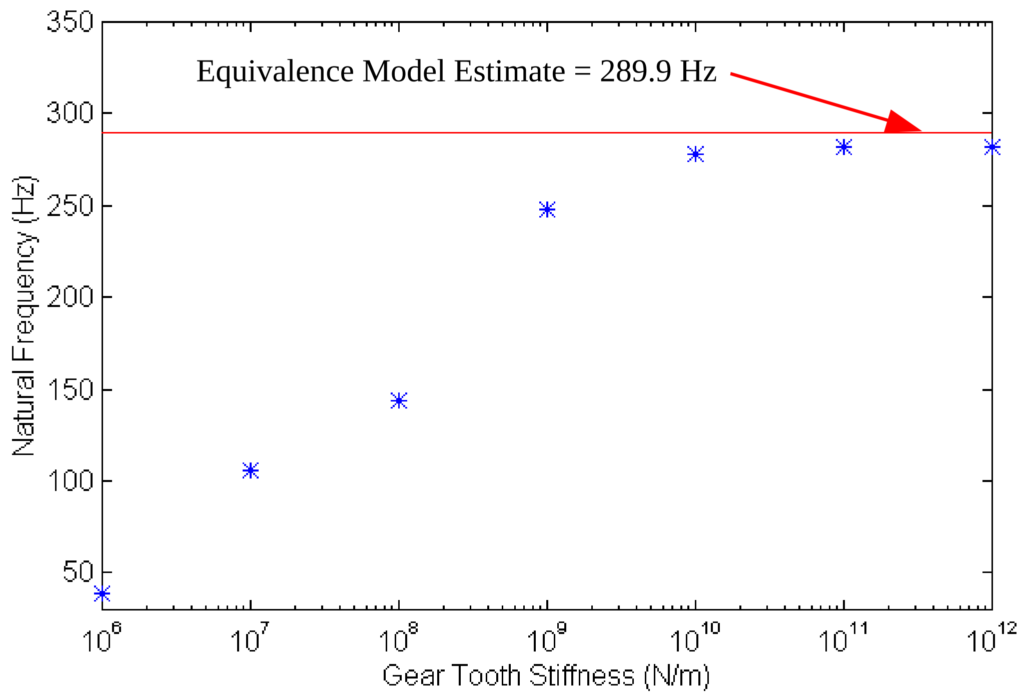

Figure 5.16: Variation of the Transmission's Second Oscillatory Natural Frequency for a Range of Linear Gear Tooth Stiffness Values

From Figures 5.15 and 5.16 it becomes apparent the magnitude of the gear stiffness values within a system can affect the system's natural frequencies. The significance of that effect is dependent on the actual gear tooth flexibility. Whether the significance is large or small, *Torsion 1* allows the user to easily include a tooth flexibility in the system model. Therefore, the multi-rotor models created using *Torsion 1* have the potential to more accurately represent a geared-torsional system.

This example demonstrates the capabilities of *Torsion 1* not only to model a system accurately but also to do so with ease. Creating the system model shown in Figure 5.14 requires no equivalence calculations, and the user-interface of the program makes the model building process a straightforward one. It should also be noted that in order to model the second and third gear configurations of this system, only the boundary conditions on the model shown in Figure 5.14 need be altered. For example, to put the system in its second gear configuration the right end of the ring gear in gear set 3 should be "free" and the ring gear in gear set 2 should be "fixed". In the actual vehicle transmission this process of making the gears "fixed" or "free" is accomplished with a series of clutches.

Chapter 6. Conclusions and Recommendations

6.1 Conclusions

A computer-aided design tool for torsional analysis of multi-rotor systems has been developed. This computer program, *Torsion 1*, makes use of an extended transfer matrix technique that allows the user to create an accurate system model with relative ease. *Torsion 1* can be used to obtain forced-response results for torsional models with a static or harmonically varying excitation. The program also has the capability to determine the eigenvalues and eigenvectors of systems with or without damping. The system eigenvalues can be found using a Muller-Method automatic root-search routine or a user-guided false-position root-search algorithm. Results are displayed in a graphical format that is easy to interpret and can be exported to files for use with other programs. The benchmark solutions in Chapter 5 verify that the program provides valid results that can be compared with previous solutions.

The *Torsion 1* program has the capability to model systems with a wide variety of components or characteristics which include: lumped inertias, massless shafts, viscous dampers, structural damping, uniformly distributed loads, pendulum absorbers, visco-elastic dampers, shafts with continuously distributed mass, foundations with uniformly distributed flexibility, gear meshes with a constant gear tooth stiffness, and planetary gear trains. These modeling capabilities allow the program user to create a system model that is representative of the machinery or component being analyzed.

6.2 Recommendations for Future Work

The following is a list of suggestions for improving the computer program, *Torsion 1*:

- The Model Editor form could be modified to aid the user in calculating such model parameters as polar inertias or torsional constants based on the geometry and dimensions of the system components.
- A material database could be included on the Model Editor form which could store material properties such as the shear modulus and density for common materials.
- The schematic model representation on the Model Editor form could be made to recognize the selection of a model element by way of a mouse click. This would allow the user to interact more directly with the system model.
- Rather than modeling a visco-elastic damper with a point matrix as is demonstrated in Section 2.5, *Torsion 1* could be modified to model the seismic mass as a separate rotor. This technique would allow the program to keep track of the response of the seismic mass as well as the main system.

- The pendulum absorber transfer matrix could be modified to include the effects of distributed pendulum mass using the relations developed for this type of system by Mitchiner and Leonard[55].
- The analysis capabilities of the program could be expanded to include a frequency-response analysis module that would allow the user to determine the forced response of a system over a range of excitation frequencies.
- The Muller-Method root-search routine could be modified to allow the user to guide it in searching a particular range of frequencies for the roots of the characteristic determinant.
- The forced-response capabilities of the program could be improved by allowing the user to model a series of torques with different phase values.
- Currently the speed ratios of compound planetary gear trains can be determined by making the output shaft "fixed" and applying a known torque value to the input. The speed ratio can then be determined as the inverse of the torque ratio. This could be accomplished more directly if the program allowed the user to prescribe a displacement for the input shaft. The speed ratio could then be calculated as the ratio of the displacement of any component to the displacement of the input. This method would not require applying the artificial "fixed" boundary condition to the output, and the speed ratios could be calculated simultaneously for all of the components rather than just the output. In fact, this type of analysis could be easily automated.
- The gear mesh forces for standard and planetary gear trains could be an additional output of the program that would useful to a design engineer.
- A power flow analysis for complex gear trains could be another simple adaptation of this transfer matrix technique. Once a force analysis and a speed ratio analysis have been performed, calculating power flows becomes a simple matter. Other techniques for performing this type of analysis have been reported in the literature by Freudenstein and Yang[56], Pennestri and Freudenstein[57], Saggere and Olson[58], Sanger[59], and Wojnarowski[60].
- The planetary gear mesh transfer matrix could be developed for systems with multiple planets.
- Axial and lateral vibration modeling capabilities could be coupled with the torsional modeling capabilities demonstrated here to create a universal multi-rotor transfer matrix program.
- A different programming platform could be used to improve the execution speed of the program's operations. Visual Basic 4.0 is an interpreted language such that an executable file is not processed by a computer as efficiently as is possible with other languages. Visual Basic 5.0 has eliminated this problem and may be the logical solution.
- The process of assembling the global transfer matrix could be made more efficient by a technique used to store and manipulate only the non-zero quantities in the matrices. For multi-rotor models with many shafts, a large number of the transfer matrix elements can be equal to zero. In such a case, carrying those zero elements of the matrices along as the global matrix is assembled can expend a lot of processing time unnecessarily. This would be

even more critical if the program's capabilities were expanded to model axial and lateral responses in addition to the torsional response.

Appendix A. Catalogue of Additional Transfer Matrices for Torsional Systems

A.1 State Vector

The torsional state vector corresponding to the transfer matrices listed in this appendix is given as follows:

$$\vec{z} = \begin{Bmatrix} q \\ T \\ \hdashline 1 \end{Bmatrix} \tag{A.1}$$

A.2 Massless, Elastic Shaft with Uniformly Distributed Torque

Pilkey and Chang[61] provide the transfer matrix shown in Equation (A.2).

$$\left[\begin{array}{cc:c} 1 & \dfrac{l}{JG} & \dfrac{-tl^2}{2JG} \\ 0 & 1 & -tl \\ \hdashline 0 & 0 & 1 \end{array}\right] \tag{A.2}$$

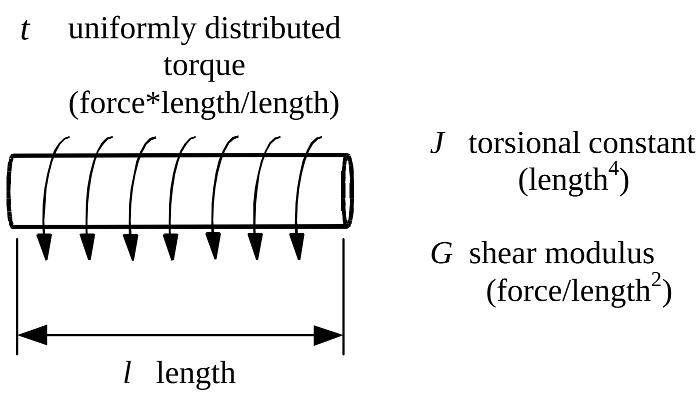

Figure A.1: Massless, Elastic Shaft with Uniformly Distributed Torque

A.3 Massless, Elastic Shaft on Elastic Foundation with Uniformly Distributed Torque

Pilkey and Chang[62] provide the transfer matrix shown in Equation (A.3).

$$\left[\begin{array}{cc:c} \cosh(\beta l) & \sinh(\beta l) & \dfrac{-t\langle -1+\cosh(\beta l)\rangle}{GJ\beta^{2}} \\ GJ\beta\sinh(\beta l) & \cosh(\beta l) & -t\dfrac{\sinh(\beta l)}{\beta} \\ \hdashline 0 & 0 & 1 \end{array}\right] \tag{A.3}$$

Where:

$$\beta^{2}=\frac{K_t}{GJ} \tag{A.4}$$

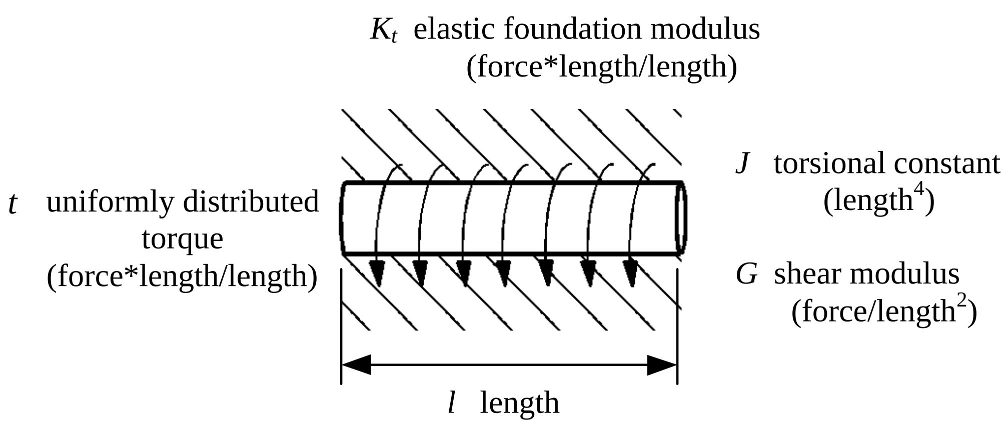

Figure A.2: Massless, Elastic Shaft on Elastic Foundation with Uniformly Distributed Torque

A.4 Elastic Shaft with Continuously Distributed Mass and Uniformly Distributed Torque

The following transfer matrix for an elastic shaft with continuously distributed mass can be found in Pestel and Leckie[63] without the extension column for loading. The same transfer matrix can be found in Pilkey and Chang[64] with the additional loading terms. However, the reader should be aware that this transfer matrix is incorrectly labeled in Pilkey and Chang as the transfer matrix for a “Rigid Bar”.

$$\left[\begin{array}{cc:c} \cos(bl) & \dfrac{\sin(bl)}{GJb} & \dfrac{-t}{GJb^{2}}\left\langle 1-\cos(bl)\right\rangle \\ -JGb\sin(bl) & \cos(bl) & \dfrac{-t}{b}\sin(bl) \\ \hdashline 0 & 0 & 1 \end{array}\right] \tag{A.5}$$

Where:

$$b = w\sqrt{\frac{r\, r_p^2}{GJ}} \tag{A.6}$$

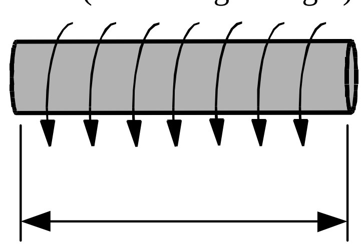

Figure A.3: Elastic Shaft with Continuously Distributed Mass and Uniformly Distributed Torque

A.5 Field Stiffness and Viscous Damping

The transfer matrix for a spring and viscous damper in parallel as shown in Figure A.4 is given by Pestel and Leckie[65] and is presented here in Equation (A.7).

$$\left[\begin{array}{cc:c} 1 & \dfrac{1}{k+jcw} & 0 \\ 0 & 1 & 0 \\ \hdashline 0 & 0 & 1 \end{array}\right] \tag{A.7}$$

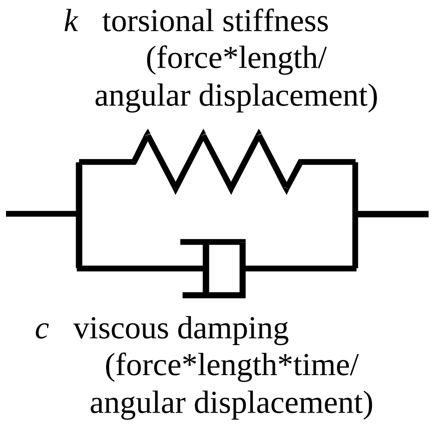

Figure A.4: Torsional Spring and Viscous Damper in Parallel

A.6 Viscous Point Damping to Ground

Pestel and Leckie[66] provide the transfer matrix used for modeling viscous damping at a point as shown in Figure A.5.

$$\left[\begin{array}{cc:c} 1 & 0 & 0 \\ jc\omega & 1 & 0 \\ \hdashline 0 & 0 & 1 \end{array}\right] \tag{A.8}$$

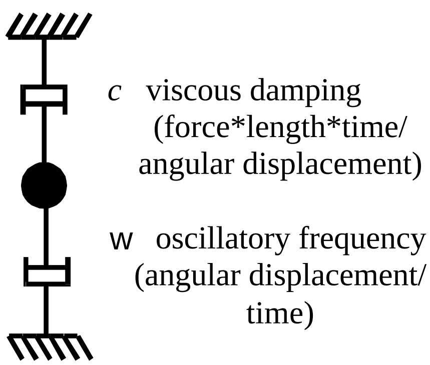

Figure A.5: Viscous Point Damping to Ground

Appendix B. Listing of the Model Parameter Values for an Automatic Vehicle Transmission

A listing of the model parameter values for the automatic vehicle transmission discussed in Section 5.6 is presented on the following pages. Figure B.1 shows the point and shaft numbers of the transmission components that correspond to those in the model listing.

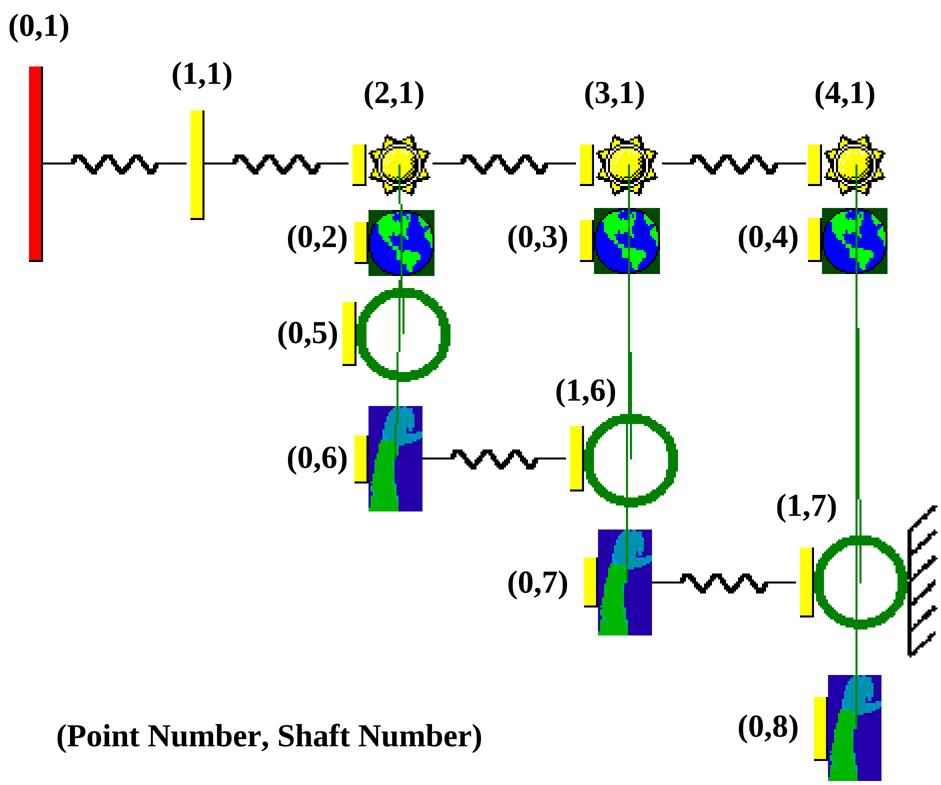

Figure B.1: Automatic Vehicle Transmission Schematic with Point Numbers

```
Model Listing:


    Shaft  1:
    Boundary Conditions:  Free - Free

      For point # 0:
      Type of point.................................  Regular
        Polar Inertia..............................=   1.607E+00   kg-m^2

      For field # 1:
      Type of field.................................  Spring-Damper
        Length of this section.....................=   1.000E+00   m
        Inline Stiffness...........................=   1.2263E+05   N-m/rad

      For point # 1:
      Type of point.................................  Regular
        Polar Inertia..............................=   3.30182E-01   kg-m^2

      For field # 2:
      Type of field.................................  Spring-Damper
        Length of this section.....................=   1.000E+00   m
        Inline Stiffness...........................=   1.605E+05   N-m/rad

      For point # 2:
      Type of point.................................  Sun Gear
        Polar Inertia..............................=   6.027E-04   kg-m^2
        Gear Base Radius...........................=   3.700E-02   m
        Gear Tooth Stiffness.......................=   1.000E+09   N/m

      For field # 3:
      Type of field.................................  Spring-Damper
        Length of this section.....................=   1.000E+00   m
        Inline Stiffness...........................=   8.936E+05   N-m/rad

      For point # 3:
      Type of point.................................  Sun Gear
        Polar Inertia..............................=   2.186E-04   kg-m^2
        Gear Base Radius...........................=   2.700E-02   m
        Gear Tooth Stiffness.......................=   1.000E+09   N/m

      For field # 4:
      Type of field.................................  Spring-Damper
        Length of this section.....................=   1.000E+00   m
        Inline Stiffness...........................=   1.5864E+06   N-m/rad

      For point # 4:
      Type of point.................................  Sun Gear
        Polar Inertia..............................=   3.462E-04   kg-m^2
        Gear Base Radius...........................=   2.700E-02   m
        Gear Tooth Stiffness.......................=   1.000E+09   N/m
```

```
Shaft  2:
Boundary Conditions:  Free - Free

  For point # 0 :
  Type of point..................................  Planet Gear
    Polar Inertia.............................=   9.360E-05   kg-m^2
    Gear Base Radius..........................=   1.600E-02   m
    Gear Tooth Stiffness......................=   1.000E+09   N/m


Shaft  3:
Boundary Conditions:  Free - Free

  For point # 0:
  Type of point..................................  Planet Gear
    Polar Inertia.............................=   2.828E-04   kg-m^2
    Gear Base Radius..........................=   2.100E-02   m
    Gear Tooth Stiffness......................=   1.000E+09   N/m


Shaft  4:
Boundary Conditions:  Free - Free

  For point # 0:
  Type of point..................................  Planet Gear
    Polar Inertia.............................=   6.580E-04   kg-m^2
    Gear Base Radius..........................=   2.100E-02   m
    Gear Tooth Stiffness......................=   1.000E+09   N/m


Shaft  5:
Boundary Conditions:  Free - Free

  For point # 0:
  Type of point..................................  Ring Gear
    Polar Inertia.............................=   3.64134E-02   kg-m^2
    Gear Base Radius..........................=   7.100E-02   m
    Gear Tooth Stiffness......................=   1.000E+09   N/m


Shaft  6:
Boundary Conditions:  Free - Free

  For point # 0:
  Type of point..................................  Planet Arm
    Polar Inertia.............................=   4.7759E-03   kg-m^2

  For field # 1:
  Type of field..................................  Spring-Damper
    Length of this section....................=   1.000E+00   m
    Inline Stiffness..........................=   1.000E+10   N-m/rad

  For point # 1:
  Type of point..................................  Ring Gear
    Polar Inertia.............................=   4.63192E-02   kg-m^2
    Gear Base Radius..........................=   7.100E-02   m
    Gear Tooth Stiffness......................=   1.000E+09   N/m
```

```
Shaft  7:
Boundary Conditions:  Free - Fixed

  For point # 0:
  Type of point.................................  Planet Arm
    Polar Inertia.............................=   6.0934E-03   kg-m^2

  For field # 1:
  Type of field.................................  Spring-Damper
    Length of this section....................=   1.000E+00   m
    Inline Stiffness..........................=   1.000E+10   N-m/rad

  For point # 1:
  Type of point.................................  Ring Gear
    Polar Inertia.............................=   6.16455E-02   kg-m^2
    Gear Base Radius..........................=   7.100E-02   m
    Gear Tooth Stiffness......................=   1.000E+09   N/m


Shaft  8:
Boundary Conditions:  Free - Free

  For point # 0:
  Type of point.................................  Planet Arm
    Polar Inertia.............................=   4.00545E-02   kg-m^2

Gear Connections:
    Planetary Gear Mesh  1:
          Sun Gear......(Point  2 , Shaft  1 )
          Planet Gear...(Point  0 , Shaft  2 )
          Planet Arm....(Point  0 , Shaft  6 )
          Ring Gear.....(Point  0 , Shaft  5 )
    Planetary Gear Mesh  2:
          Sun Gear......(Point  3 , Shaft  1 )
          Planet Gear...(Point  0 , Shaft  3 )
          Planet Arm....(Point  0 , Shaft  7 )
          Ring Gear.....(Point  1 , Shaft  6 )
    Planetary Gear Mesh  3:
          Sun Gear......(Point  4 , Shaft  1 )
          Planet Gear...(Point  0 , Shaft  4 )
          Planet Arm....(Point  0 , Shaft  8 )
          Ring Gear.....(Point  1 , Shaft  7 )

                        *** END OF LISTING ***
```

References

[1] Mabie, H. H. and C. F. Reinholtz, *Mechanisms and Dynamics of Machinery*, 4th Edition, John Wiley and Sons, Inc., New York, 1987, pp. 450-456.

[2] Wilson, W. K., *Practical Solution of Torsional Vibration Problems, Volume One: Frequency Calculations*, 3rd Edition, John Wiley and Sons, Inc., New York, 1956, pp. xiii–xxxii.

[3] Reference 2, pp. 157–661.

[4] Nestorides, E. J., *A Handbook on Torsional Vibration*, Cambridge University Press, Cambridge, 1958, pp. 1–241.

[5] Pestel, E. C. and F. A. Leckie, *Matrix Methods in Elastomechanics*, McGraw-Hill Book Company, New York, 1963, pp. 51–129.

[6] Pilkey, W. D. and P. Y. Chang, *Modern Formulas for Statics and Dynamics: A Stress-and-Strain Approach*, McGraw-Hill Book Company, New York, 1978, pp.118-122.

[7] Reference 5, pp. 153-169.

[8] Sankar, S., "On the Torsional Vibration of Branched Systems Using Extended Transfer Matrix Method", *Transactions of the ASME, Journal of Mechanical Design*, Vol. 101, October 1979, pp. 546-553.

[9] Reference 5, p. 162.

[10] Abhary, K., "Application of Bond Graphs In Rectilinear Modeling of Lumped Parameter Torsional Vibratory Systems", *Proceedings of the 1995 Design Engineering Technical Conferences, Volume 1: Advances in Design Automation*, ASME, New York, held at Boston, Massachusetts, September 17-20, 1995, pp. 733-740.

[11] Mitchell, L. D., "A New Branching Technique for the Static and Dynamic Analysis of Geared Systems", *Proceedings of the Second International Conference – Vibrations in Rotating Machinery*, The Institution of Mechanical Engineers, London, England, held at Cambridge, England, September 2-4, 1980, pp. 37-42.

[12] Hibner, D. H., "Dynamic Response of Viscous-Damped Multi-Shaft Jet Engines", *Journal of Aircraft*, Vol. 12, No. 4, April 1975, pp. 305-312.

[13] Blanding, J. M., "An Analytical Study and Computer Analysis of Three-Dimensional, Steady-State Vibration of Multishaft Geared-Rotor Systems", Ph.D. Dissertation, Virginia Polytechnic Institute and State University, Blacksburg, VA 24061, May 1985.

[14] Tsai, J. H., and J. H. Kuang, "An Improved Branch Method for Gear-Coupled Systems", *Proceedings of the 9th International Modal Analysis Conference*, SEM, Bethel, Connecticut, held at Florence, Italy, April 15-18, 1992, pp.1293-1301.

[15] Doughty, S. and G. Vafaee, “Transfer Matrix Eigensolutions for Damped Torsional Systems”, *Transactions of the ASME, Journal of Vibration, Acoustics, Stress, and Reliability in Design*, Vol. 107, January 1985, pp. 128-132.

[16] Huang, Y. M. and C. D. Horng, “Eigenvalues and Eigenvectors of Damped Branched Torsional Systems”, Proceedings of the 1992 Pressure Vessels and Piping Conference: DOE Facilities Programs, Systems Interaction, and Active/Inactive Damping, ASME, New York, held at New Orleans, Louisiana, June 21-25, 1992, pp. 121-126.

[17] Daws, J. W., “An Analytical Investigation of Three-Dimensional Vibration in Gear-Coupled Rotor Systems”, Ph.D. Dissertation, Virginia Polytechnic Institute and State University, Blacksburg, VA 24061, May 1979, pp. 53-119.

[18] Reference 13, pp. 26-48.

[19] Neriya, S. V., R. B. Bhat, and T. S. Sankar, “Dynamic Tooth Load and Response of a Torsion-Flexure Coupled Geared Shaft System Due to Internal Excitations”, *Proceedings of the 1990 ASME Design Technical Conferences: Cams, Gears, Robot and Mechanism Design*, ASME, New York, held at Chicago, Illinois, September 16-19, 1990, pp. 373-384.

[20] Oswald, F. B., D. P. Townsend, B. Rebbechi, and H. H. Lin, “Dynamic Forces in Spur Gears – Measurement, Prediction, and Code Validation”, *Proceedings of the 1996 Design Engineering Technical Conferences: Power Transmission and Gearing Conference*, ASME, New York, held at San Diego, California, October 6-9, 1996, pp. 9-15.

[21] Kuang, J. H. and Y. T. Yang, “An Estimate of Mesh Stiffness and Load Sharing Ratio of a Spur Gear Pair”, Proceedings of the 1992 Design Engineering Technical Conferences: International Power Transmission and Gearing Conference, Volume 1, ASME, New York, held at Scottsdale, Arizona, September, 13-16, 1992, pp. 1-7.

[22] Burden, R. L. and J. D. Faires, *Numerical Analysis*, Fourth Edition, Pws-Kent Publishing Company, Boston, 1989, pp. 73-81.

[23] Reference 5, p. 52.

[24] Reference 5, p. 54.

[25] Reference 5, p. 52.

[26] Reference 5, p. 54.

[27] Reference 5, p. 54.

[28] Reference 5, pp. 82-90.

[29] Wilson, W. K., Practical Solution of Torsional Vibration Problems, Volume Four: Devices for Controlling Vibration, 3rd Edition, Chapman and Hall Ltd., London, 1968.

[30] Doughty, S., “The Viscous Shear Damper in Natural Frequency Calculations”, *ASME Paper 95-ICE-14*, New York, 1995, pp. 1-8.

[31] Thomson, W. T. and M. D. Dahleh, *Theory of Vibration with Applications*, Fifth Edition, Prentice Hall, Upper Saddle River, NJ, 1993, pp. 144-151.

[32] Reference 31, p. 147.

[33] Reference 6, pp. 118-122.

[34] Reference 6, p. 119.

[35] Reference 11, pp. 37-42.

[36] Reference 11, p. 42.

[37] Shigley, J. E. and C. R. Mischke, *Mechanical Engineering Design*, Fifth Edition, McGraw-Hill, Inc., New York, 1989, p. 534.

[38] Reference 11, p. 42.

[39] Reference 1, p. 248.

[40] Reference 2, pp. 499-561.

[41] Reference 4, pp. 3-34.

[42] Reference 17, pp. 53-68.

[43] Reference 1, p. 147.

[44] Reference 6, p. 133.

[45] Reference 6, p. 133.

[46] Wilson, W. K., Practical Solution of Torsional Vibration Problems: Volume Two: Amplitude Calculations, 3rd Edition, Barnes and Noble, Inc., New York, 1963, pp. 61-66.

[47] Reference 15, pp. 128-132.

[48] Reference 15, p. 131.

[49] Reference 15, p. 131.

[50] Reference 2, p. 299-301.

[51] Reference 2, p. 293.

[52] Reference 25, pp. 265-266.

[53] Reference 25, p. 265.

[54] Mandal, B., P. Sivakumar, S. Kumar, "Torsional Vibration Analysis of an Automatic Transmission", Proceedings of the IUTAM-IITD International Winter School on Optimum Dynamic Design Using Modal Testing and Structural Dynamic Modification, Allied Publishers Limited, New Delhi, held at New Delhi, December 15-19, 1997, pp. 431-444.

[55] Mitchiner, R. G. and R. G. Leonard, "The Theory of Centrifugal Pendulum Vibration Absorbers", *Proceedings of 1987 ASME Design Technology Conferences: Vibration Control and Active Vibration Suppression*, ASME, New York, held at Boston, MA, September, 1987, pp. 1-4.

[56] Freudenstein, F. and A. T. Yang, "Kinematics and Statics of Coupled Epicyclic Spur Gear Trains", *Mechanism and Machine Theory*, Vol. 7, pp. 263-375.

[57] Pennestri, E. and F. Freudenstein, "A Systematic Approach to Power-Flow and Static Force Analysis in Epicyclic Spur Gear Trains", *Proceedings of the 1990 ASME Design Technical Conferences: Cams, Gears, Robot and Mechanism Design*, ASME, New York, held at Chicago, Illinois, September 16-19, 1990, pp. 63-70.

[58] Saggere, L. and D. G. Olson, "A Simplified Approach for Force and Power-Flow Analysis of Compound Epicyclic Spur-Gear Trains", *Proceedings of the 1992 Design Technical Conferences: Advances in Design Automation – Volume 2*, ASME, New York, held at Scottsdale, Arizona, September 13-16, 1992, pp. 83-89.

[59] Sanger, D. J., "Determination of Power-Flow in Multiple-Path Transmission Systems", *Mechanisms and Machine Theory*, Vol. 7, 1972, pp. 103-109.

[60] Wojnarowski, J., "The Graph Method of Determining the Loads in Complex Gear Trains", *Mechanism and Machine Theory*, Vol. 11, 1976, pp. 103-121.

[61] Reference 6, p. 110.

[62] Reference 6, p. 110.

[63] Reference 5, p. 377.

[64] Reference 6, p. 111.

[65] Reference 5, p. 111.

[66] Reference 5, p. 112.

Vita

Timothy R. Griffin was born on January 27, 1974 in Valdosta, Georgia and later grew up in Hendersonville, Tennessee. He graduated as valedictorian from Hendersonville High School in 1992. After graduating from high school he attended college at Tennessee Technological University. As an undergraduate he worked on co-op assignments with BellSouth, Specialty Plastics Products of Tennessee, and Hoeganaes. He received the 1996 Engineering Award at Tennessee Tech before graduating with a BS in Mechanical Engineering that same year. In the fall of 1996 he began graduate school at Virginia Tech where he worked for the Mechanical Engineering Department as a graduate teaching assistant for four semesters. Upon completion of his Masters degree Tim plans to begin work with Exxon Production Research Company in Houston, Texas.